AD-A191 924 UNDRAINED STRESS-STRAIN BEHAVIOR OF UNSATURATED SANDS VOLUME 1(U) WISCONSIN UNIV-MADISON R G BOEHM ET AL. 25 JAN 88 AFOSR-TR-88-0155 AFOSR-84-0090 1/2

UNCLASSIFIED F/G 8/10 NL

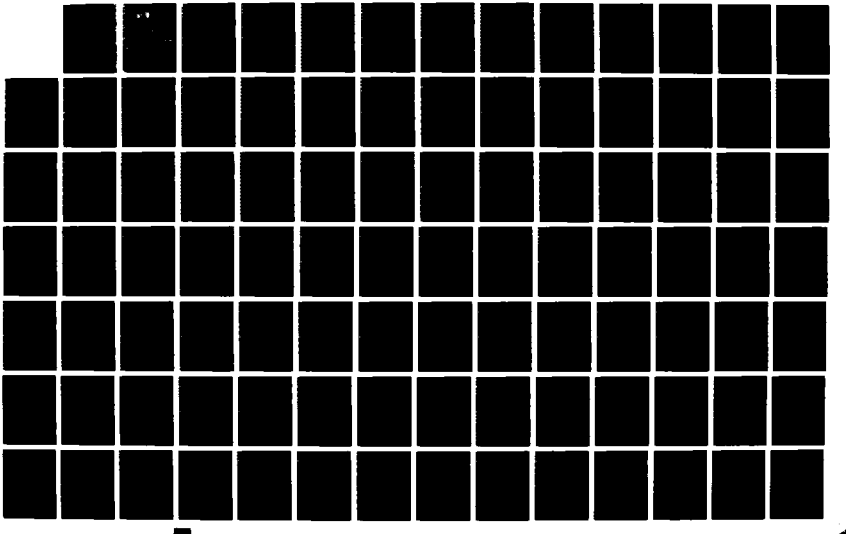

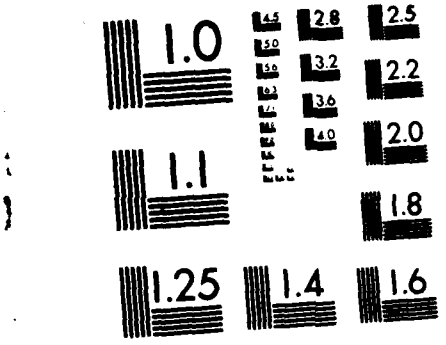

UNCLASSIFIED

DTIC FILE COPY

(2)

DOCUMENTATION PAGE

Form Approved OMB No. 0704-0188

AD-A191 924

DTIC ELECTE FEB 29 1988 S D

1b. RESTRICTIVE MARKINGS

3. DISTRIBUTION/AVAILABILITY OF REPORT
Approved for Public Release; Distribution Unlimited

2b. DECLASSIFICATION/DOWNGRADING SCHEDULE

4. PERFORMING ORGANIZATION REPORT NUMBER(S)

5. MONITORING ORGANIZATION REPORT NUMBER(S)
AFOSR-TR- 88-0155

6a. NAME OF PERFORMING ORGANIZATION	6b. OFFICE SYMBOL (If applicable)	7a. NAME OF MONITORING ORGANIZATION
University of Wisconsin		AFOSR/NA

6c. ADDRESS (City, State, and ZIP Code)	7b. ADDRESS (City, State, and ZIP Code)
2304 Engineering Building University of Wisconsin, Madison 53706.	Bldg. 410 Bolling AFB, DC 20332-6448

8a. NAME OF FUNDING/SPONSORING ORGANIZATION	8b. OFFICE SYMBOL (If applicable)	9. PROCUREMENT INSTRUMENT IDENTIFICATION NUMBER
AFOSR	NA	AFOSR-84-0090

8c. ADDRESS (City, State, and ZIP Code)	10. SOURCE OF FUNDING NUMBERS			
	PROGRAM ELEMENT NO.	PROJECT NO.	TASK NO	WORK UNIT ACCESSION NO.
Bldg. 410 Bolling AFB, DC 20332-6448	6.1102F	2302	C1	

11. TITLE (Include Security Classification) (U)
Undrained Stress-Strain Behavior of Partly Saturated Sands

12. PERSONAL AUTHOR(S)
R. Poehr, and J. K. Tevaoalan

13a. TYPE OF REPORT	13b. TIME COVERED	14. DATE OF REPORT (Year, Month, Day)	15. PAGE COUNT
Final-Volume 1 of 2	FROM 4-1-84 TO 9-30-87	25 Jan 88	96

16. SUPPLEMENTARY NOTATION

17. COSATI CODES			18. SUBJECT TERMS (Continue on reverse if necessary and identify by block number)
FIELD	GROUP	SUB-GROUP	

19. ABSTRACT (Continue on reverse if necessary and identify by block number)

This final report provides the details of an investigation on the undrained stress-strain behavior of partly saturated sands under controlled laboratory conditions. A new triaxial test setup was developed during the previous years of this research study. Thus, the two purposes of the investigation reported in this report were a) to evaluate the usefulness of the new soil test procedure, and b) to determine the behavior of the unsaturated sand samples. An axis translation technique was used to monitor pore water pressure changes during the tests and this appeared to work well. A special ceramic porous stone was used to be able to measure pore water and air pressures separately. The conclusions drawn from this research are that the stress-strain behavior changes little with respect to saturation level unitl the level approaches about 95 %. The initial tangent modulus decreased with an increase in saturation. For lower saturated samples, there seems to be no difference between an undrained and a drained test. The dilation potential of the sand increased with strain rate. The strain rate had some effect on the initial modulus of only the dense samples of sand.

20. DISTRIBUTION/AVAILABILITY OF ABSTRACT
☒ UNCLASSIFIED/UNLIMITED ☐ SAME AS RPT ☐ DTIC USERS

21. ABSTRACT SECURITY CLASSIFICATION
UNCLASSIFIED

22a. NAME OF RESPONSIBLE INDIVIDUAL	22b. TELEPHONE (Include Area Code)	22c. OFFICE SYMBOL
Major Steven C. Boyce	(202) 767-6963	AFOSR/NA

DD Form 1473, JUN 86 Previous editions are obsolete. SECURITY CLASSIFICATION OF THIS PAGE

UNCLASSIFIED

UNDRAINED STRESS-STRAIN BEHAVIOR OF UNSATURATED SANDS

By

Rolland G. Boehm

and

Jey K. Jeyapalan

2304 Engineering Building
University of Wisconsin
Madison, Wisconsin, 53706.

Report to the

Air Force Office of Scientific Research
Bolling Air Force Base
Washington, DC

25 January 1988

TABLE OF CONTENTS

ACKNOWLEDGEMENTS

This investigation was conducted at the University of Wisconsin-Madison in the Department of Civil and Environmental Engineering under the sponsorship of the Air Force Office of Scientific Research. Professor J.K. Jeyapalan initiated the project and served as the author's advisor.

The financial support by the Air Force Office of Scientific Research and the guidance and trust of Professor J.K. Jeyapalan are gratefully acknowledged.

Acknowledgement is also extended to Mr. Ernie R. Hanna and Mr. Norm H. Severson for their help in familiarizing me with the test equipment, as well as helpful suggestions.

Finally, I would like to thank my wife Wendy K. Boerm, for typing and editing the manuscript, but more importantly for her continued support during my entire graduate studies.

LIST OF FIGURES

Figure | Page

I. INTRODUCTION

The stress-strain behavior of a partially saturated soil can be dramatically different than that of the same soil in a saturated state. The difference in behavior can be attributed to the soil's suction characteristics. Soil suction is a function of the soil type, gradation, location of the water table, and the environmental conditions.

Partially saturated soil behavior has been studied almost since the birth of soil mechanics, realizing that the majority of surface or near surface soil deposits are partially saturated. Early investigators recognized that Terzaghi's effective stress equation was inadequate to describe the effective stress of partially saturated soils. The mechanisms involved are very complex. Many general effective stress formulae have been developed, but most have been met with criticism and/or are of limited use.

The first objective of this research project was to evaluate the testing apparatus and procedures used for unsaturated soils. The second objective was to study in detail the stress-strain-strain rate behavior of an unsaturated fine sand.

A series of undrained modified triaxial tests were performed on the fine sand. Five parameters were varied during the test program. These include: density, saturation, initial back pressure, effective confining pressure and the strain rate. The reduced data include: stresses, axial and volumetric strains, pore pressures and the initial tangent modulus.

II. PRELIMINARY CONSIDERATIONS

2.1 General

The physical laws that govern a partially saturated soil differ from those of saturated soils. One must understand these physical differences before a characterization of the stress-strain behavior of an unsaturated soil can be made.

2.2 Surface Tension

Surface tension is a phenomenon that occurs at the intersection between different materials. For soils, it occurs at the interface between the water, mineral grains, and the air. Fundamentally, surface tension results from differences in forces of attraction between the molecules of the material at the interface (Holtz and Kovacs, 1981). Surface tension is the fundamental reason behind the differences in saturated and unsaturated soil. The following formula expresses the total surface tension force generated by a water menicus between two spheres.

$$T_f = 2\pi r T \left(\frac{\mathrm{Sin}\Theta + \mathrm{Cos}\Theta - 1}{\mathrm{Cos}\Theta} \right) \qquad [1]$$

Where T is the surface tension of water (73 dynes per cm @ 20 C), and all other variables are defined in Fig. 1.

2.3 Soil Suction

Soil suction is due to the soils' ability to lift or hold water in soil matrix. Thus, soil suction can be considered stored or

potential energy. there are typically three compoonents to soil suction.

1. Pressure Head
2. Adsorptive Head
3. Osmotic Head

The total suction is the addition of the above three components. The first two are often combined and referred to as the matrix suction. The matrix suction is the negative gage pressure at a point in the soil-water relative to the external gas pressure. It results from the capillary and adsorptive forces arising from the soil matrix. Osmotic suction arises from the differences in the concentration of soil-water at different points in a soil. The following formula describes the water pressure in a soil due to matrix suction.

$$P = \frac{T\cos\theta}{r}\left(\frac{1}{(1-\cos\theta)} - \frac{1}{(\sin\theta+\cos\theta-1)}\right) \qquad [2]$$

Where T is the surface tension of water and all other variables are described in Fig. 1.

Typically water will vaporize at pressures below a -1 atmosphere (-14.7 psi). However, if the pore diameter is small enough, the water will not be able to cavitate, because the surface tension forces will be too high for an air bubble to form (Terzaghi and Peck, 1967). It is for this reason, capillary rise can occur to a height far greater than expected. In fact, most clays will have a capillary rise in excess of 30 feet. This for sands rarely exceeds 5-6 feet.

2.4 Effective Stresses in Unsaturated Soil

If a soil is saturated the effective stress is simply the total stress minus the pore water pressure (Terzaghi, 1936), regardless of whether or not the pore pressures are negative or positive. If on the other hand, the soil is partially saturated, the mechanisms of effective stress become far more complex. Partially saturated soils form menisci at the soil grain/water/air interfaces. The relative amount of water capable of being held in this pocket or column of water is a function of the grain geometry and soil type. The water held in this position will be in tension (negative pressure), which results in intergranular forces. As the meniscus becomes smaller, the pressures become more negative, but acting over a smaller area. Thus, the addition of strength attributed to soil suction is both a function of degree of saturation and soil structure. The following formula describes the effective stress for a partially saturated idealized material made of spheres.

$$\bar{\sigma} = \frac{p\pi}{4}\left(\frac{\mathrm{Sin}\Theta+\mathrm{Cos}\Theta-1}{\mathrm{Cos}\Theta}\right)^2 - \frac{\pi T}{2r}\left(\frac{\mathrm{Sin}\Theta+\mathrm{Cos}\Theta-1}{\mathrm{Cos}\Theta}\right) \qquad [3]$$

where p= (as given by equation 2)

T= the surface tension of water (73 dynes/cm)

r= the radius of water menicus

Θ= (as given in figure 1)

If a partially saturated cohesionless soil is tested with a conventional triaxial setup and procedures, the Mohr-Coulomb diagram will show a cohesion intercept. In reality, the exact locations for the Mohr's circles can only be determined if the stresses attributed by soil suction are included.

2.5 General Gas Law

Theoretical changes in pore water pressures for a given soil volume decrease under undrained conditions, has been derived by Hamilton (1939). The assumption being that the pore air and pore water pressures are equal (no soil suction). Hamilton's formula is expressed as follows:

$$Po = (Vao + 0.2Vw) = Pc (Vac + 0.02Vw) \qquad [4]$$

where Po= initial absolute air pressure

Pc= absolute air pressure after compression

Vao= initial free air volume at Po

Vac= volume of air at Pc

Vw= volume of water in soil

This equation can illustrate how a relatively small amount of air in the soil can drastically effect the pore pressures. It's usefulness is limited to soils with little or no soil suction.

III. LITERATURE REVIEW

3.1 Modified Effective Stress Equation

Bishop (1959) was one of the first investigators to develop a general effective stress equation. His original work resulted in the following equation:

$$\sigma' = (\sigma - Ua) + X(Ua-Uw) \qquad [5]$$

where σ = total stress

Ua= pore air pressure

Uw= pore water pressure

X= empirical parameter

The empirical parameter was thought to be a function of soil structure and saturation level. The basic assumption in this being able to quantify the parameter X was that an increase in the matrix suction term X(Ua-Uw) is equivalent to an increase in confining pressure. Blight presented a method for determining this parameter. The method required several sets of test on similar samples. One set is tested in a saturated state. A graphical procedure then relates the two sets of laboratory tests.

Aitchison (1960) performed some theoretical work which described Bishop's empirical parameter X as a function of the matrix suction (Ua-Uw), the level of saturation, and the soil structure.

Sparks (1963) suggested that Bishop's equation was incorrect, because the effect of surface tension was ignored in the derivation. Sparks developed the following equation that considers the surface

tension force.

$$\sigma_x' = \sigma_x - \alpha Ua - \beta Uw + \gamma T \qquad [6]$$

Where T is the surface tension at the air water interface. If the pores are filled with water $\alpha = \gamma = 0$, and if filled with air $\beta = \gamma = 0$.

Donald (1963) attempted to generate a general formula for the X parameter. Donald felt that the equation must include the surface tension forces. By definition

$$X = S + (f(s)/(Ua-Uw)) \qquad [7]$$

where S is the degree of saturation of the pores and f(s) is a function that takes into account the numerical value of the surface tension forces.

Burland and Jennings (1962) and Burland (1965) pointed out that surface tension forces produce only normal intergranular stresses. They also questioned the validity of the underlying assumption used in determining the X parameter. Namely, that an increase in the matrix suction term is equivalent to an increase in confining pressure. Their test results suggested that for a given soil structure and type, there is a critical degree of saturation, and below this value, the above assumption is incorrect.

Blight (1967) reinstated Bishop's equation but recognized its limitations. Blight suggested that the X parameter could not be determined from some unique function. But instead had to be evaluated for each soil type, structure, saturation level, and applied matrix suction.

Tower and Childs (1972) attempted to calculate the effective stress that would operate in an unsaturated soil as a sum of two components: one arising from continuous water at an externally measured suction in unemptied pores, the other from isolated bodies of water in nominally emptied pores at suctions approximating to the suctions at which those pores were emptied. Their findings were that an average degree of saturation specified for an unsaturated soil may not be a particularly relevant factor in determining its behavior.

Gulhati and Satija (1979) took a slightly different approach in examining unsaturated soil stresses. They presented the following equation:

$$\frac{(\sigma_1 - \sigma_3)_f}{2} = a + (\sigma_3 - Ua)_f \tan\alpha + (Ua - Uw)\tan\beta \qquad [8]$$

where a, α, and β are coefficients to be determined from laboratory tests. Their approach was to vary the $(\sigma_3 - Ua)_f$ and $(Ua - Uw)_f$ terms and plot all three (including $(\sigma_1 - \sigma_3)_f/2$) values on a 3-D plot from which a, α, and β can be determined. Gulhati and Satija believed that the above approach was better for determining relative gains in shear strength as a function of soil suction.

Ho and Fredlund (1982) presented the following shear strength equation for unsaturated soils:

$$\tau = c' + (\sigma - Ua)\tan\phi' + (Ua - Uw)\tan\phi^b \qquad [9]$$

where ϕ^b equals the friction angle with respect to changes in (Ua-Uw) when $(\sigma - Ua)$ is held constant. Ho and Fredlund felt this approach was

valid providing ϕ^b was determined for each soil type and condition. It is necessary to recognize that the applied matrix suction (Ua-Uw) will control the saturation level up to some critical value, at which point the water in the specimen will be completely dispersed throughout the soil matrix (no capillary rise). The ϕ^b parameter can be determined from a 3-D graphical approach. This approach must include a series of saturated tests.

3.2 Unsaturated Soil Testing Equipment

Hilf (1956) was one of the first to measure negative pore pressures. He developed a device which consisted primarily of a pressure vessel, in which the soil specimen was placed. A saturated porous ceramic tip was placed into the specimen. This probe was connected by a tube, filled with de-aired water, that was connected to a null type pressure measuring system. The measuring system would register a negative pressure as the water had a tendency to travel into the sample. By raising the air pressure in the pressure vessel the tendency for water movement could be stopped. This point was considered equilibrium and the soil suction was determined by taking the pressure difference between pore air and pore water.

Bishop (1959) was the first to utilize the high air entry ceramic disk in a triaxial setup. Thus, allowing measurement of pore water pressures independently from pore air pressures. As with the pressure vessel, an axis translation technique was used. The system was closed in regards to outside air. A self-compensating mercury control was used to maintain cell pressure and pore air pressure. Two colored

kerosene and water interfaces were introduced into the layout. This allowed measurement of water into or out of both the sample and triaxial cell.

Bishop and Donald (1961) used mercury (Hg) as the confining fluid. They also introduced a means of collecting and measuring the dissolved air that passed through the ceramic disk (bubble pump). Air has a tendency to come out of the solution under the ceramic disk if the pressure is less. This ultimately causes problems in obtaining accurate pore pressure readings.

To date most of the advancements in testing equipment have been in the form of increasing the accuracy of the volume change and pore pressure measurements, simplifying the layout by making use of pressure regulators, and using electrical strain and pressure gauges. Hanna and Jeyapalan (1986) used the forementioned ideas in conjuction with an automated data aquisition system to develop the most recent state-of-the-art unsaturated soils testing system. However, problems with air diffusing into the cell and through the ceramic stone still persist.

3.3 Stress-Strain Behavior of Unsaturated Soil

Bishop and Donald (1961) presented unsaturated test results on Braehead silt. Using the results they developed, a curve was established for the X parameter (for the silt) used in the modified effective stress equation. A sample of their results is shown in Fig. 2.

Donald (1963) performed undrained triaxial tests on a partially saturated compacted clay. A series of Mohrs circle diagrams showed in a relative way the effects of soil suction on shear strength, as given in Fig. 3.

Bishop and Blight (1963) performed an extensive testing program on unsaturated soils. Their results concluded that a modified effective stress equation was useful in defining shear strength. However, its usefulness in determining volume change is very difficult.

Burland (1965) discussed volumetric behavior qualitatively in terms of intergranular forces and drew a contrast between the changes in intergranular forces arising from increases in external stresses (which tend to induce grain slippage) and those arising from changes in negative pore water pressure in the menisci (which tend to act as blobs of glue, holding the grains together). Because there are fundamental differences in the way applied stresses and pore pressures are transmitted through the grain structure there can be no equivalence between change in applied isotropic stresses and any function of a change in the pore suction.

Blight (1967) presented test results that showed the shear strength increase due to applied suction, as given in Fig. 4. He also concluded, based on test data that the X parameter changes with axial strain. His results also indicated that changes in volume of an unsaturated soil appear to be related to the modified effective stress equation.

Towner and Childs (1972) presented data to show that the stress path for an unconfined, unsaturated sand is dependent not only on the applied suction, but also on whether the soil is in a drying or wetting process. The results of this study are shown in Fig. 5.

Edil, Motan and Toha (1981) applied various matrix suctions to an unsaturated clay. Upon equilibrium, an unconfined compression test was performed. As expected, the strength increased with initial matrix suction. But more interestingly, the initial modulus increased linearly up to some critical matrix suction, where it then declined. The poisson ratio was also determined as a function of initial matrix suction. The results of this study are shown in Fig. 6.

3.4 Strain Rate Effects

Soils under rapid or dynamic loading usually exhibit differences in their strength and deformation modulus when compared to static loading. The following will be a brief review of the work to date in this area.

Casagrande and Shannon (1948) presented the results of triaxial test on dry sand in which the load was applied by a falling beam type apparatus. They found an increase in the ultimate shearing strength of 10 of 15 percent and an increase in the modulus of deformation of about 30 percent when the load was applied dynamically rather than statically. The modulus of deformation was defined by a secant modulus obtained by passing a straight line through the origin and a point on the stress-strain curve at one half the ultimate stress.

Casagrande and Shannon also conducted similar tests on unsaturated clay. They found that the percentage increase of the fast transient strength over the static compressive strength was greatest for specimens of the lowest water content. With the highest water content the modulus of deformation increased by two times.

Whitman (1954) evaluated the strain rate effect on ten different cohesive materials. Generally, an increase in the strain rate from static to 1000 percent per second increased the ultimate strength by a factor of 1.5 to 3.0, which is of the same order of magnitude as that found by Casagrande and Shannon.

Seed and Lundgren (1954) investigated the strength and deformation characteristics of saturated specimens of a fine sand and of a coarse sand under dynamic loadings. They found an increase in strength of 15 to 20 percent and an increase in the modulus of deformation (secant) of about 30 percent under the dynamic loading conditions. They noted that dilatancy effects and lack of drainage contributed to the strength under dynamic loads.

Nash and Dixon (1961) developed a dynamic pore pressure measuring device with which they successfully recorded pore pressure changes in triaxial tests on saturated sands under strain rates up to 8000 percent per minute or loading rates up to about 220 inches per minute.

Richart (1977) summarized previous work on strain rate effects on shear strength: (a) for dry sands the strain rate factor is less than 1.1 to 1.15 for strain rates varying from about 0.02% to 1000%

per second, (b) for saturated cohesive soils the strain rate factor was 1.5 to 3.0 and (c) for partially saturated soils the strain rate factor was 1.5 to 2.0.

Gulhati and Satija (1979) found that the strain rate has a pronounced effect on the measured soil suction during drained modified triaxial tests on clay. They showed that during shearing the specimens change volume. A changing soil structure resulted in a changing matrix suction. But at fast strain rates, an equilibrium condition was not possible, resulting in excess pore pressures (drop in soil suction).

Richart, Wu and Gray (1984) performed dynamic shear modulus tests on partially saturated sands. They concluded that the maximum capillary influences occurred at degrees of saturation between 5% to 20% for the soils tested. The increase in the shear modulus over the dry samples was about 1.65 and 2.0 for average confining pressures of 3.6 psi and 14.2 psi, respectively.

IV. EVALUATION OF EQUIPMENT AND TEST PROCEDURES

4.1 Apparatus

The testing system used in this research program is the same system that was developed and used by Hanna and Jeyapalan (1986). There were several minor modifications that increased the overall accuracy of the measurements, but the system basically remained the same. A schematic diagram of the setup is shown in Fig. 7. In short, two thick rubber balloons enclosed in a chamber are pressurized via a regulator. The pressurized water (in the chamber) is then transmitted to the cell fluid or pore water. A regulated air supply is transmitted to the top of the soil specimen. Transducers, placed in the appropriate places, allow measurement of cell, pore water and pore air pressures.

There are several features about the apparatus that should be discussed in detail. The first is the colored kerosene interface. This interface allows measurement of water into or out of the cell or sample. For instance, if the sample were to dialate, water would be forced out of the cell and into the pressure chamber, where the balloon would collapse by the appropriate amount. The amount of water forced into the pressure chamber would be measured by the travel distance of the kerosene/water interface. The second major point of interest is the ceramic stone. This special disk allows water to travel through its pores, but not air. So ultimately, one can measure pore water pressure independently from pore air. The ceramic stone

used during this testing program had an air entry value of 80 psi. This means that the ceramic stone could hold back up to 80 psi of air pressure. One of the major drawbacks to the high air entry value is the decrease in permeability compared with conventional porous stones. The particular ceramic stone used has a permeability of 1.0×10^{-7} cm/sec. Because dissolved air can pass through the stone, a special port was drilled into the base and pedestal in order to provide a flushing system for air entrapped under the ceramic disk.

The loading frame used was similar to those used in most triaxial setups. The loading was applied at a constant strain rate, which was regulated by a hydraulic system. A load cell incorporated into the loading shaft provided electronic measurement of the applied load. Sample deformations were measured as the travel distance of the loading shaft. An LVDT was used to measure the deformations electronically.

A data ecquisition system (SYSTEM 4000) was used to acquire and reduce the raw data from the gauges. The information could then be transformed directly onto the computer monitor. A computer program provided with the system allows the user to automatically record data at desired time intervals. Once recorded onto a floppy disk, the data could be reduced and printed at any future time.

4.2 Test Procedure

Sample preparation-

1. Mix weighed amounts of soil and water.

2. Place two rubber membranes on the base pedestal and secure with rubber O-rings. A thin film of silicone grease on the pedestal provides a water tight seal.
3. Place molding jacket on the pedestal. Lift rubber membranes up through the jacket and pull up and over jacket.
4. Place soil into the rubber lined jacket in five lifts, each compacted to roughly the same degree.
5. Place top cap on specimen. Lift rubber membranes up and over top cap. Secure the membranes to the top cap with rubber O-rings.
6. Measure the height and diameter of sample.

Preparation for Consolidation/Equilibrium-

1. Place cell jacket on base.
2. Connect the air supply valve (on cell cover) to the top cap.
3. Secure cell jacket to base.
4. Push piston down onto the sample and secure.
5. Fill cell with properly de-aired water.
6. Flush the entire system, including transducers.
7. Start up data acquisition system.
8. Zero out transducers.
9. Bring pressures up in small intervals.
10. Do not apply more suction (Ua-Uw) than the maximum potential of the soil.

11. Monitor changes in samples volume and moisture content (reading burettes).
12. Make sure the water in the sample is in equilibrium (no flow in or out of sample) before proceeding ahead with the shearing.

Shearing Process-

1. Place triaxial cell under deviator/load cell. Release piston such that it lifts off of the sample by approximately 1/4 inch.
2. Place strain gauge in an appropriate position.
3. Set the deformation rate.
4. Start the deviator movement.
5. Zero out the load cell while piston is in travel, but not yet back onto sample.
6. Just as a non-zero deviator reading is noted on the monitor, zero out strain gauge.
7. Set computer to take readings at desired intervals.
8. Close pore water pressure valve (and pore air if desired).
9. Take burette readings for sample volume change.
10. At the conclusion of the test it is important not to release the cell pressure before the pore pressures. If both the cell and pore air pressures are released before the pore water, cracking of the ceramic disk is probable.

4.3 Conclusions

One of the major objectives of the research project was to evaluate the unsaturated soils testing apparatus and procedures developed by Hanna and Jeyapalan (1986). The criteria for evaluation is as follows:

1. In general, the degree of saturation is dependent upon the applied matrix suction (Ua-Uw) only up to some critical value. After which, the degree of saturation should remain at its initial conditions.
2. The shear strength will in general increase with an increase in applied matrix suction only up to some critical value. After which, the applied matrix suction will have no continued effect on the shear strength.
3. Soil suction should decrease the dilatancy potential of the soil.
4. As the specimen changes volume, so should the matrix suction potential.
5. The measurement of pore water pressures are both representative and an accurate account of true pore water pressures.

Three triaxial tests on a silty soil were performed in order to generate data by which an evaluation could be performed. The silt was choosen for two reasons.

1. There is clear evidence that silt has a significant change in its stress-strain behavior when it becomes

unsaturated, compared to being saturated.

2. Several key investigators have used silt in their test program from which, data can be compared.

The three soil specimens were compacted to a void ratio of 0.59 and a saturation level of 60%. The length to diameter ratio was approximately 2.0. Each specimen was tested at a constant confining pressure minus pore air pressure (σ_3 -ua) of 10 psi.

The results of the triaxial tests are shown in Fig. 8. Note how the saturation increased when the applied matrix suction was either 0 or 2.5 psi. This is due to capillary rise in the soil specimen. When the applied matrix suction was 10 psi, the level of saturation decreased, which is indirectly a consequence of the axis translation technique employed. During the axis translation technique, the confining pressure and the pore air and water pressures are simultaneously increased by an equal amount. The soil structure feels the increase in confining pressure immediately, but the pore air pressure requires air flow into the specimen in order to achieve the desired pore air pressure. The air flow takes with it water that is in the upper portion of the specimen and drives it toward the bottom. The amount of water in the specimen and the rate of pore air pressure application are the controlling factors. If the pore air pressure can be brought up to the desired level very slowly and the saturation is not exceedingly high, than the movement of water should be a minimum. This effect is clearly illustrated by the fact that the saturation level of specimen 1,a dropped in saturation from 60% to 3b%. Water at the bottom

of the specimen is flushed out through the ceramic disk, providing the applied matrix suction is great enough to counteract the capillary rise within the specimen. The time for achieving the equilibrium saturation level was quite high, due to the small gradient and low permeability of the ceramic disk. The specimens were considered to be in equilibrium when there was no recorded flow of water into or out of the specimens during a 24 hour period.

Figure 8.a clearly illustrates how the shear strength increases with a decrease in saturation. This is evidence to the fact that as the water menicus becomes smaller, the pressure within the menicus drops. Specimen 1.b, whose saturation level was 70%, was comparable in strength to the fully saturated specimen (1.c), more so than the 35% saturated specimen (1.a). Specimen 1.b probably has both a dispersed water distribution and capillary rise. The water pressure in a column of water (capillary rise) is not of the same magnitude as a single water menicus between soil particles. In fact, the water pressure in a column of water within a specimen is distributed from a maximum negative pressure at the bottom of the specimen, to atmospheric pressure at the top of the column. However, due to the axis translation technique, the water pressures are always positive with the lowest positive water pressure at the bottom of the specimen. Thus, the matrix suction changes within the height of the specimen (if capillary rise is present). It is important to note that capillary rise within a specimen may not be uniform, owing to the fact that pore spaces within a soil specimen may not be uniform.

One of the criteria for evaluation of the apparatus and procedures was that the shear strength not increase after some critical applied suction for a given initial saturation. This critical value is the point where capillary rise is negated. To fully verify this criteria, at least one more test at an applied suction greater than 10 psi should have been performed. But even still, with specimen 1.a changing its saturation level due to the axis translation technique, an additional test would have been in all likelihood inconclusive. Reiterating the conclusion that the axis translation technique must be applied simultaneously and in small incremental pressure changes.

The lower the saturation the higher the average matrix suction within the specimen. The higher matrix suction should result in less dilantancy potential during the shearing process. The small water menisci act like blobs of glue, holding the specimen together. Figure 8.b does verify this tendency. The lower saturated specimen seems capable of holding off on dialation longer (higher axial strains).

As the soil structure changes so should the matrix suction, provided the specimen is initially at equilibrium. Figure 8.c does show changes in matrix suction as a function of axial strain. However, the values appear to be unreliable. For instance, specimen 1.a was equalized at an applied matrix suction of 10 psi, yet when the pore water pressure supply was closed off, the pore water pressure began to increase immediately. When the applied matrix suction is past the critical point it will not be representative of the true

matrix suction for a specimen that has a completely dispersed soil water distribution. Therefore, by closing off the water pressure supply, the measuring device will tend to measure the water pressure of the menisci, which should result in the true matrix suction. However, there are further complications due to the fact that the shape of the menisci at the interface between the specimen and the ceramic stone may not be representative of the entire sample. In addition the moisture content near the bottom was found to be higher than that at the top of the specimen (probably due to the axis translation technique). This results in a larger water menisci near the bottom as opposed to the top of the specimen.

When the specimen compresses, the grains become closer together which results in a larger radius water menicus (pre-existing menicus). This results in an increase in water pressure (positive change). This phenomenon can be seen in Fig. 8 (i.e. suction drops during the compressive stage). However, in the case where there is capillary rise, a decrease in the void ratio should result in an increase in matrix suction. This could not be checked from the single specimen (1.b) for which there was capillary rise as a result of a small applied matrix suction. The reason being, there was no volume decrease for that specimen during shear.

It is worth noting that after the onset of dilation the matrix suction remained fairly constant. This was probably because the

dilation was occuring predominately in the middle of the specimen, due to end restraints.

Overall, the apparatus and procedures provide an excellent means of obtaining qualitative data in regards to both shear strength and volume change characteristics as a function soil structure and saturation level. However, the accuracy of the matrix suction data is under scrutiny.

In order to quantify the stress-strain behavior, the principal effective stresses are required. Bishop (1959) has outlined a method for determining the effective stresses in an unsaturated soil. However, the technique is still under scrutiny. The technique requires an accurate account of the matrix suction, which is difficult to obtain with the present apparatus and procedures.

V. PRESENTATION AND DISCUSSION OF RESULTS

5.1 General

The second objective of this research study was to investigate the stress-strain behavior of an unsaturated fine sand. The following studies were made:

1. Capillary rise and its effects on stress-strain behavior.
2. Magnitudes of the pore water pressures in the unsaturated sand.
3. The influence of negative pore water pressure with respect to strength and volumetric strain.
4. The stress-strain behavior of the sand in a near saturated state, under undrained loading conditions.
5. The shear strength as a function of saturation level and void ratio (undrained).
6. The initial tangent modulus as a function of saturation and void ratio (undrained).
7. Strain rate effects with respect to the shear strength and initial tangent modulus.

5.2 Capillary Rise

The magnitude of the soil suction potential is directly related to the grain size, shape and composition. In a cohesionless soil the

main factors reduce to grain size and shape. The following are the grain characteristics for the fine sand used in the testing program.

Shape - Sub-angular

10% finer (D_{10}) = 0.15 mm

50% finer (D_{50}) = 0.17 mm

Uniformity Coeff. (C_u) = 1.13

Effective Pore Dia. ($0.2*D_{10}$) = 0.03 mm

The above values clearly illustrate that the sand grains are fine and uniform in size.

The ability for the soil to increase or decrease in saturation as a function of applied matrix suction and density is shown in Fig. 9, (commonly referred to as characteristic curves). Each of the two samples were compacted on the base pedestal at a saturation level of 50%. The confining pressure during the generation of the curves was 90 psi, with the pore air pressure held constant as 80 psi, and an initial applied matrix suction of 10 psi (pore water 70 psi). Incremental changes in pore water pressure would result in changes in matrix suction. Each incremental change was induced only after equilibrium was achieved from the previous incremental change.

The shape of the characteristic curves is also dependent on whether the sample is in a wetting or drying cycle. In a wetting cycle, (drawing water into the sample) a sudden increase in the pore space diameter could reduce any further capillary rise.

Likewise, in a drying cycle the smaller pore diameter spaces in a continuous pore would control the level of saturation. The more uniform the grains the higher the likelihood that the difference between the two cycles would be insignificant. The procedure used for the generation of the characteristic curves for the fine sand was one of a wetting cycle.

A threshold value is clearly evident in both the dense and loose samples. That is, no capillary rise can develop before some clearly defined matrix suction develops. Any higher applied matrix suction would result in no further de-saturation of the sample. As expected the dense sample has a larger threshold suction (0.65 psi) than the loose sample (0.35 psi), simply because of the smaller effective pore diameter. These values appear to be in line with the estimated value of 1.4 psi obtained by assuming the effective pore diameter of 0.200^{10} and this could be explained using a capillary tube analogy.

The maximum negative pore water pressure in the field would be approximately 0.65 psi (e=0.60). The pressure within the capillary rise would be distributed in a linear fashion from -0.65 psi to atmospheric pressure, over the length of 1.5 feet. The values obtained from this study seem to be smaller that expected. This can however be attributed to the uniformity of the grain size. In view of the relatively small capillary rise it would be reasonable to assume that the negative pore pressures would be relatively

ant in terms of practicality. Therefore, capillary rise will not be condidered any further in this study. Instead, the emphasis will shift to the negative pore water pressures maintained in individual water meniscus between soil grains, in a completely dispersed soil water distribution.

5.3 Effects of a Dispersed Water Distribution

The pressure within an individual water meniscus for a completely dispersed water distribution is directly related to the size and shape of the water meniscus. A higher saturation level tends to increase the radius of the water meniscus. The negative water pressures (water in tension) in the water meniscus causes intergranular stresses, which increases the effective stress. The degree by which this mechanism effects the fine sand is studied in this section.

Two triaxial tests were performed, one on a saturated sample and the other on an unsaturated sample (Sr=60%), with an applied matrix suction of 5 psi. The 5 psi of applied matrix suction was choosen because such a value would not allow capillary rise. The special ceramic disk allowed measurement of the pore water pressures. However, as mentioned in a previous section the values may not be representative of the actual pore water pressure in the menisci distributed throughout the sample.

Observation of Fig. 10.a indicates that the effects of the water menisci are relatively unimportant (with regards to shear

strength) for a sample whose saturation level is 60%, void ratio of 0.60, and effective confining pressure of 10 psi. The shear strength was expected to increase for the unsaturated sample. Apparently the grain size is such that a 60% saturated sample forms relatively large water menisci (radius), and/or the intergranular forces created by such a mechanism act over a very small area in relation to the area of the sample.

The triaxial tests were performed at a constant strain rate of 0.095% per minute. The slow strain rate allows the change in water pressure to stabilize before additional sample deformation causes additional changes in pore water pressure. It should be noted that the negative pressure in conjunction with surface tension effects tend to make the water more viscous as opposed to free water.

The variation of matrix suction with axial strain curve, in Fig. 10.b, shows that the matrix suction decreases during the early stages of the test, and then levels off to a fairly constant value. During the early stages of the test the sample compresses. As the soil grains come closer together a given amount of water in the meniscus tends to increase the radius of the water meniscus. This increase in radius causes the water pressure to increase (positive direction). The limiting value would be the ambient air pressure (matrix suction equals zero). As the test progresses, the sample starts to dilate until some point showing a positive dilation. One would expect the pore water pressure to decrease at this stage, (due to grains

moving apart). This trend is evident only slightly in Fig. 10.b. The reason for such a slight observation is probably due to the end restraints, which tend to constrain the sample from dilating at the ends.

The graph of variation of volumetric strain with axial strain is shown in Fig. 10.c. There does not appear to be any significant difference between the two samples with regards to volumetric change. On one hand, this is expected, since the shear strengths were similar for the samples. But on the other hand, an unsaturated specimen should exhibit more compression and hold off dilation longer, due to the intergranular stresses. It seems reasonable to assume that the intergranular forces involved in this unsaturated sample are negligible.

Certainly, two triaxial tests cannot be considered as conclusive evidence to support a theory that the unsaturated sand behaves similar to the saturated sand under drained conditions. Therefore, several additional triaxial tests were performed, but without pore water pressure measurements. The water menisci in an unsaturated granular soil will hold the soil sample together under unconfined conditions, resulting in a small unconfined compressive strength. This strength should be apparent in the form of a cohesion intercept on the Mohr's circle diagram. Triaxial tests were performed at varying confining pressures, void ratios of 0.60 and 0.80, and a saturation of 70%. The results are given in Fig. 11. There is a definite cohesion intercept for both void ratios, (figures 11.a and 11.b).

The intercept can be taken to be approximately 5 psi.

Several saturated tests at a void ratio of 0.80 were performed. The Mohr circle diagram of these tests is shown in Fig. 11.c. These tests also indicate a cohesion intercept, roughly 3 psi. It is not uncommon for a sand sample in a triaxial test to show a small intercept. This small intercept is usually attributed to the rubber membrane (1-2 psi). Two rubber membranes were used on each sample throughout the testing program. Therefore, it is reasonable to expect an intercept of 3 psi. Consequently, the cohesion intercept for the unsaturated tests also includes the effects of the rubber membranes. Thus, the 5 psi intercept in reality may be closer to 2 psi. Note in Fig. 11.b and 11.c that both the unsaturated and saturated samples have the same friction angle with only the magnitude of the intercept being different. Despite the increase in the cohesion intercept for the unsaturated sample, its relative importance can still be considered insignificant. Therefore, it is suggested that in a drained condition this fine sand will behave (with regards to stress-strain) similar in both a saturated and unsaturated state. Probably, the only way to develop clear trends with regard to the differences in stress-strain behavior of the unsaturated (as opposed to a saturated) sample would be to perform a very large number of tests in order to establish statistical trends. However, considering the obviously small contributions to the effective stress generated by the water menisci, as well as equipment limitations, thorough analysis would not be practical.

5.4 Undrained Saturated Triaxial Tests

A series of undrained triaxial tests were performed on saturated samples. Upon completion of these tests it was apparent that most of the samples were at a saturation significantly below 100%. "Significantly" is a relative term and in this case a saturation level of 98% can be considered significant. In reality, a 100% saturated sample is impossible to achieve due to the dissolved air in the water. Increasing the back pressure on a sample has the effect of increasing Skempton's B parameter (B=the change in pore pressure divided by the change in confining pressure). As Skempton's B parameter increases, the combined fluids (water and air) decrease in compressibility. A perfectly incompressible fluid will have a B-value of 1.0. Normally a B-value between 0.96 and 0.99 is considered very good. Rarely will a B-value be higher than 0.99.

The test samples were compacted on the triaxial pedestal to a void ratio of 0.60. An initial confining pressure of 10 psi was applied to the samples. After applying the confining pressure, a continuous amount of de-aired water was flushed through the sample. It should be noted that the system was completely de-aired before use.

Even with the thorough flushing with de-aired water, a B-value was virtually nonexistent at zero back pressures. Subsequently, the samples were back pressured to 80 psi, in 10 psi increments. This resulted in a B-value of 0.85-0.92 for all the samples. Sand is a difficult soil to obtain a good B-value because of the high porosity.

Water in the sand can literally surround small pockets of air. The water at the air/water interface is influenced by surface tension, resulting in the difficulty with flushing air pockets out of the sample.

The stress-strain curves for the test series are shown in Fig. 12. The results were plotted for high, mid and low range values of shear strength. Most striking is the difference in magnitudes of the shear strength and tangent modulus between the high and low ranges. The low range values are roughly 40% lower in shear strength compared to the high range values. This is a significant difference considering that all the tests were performed on samples with the same density and confining pressure.

The reason for such differences in strength can be found in Fig. 13. Here the pore pressures were plotted for each range of shear strength values. It is apparent that the drop in pore pressures was much greater for the high range values. A drop in pore pressure has the effect of increasing the effective confining pressure.

The samples tested tended to show a positive volumetric change (dialation) at relatively low axial strains, with little or no compression prior to dialation. The variation of volumetric strains with axial strain is given in Fig. 14. Again, the graphs are organized in the high, mid and low range values of shear strength. It appears from the results that all the samples behaved the same in regards to volume change.

It would seem reasonable to assume that the differences in shear strength between samples could be attributed to differences in initial saturation levels. Note that the differences in B-value (0.85-0.92) indicate differences in fluid and soil compressibility.

Theorectical values of initial saturation levels can be calculated by using equation [4]. Two theoretical calculations were made, one using a high range value, and the other using a low range value. The data is given as follows:

High Range Test	Low Range Test
V total=4.40 cu. in.	V total=4.50 cu. in.
V soil=2.73 cu. in.	V soil=2.82 cu. in.
V voids=1.67 cu. in.	V voids=1.68 cu. in.
Initial Absolute Pore Pressure equals 94.72 psi @ ε_v=1.08%	Initial Absolute Pore Pressure equals 94.72 psi @ ε_v=1.07%
Absolute Pore Pressure Equals 34.72 psi	Absolute Pore Pressure Equals 52.72 psi
thus V water=1.674 cu. in. Sr=100%	thus V water=1.650 cu. in. Sr=98%

The previous calculations indicate that the high range shear strength test had an initial saturation of 100%. This of course is theoretically impossible, plus the corresponding pore pressure change curve does not suggest such a saturation level. However, it

should be realized that the measured values of Vv, Vt, Vs are not absolute. In addition, equation [4] was derived for a state of compression. Nevertheless, such a calculation does provide the evidence that the two samples had different initial saturation levels (100% vs. 98%), with the higher saturation corresponding to the higher shear strength. It should be noted that even the high shear strength tests were able to achieve only a slight negative pore pressure (back pressure equals 80 psi). It also illustrates that even a very small amount of air in the sample does play a major role in the stress-strain behavior of this soil.

5.5 Pore Pressure Response of Ceramic Stone

In the previous section the saturated (or near saturated) tests were performed using a coarse corundum stone in the base pedestal. The permeability of such a stone is compatible with the permeability of the fine sand. In unsaturated testing a fine ceramic stone is normally used to transmit the pore pressures to the measuring device. The function of such a disk is to allow measurement of pore water pressures independent of the pore air. This type of stone was used in the unsaturated tests discussed thus far.

Four saturated triaxial tests were performed with the same parameters as that of the previous test series. The tests used a ceramic stone in the base pedestal as opposed to the corundum stone. Changes in pore pressure vs. axial strain curves are compared to similar tests performed with the corundum stone. By "similar" it

is meant that the stress-strain behavior closely resemble each other. Fig. 15 and 16 illustrate these comparisons. These curves clearly indicate that the pore pressure response of the ceramic stone is inadequate for moderate strain rates.

Additional tests were conducted on the ceramic stone response time. These tests consisted of increasing the confining pressure in the triaxial cell without a soil sample. The response of the measuring system gives an indication of the efficiency of the ceramic stone with regards to pore pressure measurement. These results are shown in Fig. 17. Again, it is evident that a considerable time lag is involved with usage of the ceramic stone.

5.6 Undrained Unsaturated Test Results

An extensive series of undrained tests were performed on samples of the test sand. The pore water and pore air pressures were not measured independently. The following parameters were varied during the test series:

1. Saturation Level (Sr)
2. Void Ratio (e)
3. Effective Confining Pressure (Po)
4. Back Pressure (Po)
5. Strain Rates (.)

A complete graphical representation of each test is given in the appendix (Deviator Stress, Pore Pressure, Volumetric Strain vs. Axial Strain).

In regards to the saturation level, the first item to be investigated was the shear strength. For this purpose, tests were performed on dense and loose samples (e of 0.60 and 0.80) at saturation levels of 25, 95, and 100%. Fig. 18 illustrates how the undrained shear strength was affected by the saturation level. For the dense samples, the shear strength increased rapidly as full saturation was approached. Such behavior is expected due to the dilation characteristics of the denser samples. It is a theoretical fact that large negative fluid pressures will develop if there is an increase in volume in conjunction with an incompressible fluid. However, as pointed out earlier, the pore fluid is not truely incompressible. Consequently, the pore pressures dropped to only a small negative pressure from a back pressure of either 10 or 20 psi. Still such a pore pressure drop greatly influenced the strength of the samples whose initial confining pressures were of the same magnitudes as the pore pressure drop. It is noted in Fig. 18 that the initial effective confining pressures (20 and 10 psi) for the denser samples had no relative effect on the total shear strength. This was because the confining pressure was held constant at 30 psi with the pore pressures dropping to zero in both cases, (the back pressures were initially 10 and 20 psi respectively). It is quite evident from Fig. 18 that a slight introduction of air will dramatically affect the shear strength of the denser samples. The saturation level effects are less pronounced between the 95% and 25% saturated samples. The slight drop in strength between the 95% and 25% levels

are thought to be attributed mostly to the differences between the volumes of air in the samples, with the water menisci effects (in 25% sample) playing a limited role. No water was allowed to flow into or out of the samples before or during the tests.

The loose samples (e of 0.80) showed an entirely different relationship with saturation level, as in Fig. 18. The shear strength was virtually equal at the 100% and 25% levels. Such behavior can be attributed to the volumetric strain characteristics of the loose sample (see appendix). In the loose state the fine sand shows little volumetric strain. As a consequence the pore pressures will remain fairly constant (initial back pressure) throughout the test. Further evidence for the theory that this soil possesses a very limited effective stress increase (in an unsaturated state), is illustrated by the fact that the 100% and 25% samples (e of 0.80) have the same shear strength.

The effects of saturation level on the initial tangent modulus was also investigated. The results of such a study are shown in Fig. 19. Overall, the initial tangent modulus decreased as the saturation level increased. During the initial stages of the triaxial test, both the loose and dense samples compress slightly. Such compression results in slight increases in pore pressures. As the pore fluid approaches water saturation, the pore pressure increases become larger for a given volumetric decrease. A rise in the pore pressure will reduce the effective stress, which results in a weaker soil structure.

Fig. 20 and 21 illustrate that the behavior of the test sand at a saturation level of 25% is independent of the applied back pressure (as long as the effective confining pressure is held constant). In addition, the figures also show that an undrained test has the same stress-strain behavior as a constant water content (drained) test. Such behavior can be attributed to the large volumes of air in the samples.

To date, there has been little experimental data generated on the effects of strain rate for an unsaturated sand. Undrained tests were performed at various strain rates as part of the test series. The saturation level was held at a constant value of 25% and the void ratio of the samples were chosen to be either 0.60 or 0.80. The saturation value was chosen at 25% because it was thought that this small level would induce high negative pressures within the water menisci. High negative pressures and surface tension are thought to make the water have a higher viscosity.

The results indicate that there is no relationship between the shear strength and the strain rate, as Fig. 22. It is concluded that either the effects of the water meniscus operate over an area is too small to be a factor, or the water menisci do not act in a viscous manner. The higher strain rates seem to induce higher dilation potential, as evidenced by the volumetric strain vs. axial strain curves (appendix). As the particles move apart, a given water meniscus should have a decrease in its radius. Such a decrease in radius would cause higher negative pressures within the menisci.

However, this effect does not appear to be a factor for the given sand under the test conditions. Again, showing further evidence that the menisci in this unsaturated soil play a limited role in its stress-strain behavior.

There appears to be a slight relationship between strain rate and initial modulus for a dense sample (e of 0.60), as shown in Fig. 23. The higher strain rate samples tend to dilate even during the initial stages of the test, unlike the slow rates when a small amount of compression took place. There appears to be no relationship between strain rate and initial tangent modulus for the loose samples, Fig. 23. The samples in this case also indicated higher dilation potential, but compression did take place during the early stages of the test.

The behavior of the soil with respect to strain rate is for the most part unclear. The fastest strain rate used in this test series was 8%/min. By laboratory standards, such a rate can be considered moderately fast. It is unknown whether or not these relationships described above can be extended to strain rates far greater than 8%/min.

VI. CONCLUSIONS AND RECOMMENDATIONS

The purpose of this research has been two fold. First, to investigate the usefulness of the unsaturated testing apparatus. Second, to investigate the behavior of an unsaturated sand. The general conclusions that can be drawn from this research are given below.

The test apparatus on the whole performed satisfactorily, with duplication of test samples showing good agreement in their results. The automated data aquisition system proved to be especially useful, with a capability of recording test data every 5-6 seconds.

The axis translation technique is useful in monitoring pore water pressure changes or describing capillarity, in unsaturated soils. This is especially true for unsaturated soils which exhibit pore water pressures below -1 atmosphere. It has been mentioned that care and patience is required when applying the axis translation technique.

There is a critical value for the applied matrix suction in which the tendency for water to be drawn into the soil structure is negated. At this point the water pressure within the menisci can be taken to equal the matrix suction minus the pore air pressure. A slight decrease in the matrix suction from this critical point will cause the sample to become saturated. This is because the water needs to climb only the height of the sample, which was typically 2.5 inches in height.

By using a special ceramic stone, the pore water pressures could be monitored independently from the pore air pressures. The stone used in the testing program had a permeability of 1.0×10^{-7} cm/sec. Such a low permeability results in time lag between measurements, especially at fast strain rates. In addition, there is some question on whether the use of the ceramic stone will yield representative water pressures for a dispersed water distribution.

Constant water tests were performed on both silt and the test sand. A constant water content test allows changes in pore water pressures, while holding the pore air constant. These tests illustrated the usefulness of the test apparatus and procedures. The silt showed large increases in shear strength in an unsaturated state. Contrary, the test sand showed little or no influence from the water menisci effects.

A series of undrained saturated tests illustrated the importance of even minute amounts of air in the sand. The tests indicated that it was difficult to achieve complete saturation of the fine sand.

A series of undrained, unsaturated tests were performed, from which the following conclusions can be made:

1. The stress-strain behavior changes little with respect to saturation level, until the level approaches saturation (95%).

2. The initial tangent modulus decreased with an increase in saturation.
3. For lower saturated samples (Sr=25%) there seems to be no difference between an undrained test and a drained test.
4. The dilation potential of the sand increases with strain rate.
5. The shear strength of the fine sand seems to be realatively unaffected by the different strain rates used in the testing program.
6. The initial tangent modulus increases slightly with strain rate for dense samples.
7. The strain rate has no clear effect on the initial tangent modulus for loose samples.

It was initially thought that the fine sand would exhibit definite trends with regards to saturation level, but the tests conducted in this study indicate that the fine sand does not possess significant increases in effective stresses, due to negative pore water pressures or surface tension forces. Such behavior is probably the result of the size and uniformity of the sand grains. In addition, sand grains do not possess the physio-chemical attractive forces that are present in cohesive soils.

The following are suggestions for future improvements in the test program:

1. Higher resolution of the samples' volume change device.
2. Use of a more permeable ceramic stone if possible, i.e. soils with low to moderate suction potential do not require an air entry of 80 psi, as used in this research.
3. De-air the water under a higher vaccum.

The apparatus and procedures that have been developed thus far are unique to soils testing. Continued research in this area will no doubt prove to be valuable in the future. It is recommended that future research with the above apparatus and procedures utilize a different soil type. Unsaturated soils testing is best suited for soils with a fine grain structure and/or physio-chemical attractive forces. However, the test program will take much more time and effort.

REFERENCES

Aitchison, G.D., 1960, "Relationship of Moisture Stress and Effective Stress Functions in Unsaturated Soil", Pore Pressure and Suction in Soils, Butterworths, London.

Bishop, A.W., 1959, "The Priciple of Effective Stress", Teknisk Ukeblad, Oslo.

Bishop, A.W., and Blight, G.E., 1963, "Some Aspects of Effective Stress in Saturated and Partly Saturated Soils", The Institute of Civil Engineers, London.

Bishop, A.W., and Donald, I.B., 1961, "The Experimental Study of Partly Saturated Soil in the Triaxial Apparatus", Proceedings of the Fifth International Conference of Soil Mechanics.

Blight, G.E., 1967, "Effective Stress Evaluation for Unsaturated Soils", Journal of the Soil Mechanics and Foundations Division, Proceedings of the American Society of Civil Engineers.

Burland, J.B., 1965, "Some Aspects of the Mechanical Behavior of Partly Saturated Soils", Moisture in Soils Beneath Covered Areas, Butterworths, London.

Burland, J.B., and Jennings, J.E.D., 1962, "Limitations to the use of Effective Stresses in Partly Saturated Soils.", Geotechnique, Volume 12, Number 2.

Casagrande, H., and Shannon, W.L., 1948, "Stress Deformation and Strength Characteristics of Soils under Dynamic Loads", Proc. 2nd ICSMFE, Volume 5.

Donald, I.B., 1963, "Effective Stress Paramenters in Unsaturated Soils", Proc. of the 4th Australian-New Zealand Conference on SM and FE.

Edil, T.B., Motan, S.E., and Toha, F.X., 1981, "Mechanical Behavior and Testing Methods of Unsaturated Soils", ASTM STP 740, American Society for Testing and Materials.

Gulhati, S.K., and Satija, B.S., 1979, "Strain Rate for Shearing Testing of Unsaturated Soil", Proceedings of the 6th Asian Regional Conference on SM and FE, Singapore.

Gulhati, S.K., and Satija, B.S., 1979, "Shear Strength of Partially Saturated Soils", Proceedings of the 6th Asian Regional Conference on SM and FE, Singapore.

Hamilton, L.W., 1939, "The Effects of Internal Hydrostatic Pressure on the Shearing Strength of Soils", Proceedings of the American Society for Testing and Materials, Volume 39.

Hanna, E.R., and Jeyapalan, J.K., 1986, "An Investigation of Behavior of Unsaturated Sands", Submitted to the Air Force Office of Scientific Research, Bolling Air Force Base.

Hilf, J.W., 1956, "An Investigation of Pore Water Pressure in Compacted Cohesive Soils", Technical Memorandum Number 654, Bureau of Reclamation, United States Department of Interior, Denver, CO.

Ho, D.Y.F., and Fredlund, D.G., 1982, "A Multistage Triaxial Test for Unsaturated Soils", Geotechnical Testing Journal, GTJODJ, Volume 5, Number 1/2.

Holtz, R.D., and Kovacs, W.D., 1981, "An Introduction to Geotechnical Engineering", Prentice-Hall, Inc., New Jersey.

Nash, K.L., and Dixon, R.K., 1960, "The Measurement of Pore Pressure in Sand Under Rapid Triaxial Test", Proc. Conference on Pore Pressure and Suction in Soils, Butterworths, London.

Richart, F.E., Jr., 1977, "Field and Laboratory Measurements of Dynamic Soil Properties", Proceedings of DMSR, Volume 1, Sept., 1977, Karlsruhe.

Richart, F.E., Jr., Wu, S., Gray, D.H., 1984, "Capillary Effects on Dynamic Modulus of Sand and Silts", Journal of Geotechnical Engineering, Volume 110, Number 9.

Seed, J.B., and Lundgren, R., 1954, "Investigation of the Effect of Transient Loading on the Strength and Deformation Characteristics of Saturated Sands", Proc. ASIM, Volume 54.

Sparks, A.D.W., 1963, "Theoretical Considerations of Stress Equations for Partly Saturated Soils", Proceedings of the Third Regional Conference for Africa on Soil Mechanics and Foundation Engineering, Southern Rhodesia.

Terzaghi, K., and Peck, R.B., 1948, "Soil Mechanics in Engineering Practice", 2nd Ed., John Wiley and Sons, Inc., New York.

Towner, G.D., and Childs, E.C., 1972, "The Mechanical Strength of Unsaturated Porous Granular Material", Journal of Soil Science, Volume 23, Number 4.

Whitman, R.V., 1954, "The Behavior of Soils Under Dynamic Loadings' Final Report on Laboratory Studies, Aug., Massachusetts Inst. of Technology, Dept. of Civil and Sanitary Engineering Soil Mechanics Lab.

FIGURES

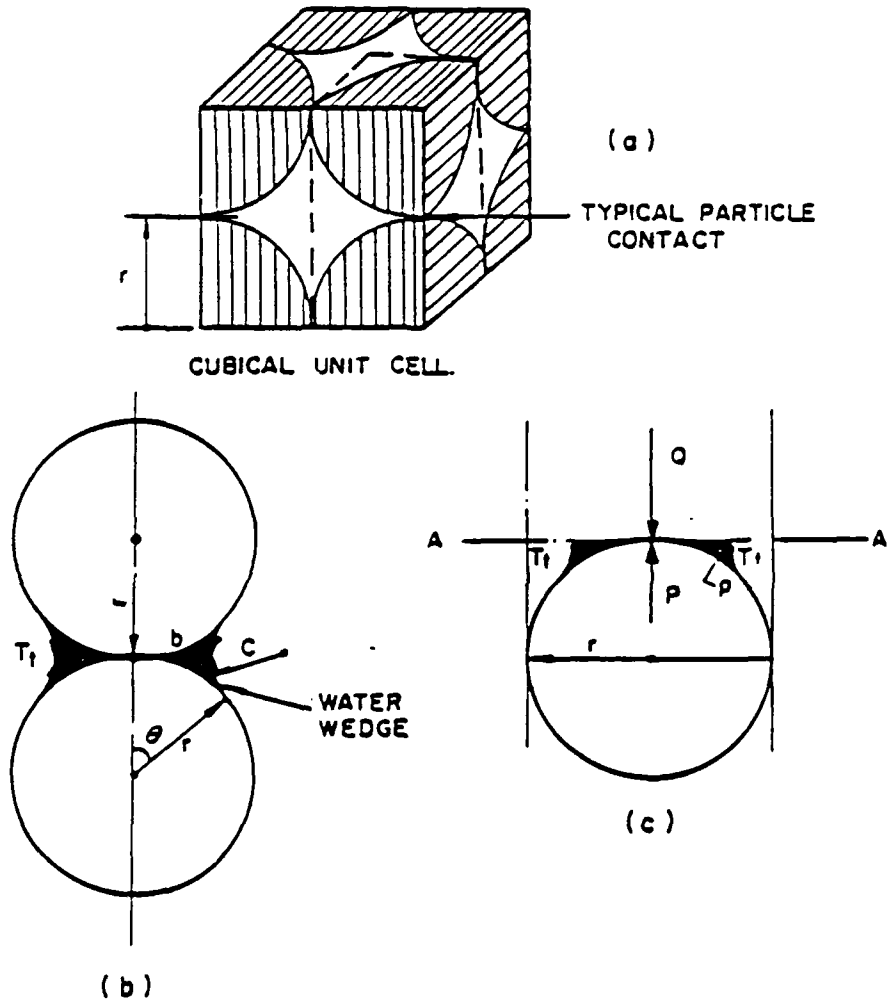

FIG. 1 TERMS USED IN ANALYSIS OF EFFECTIVE STRESSES IN IDEALIZED SOIL

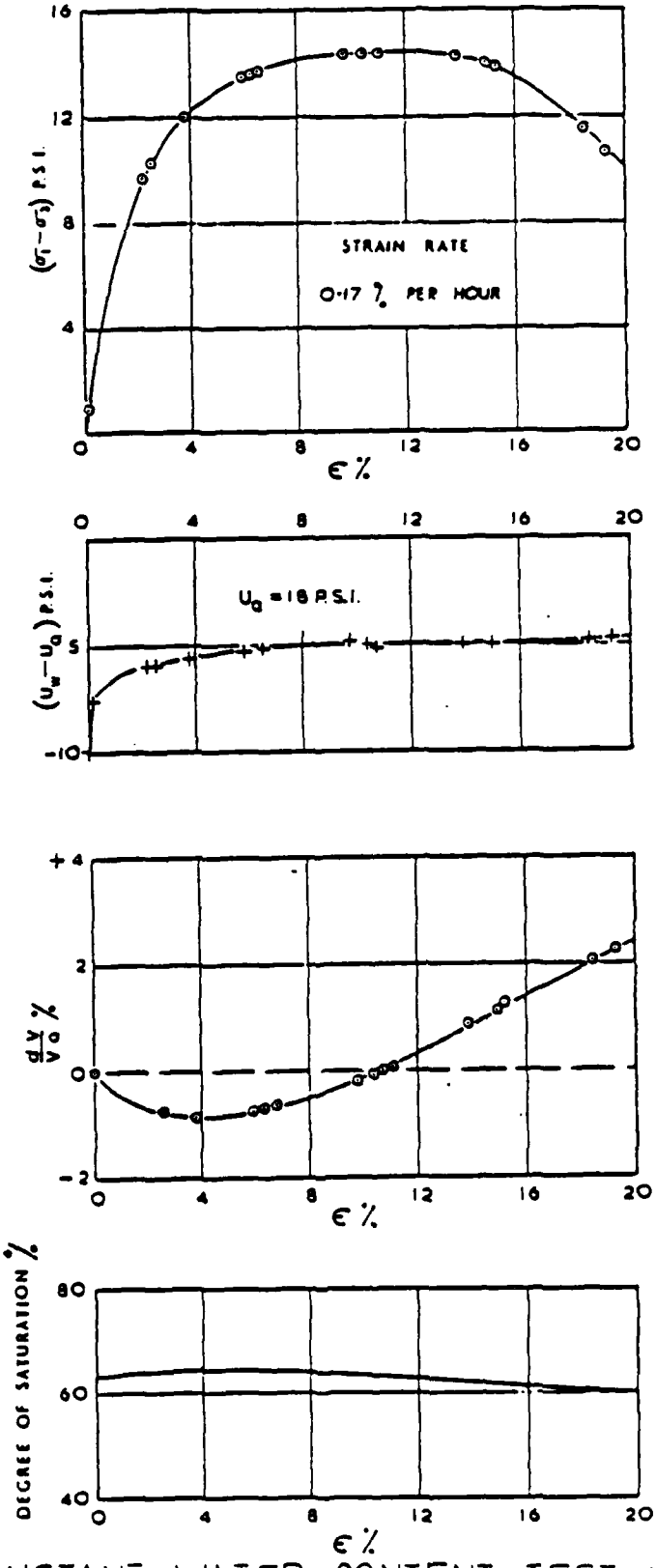

FIG. 2 CONSTANT WATER CONTENT TEST WITH CONTROLLED AIR PRESSURE ON PARTLY LOOSE SILT

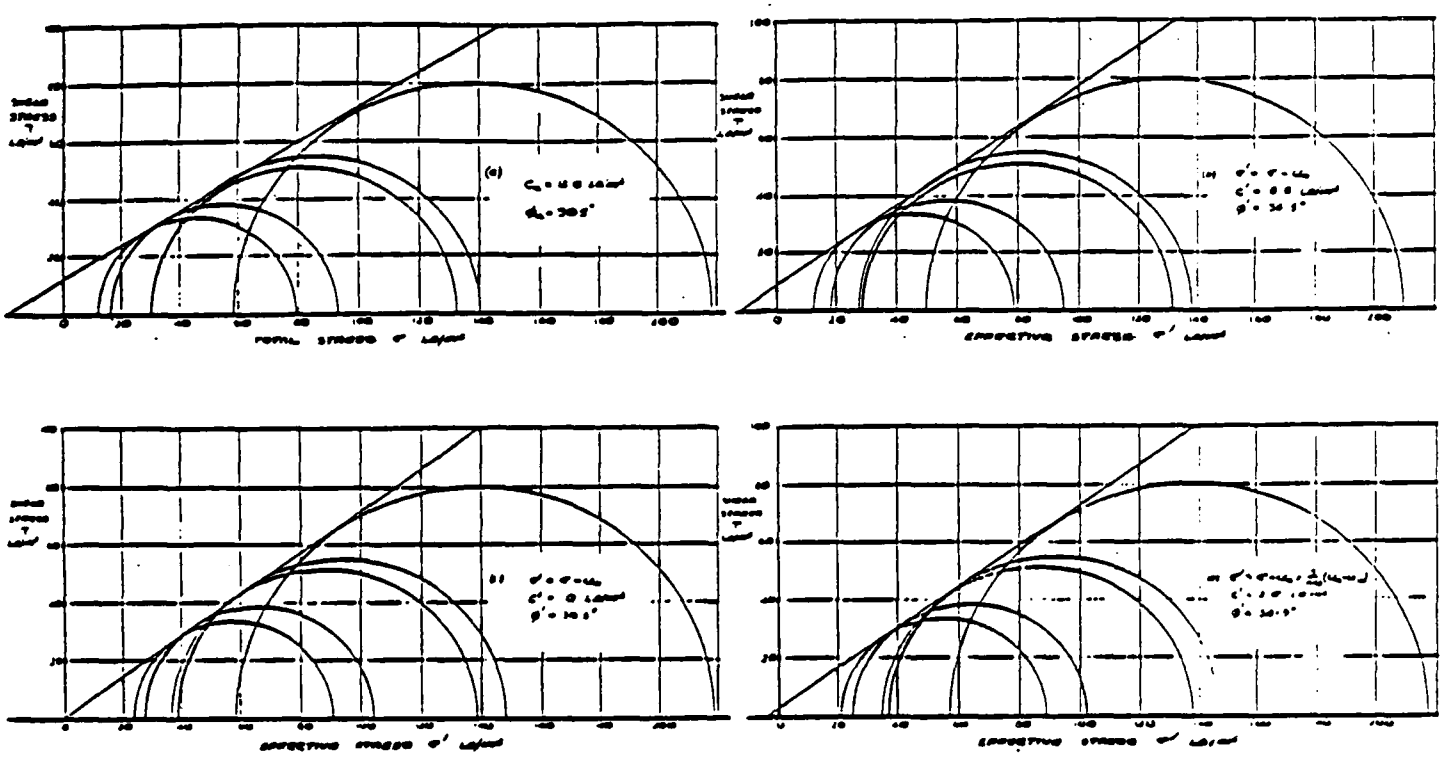

Abcissa	Apparent Cohesion	Apparent Angle of shearing Resistance
σ	c_a = 12.0 lb./in.^{2}	ϕ_a = 30.5°
$\sigma' = (\sigma - u_a)$	c' = 8.8 lb./in.^{2}	ϕ' = 34.5°
$\sigma' = (\sigma - u_w)$	c' = 0 lb./in.^{2}	ϕ' = 36.3°
$\sigma' = (\sigma - u_a) + \frac{S}{100} \times (u_a - u_w)$	c' = 2.8 lb./in.^{2}	ϕ' = 34.9°

FIG. 3 COMPARATIVE FAILURE ENVELOPES FOR PARIALLY SATURATED BOULDER CLAY

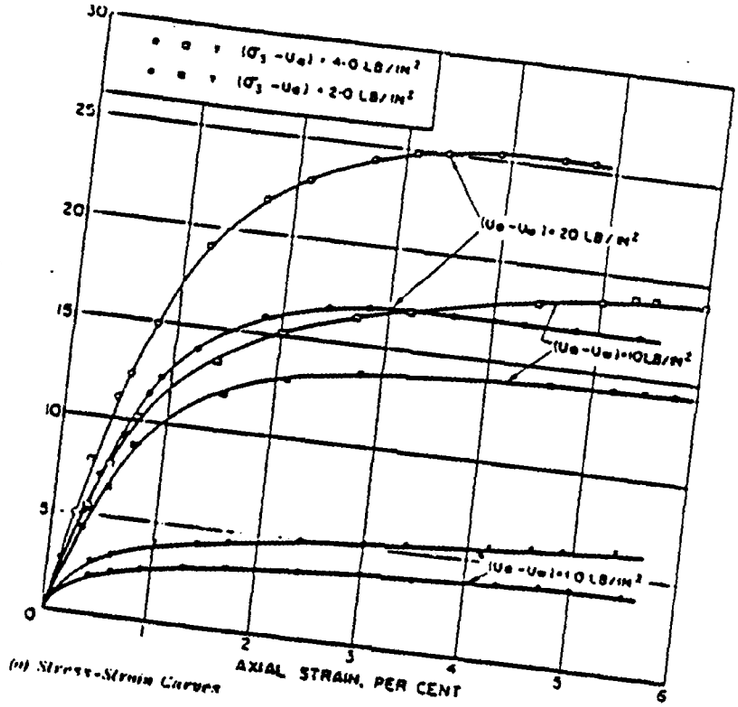

(a) Stress-Strain Curves

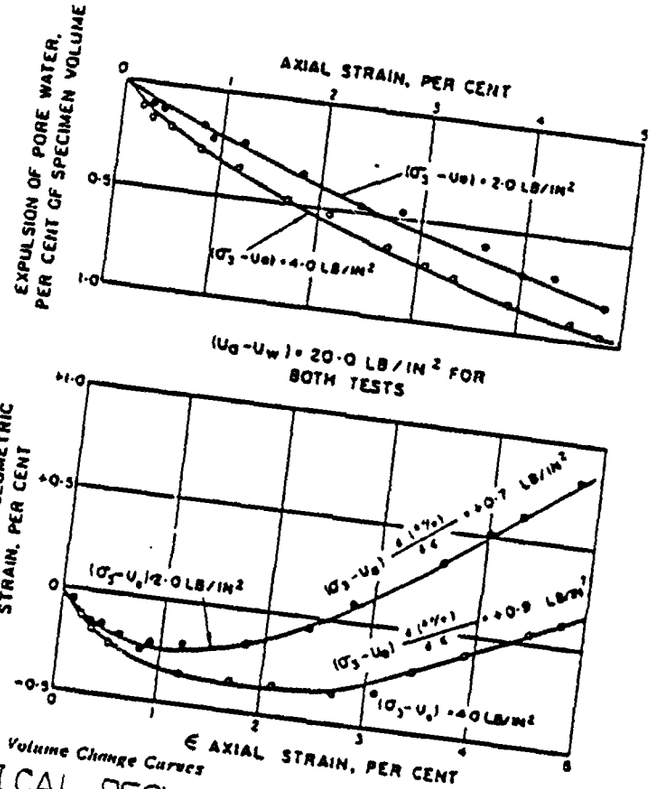

(b) Volume Change Curves

FIG. 4 TYPICAL RESULTS OF PAIRED TRIAXIAL TESTS ON UNSATURATED SILT

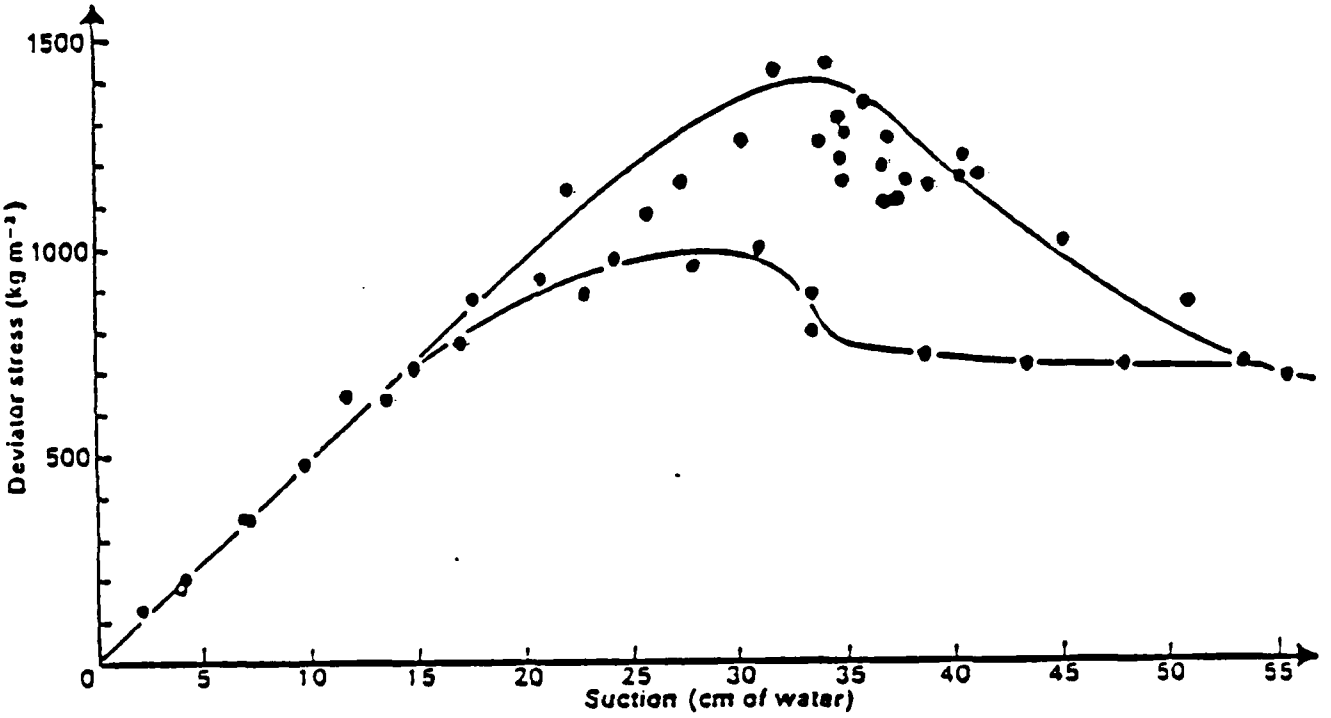

FIG.5 DEVIATOR STRESS AT FAILURE IN UNCONFINED COMPRESSION TESTS ON BRANCASTER BEACH SAND AS A FUNCTION OF SUCTION, FOR DRYING AND WETTING PROCESSES

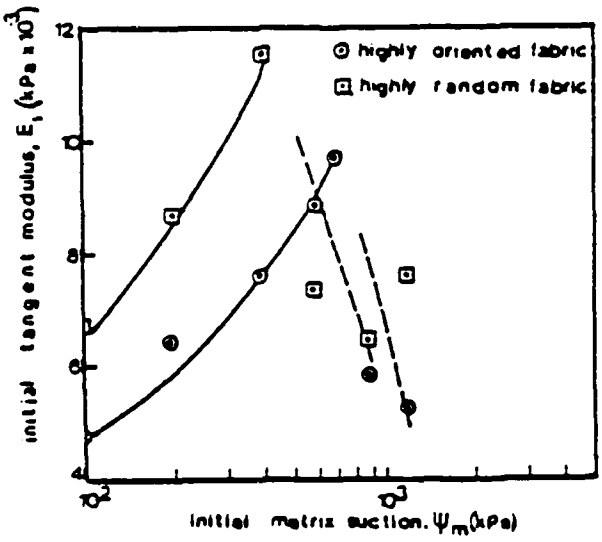

a) modulus as a function of initial matrix suction

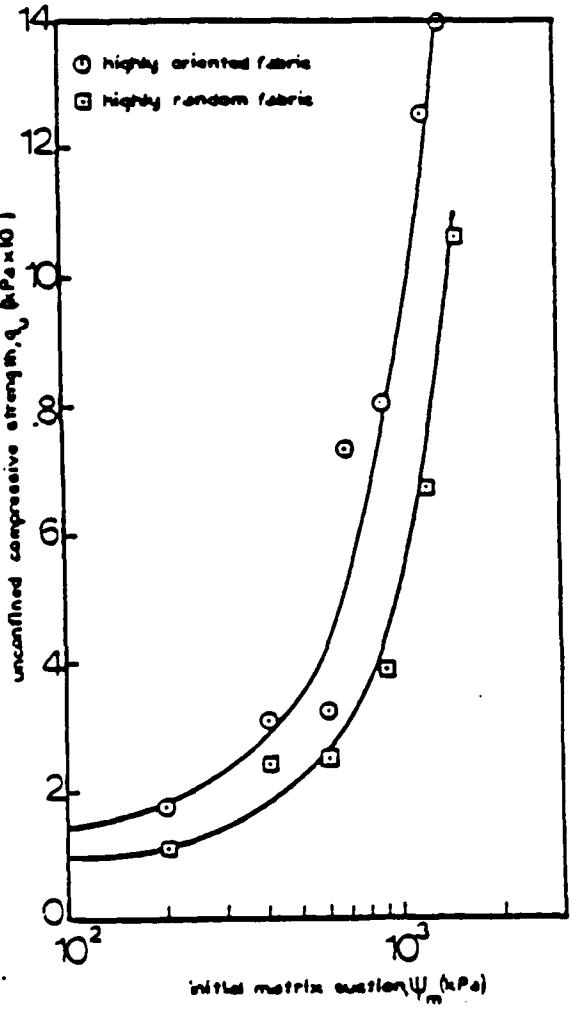

b) unconfined compressive strength as a function of initial matrix suction

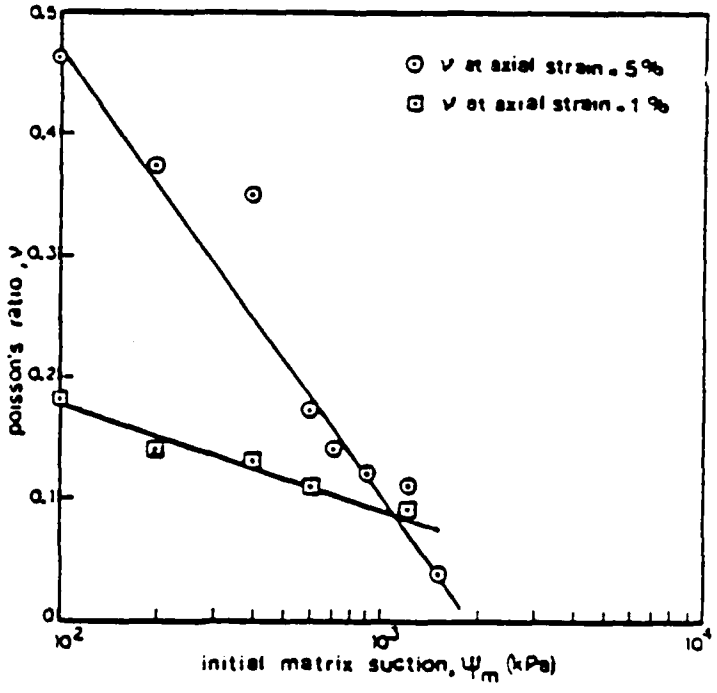

c) poisson's ratio as a function of initial matrix suction

FIG. 6 TEST RESULTS FROM AN UNSATURATED CLAY

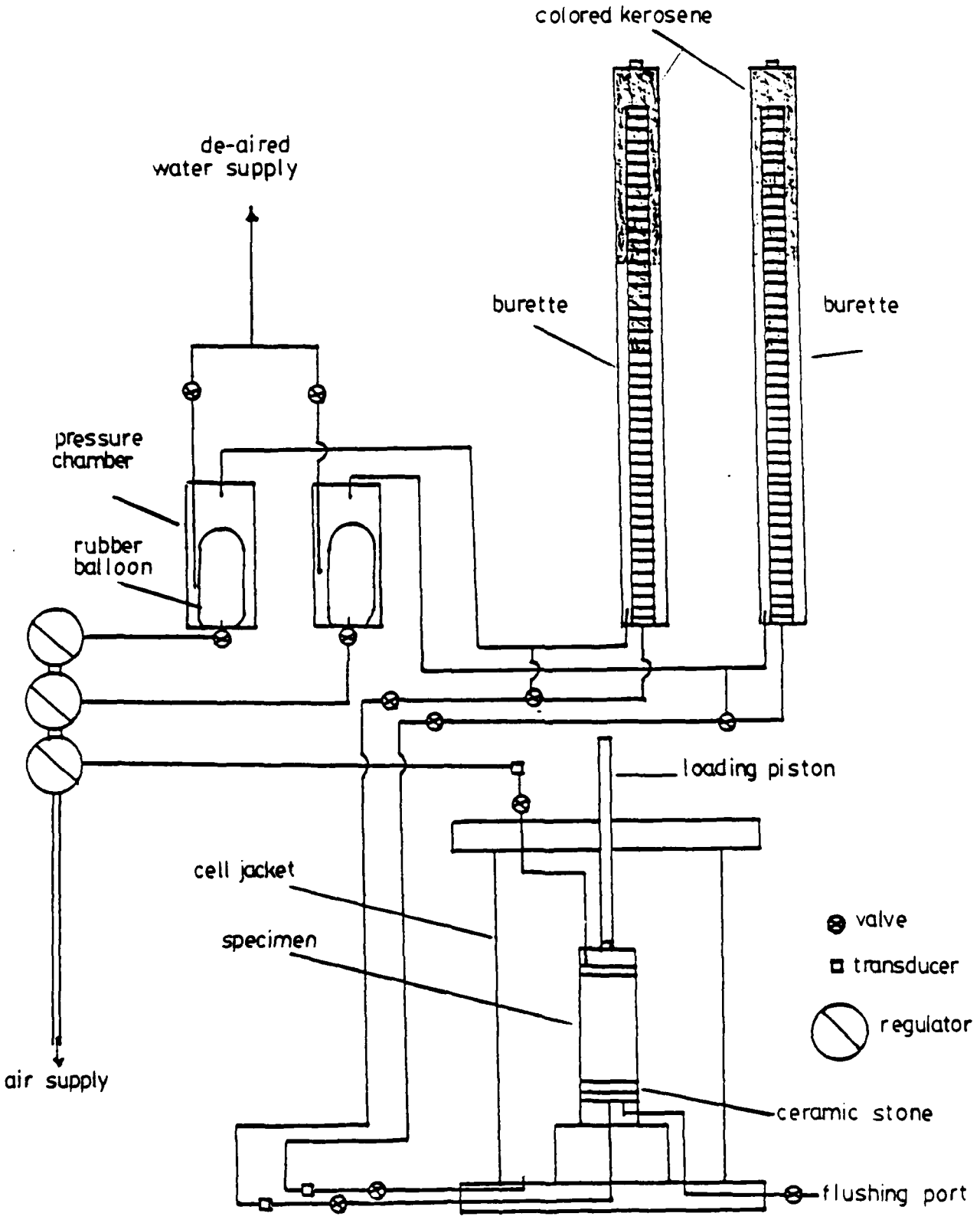

FIG.7 DIAGRAM OF TRIAXIAL SET-UP

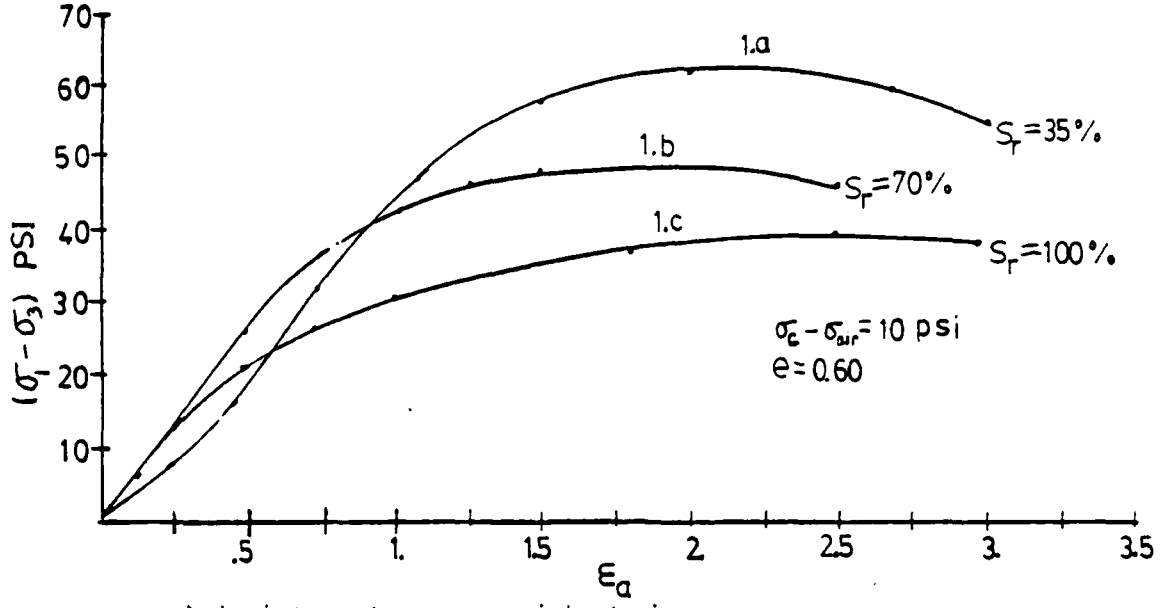

a) deviator stress vs. axial strain

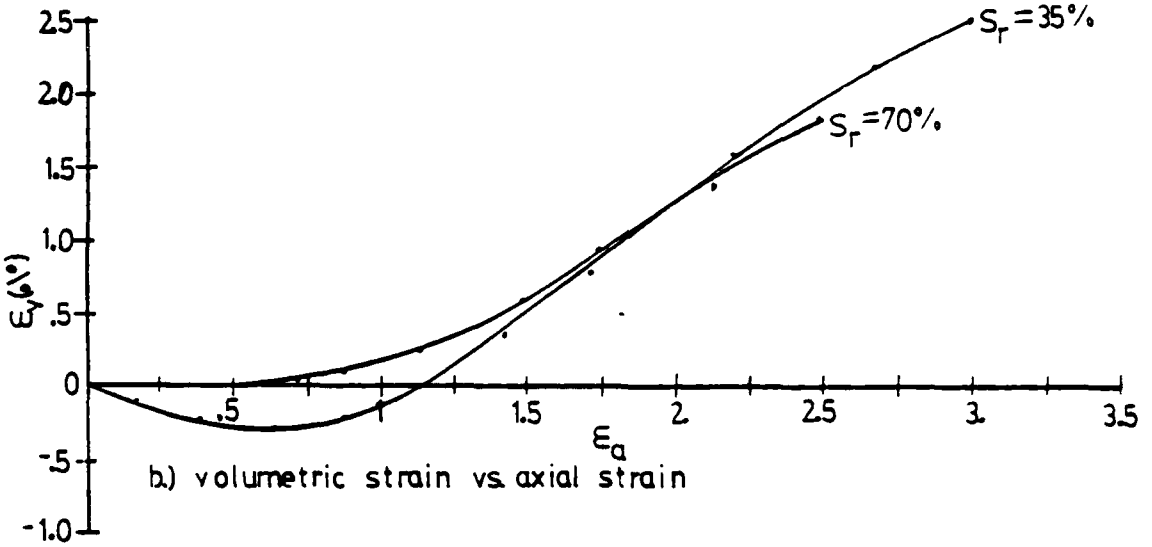

b.) volumetric strain vs. axial strain

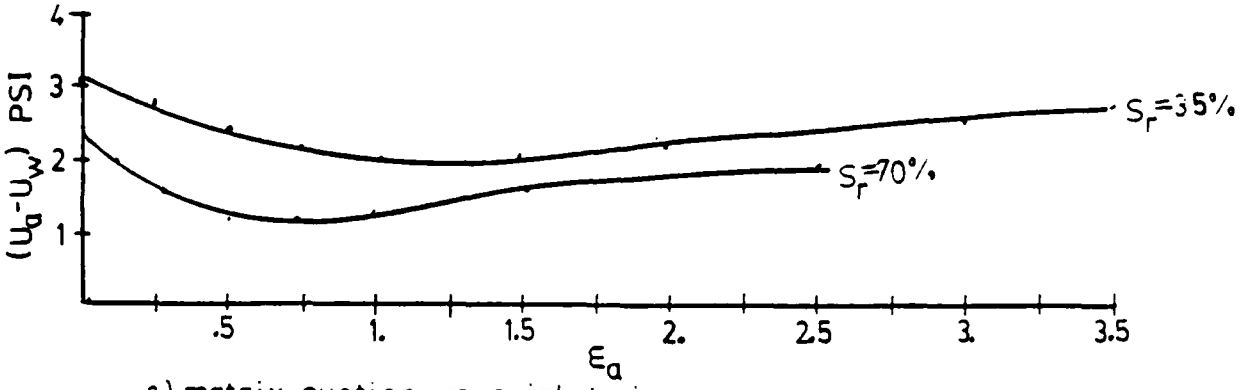

c.) matrix suction vs. axial strain

FIG. 8 TEST RESULTS ON UNSATURATED SILT

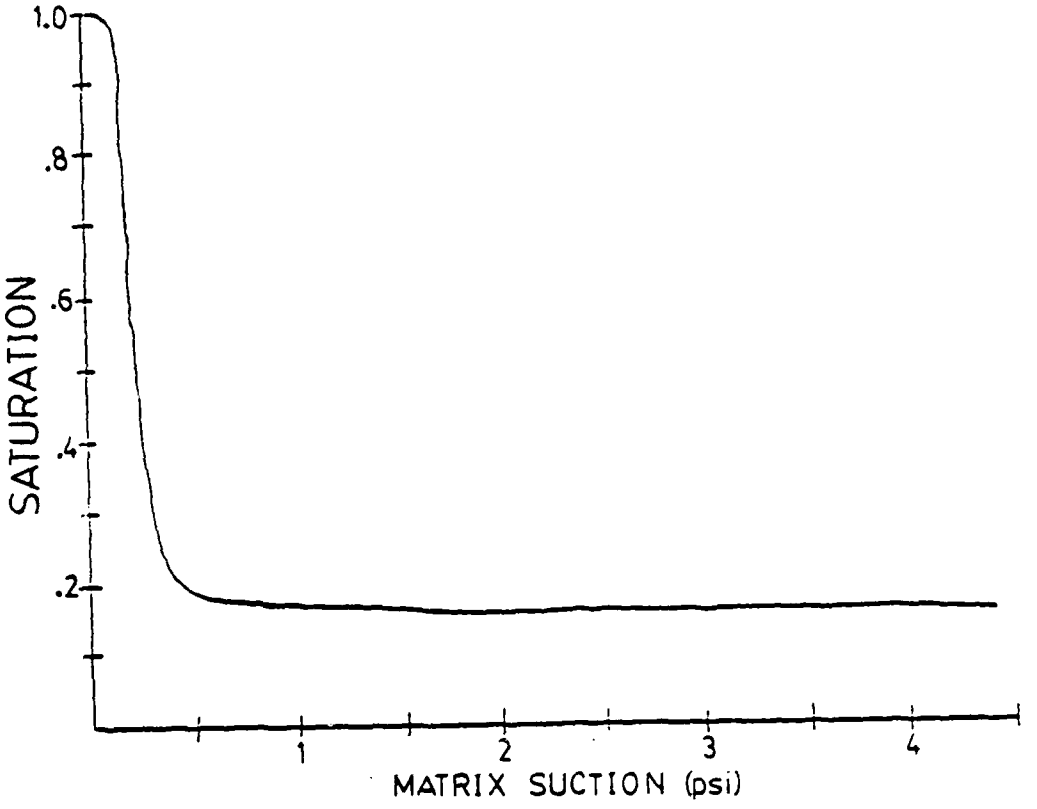

a) loose sample

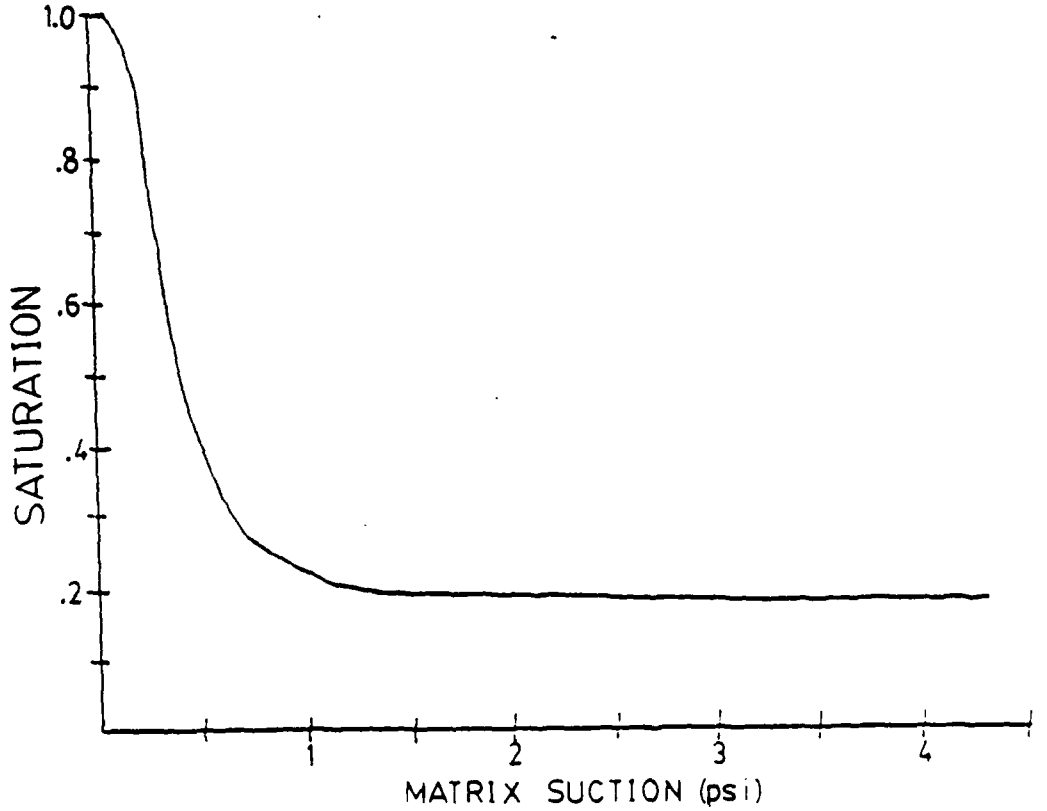

b) dense sample

FIG.9 CHARACTERISTIC CURVES FOR TEST SAND

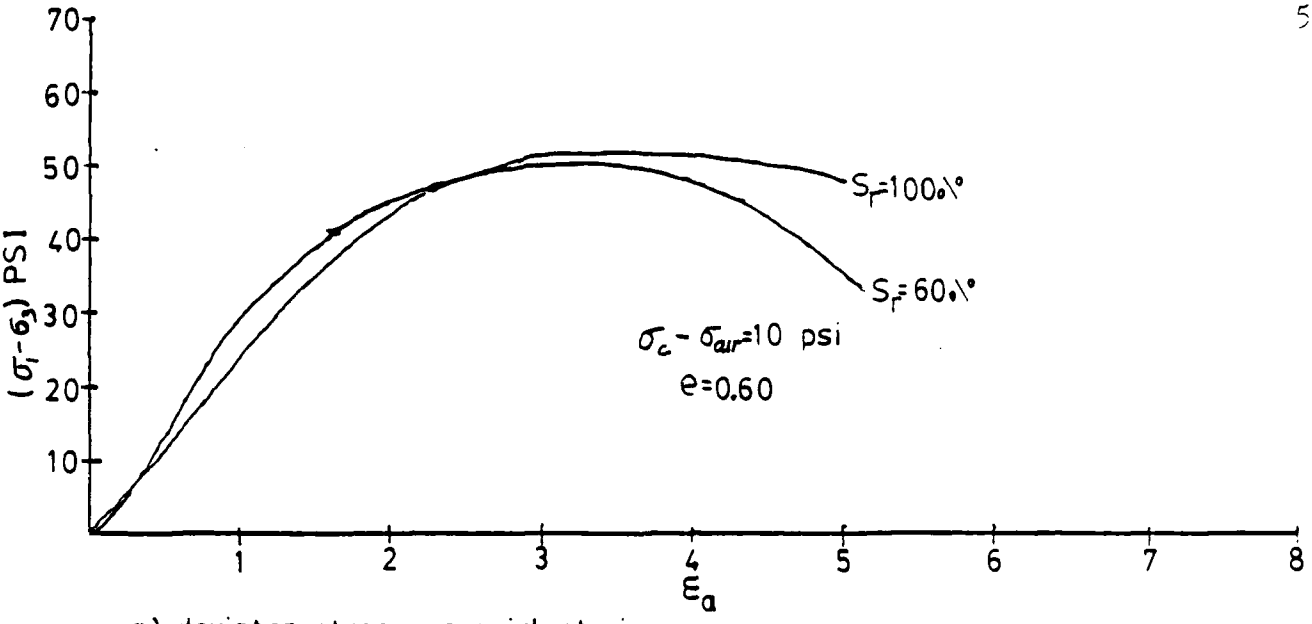

a) deviator stress vs. axial strain

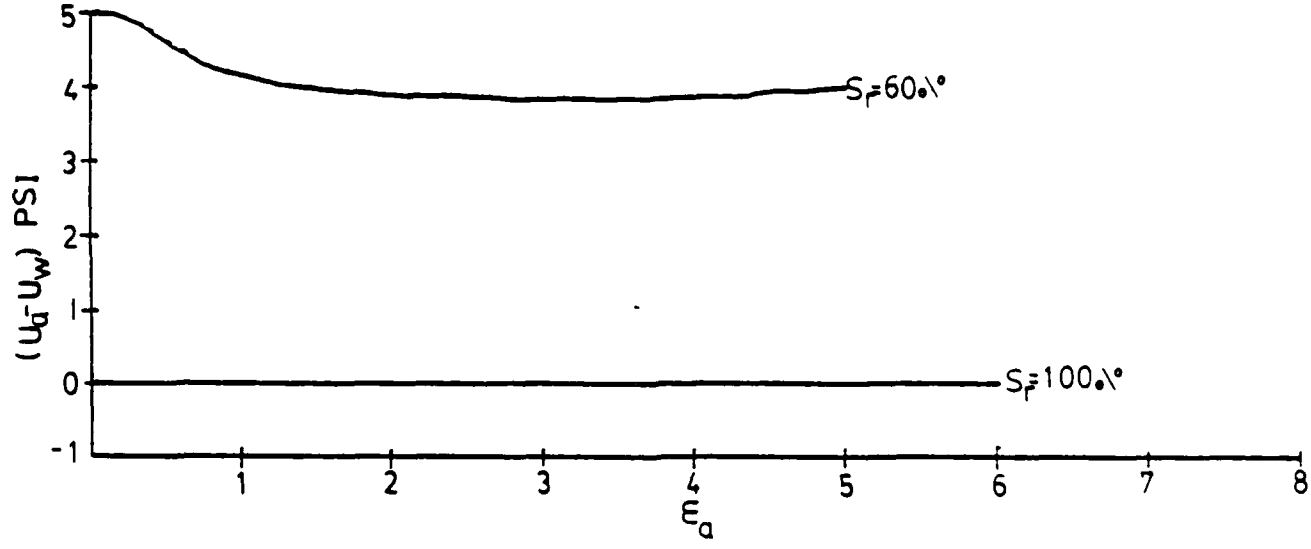

b.) matrix suction vs. axial strain

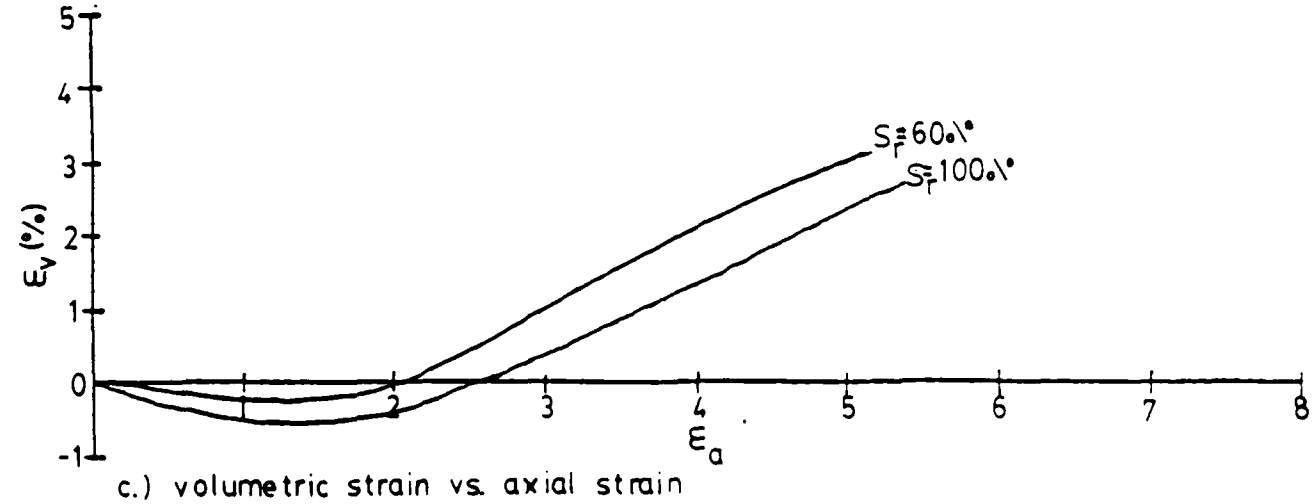

c.) volumetric strain vs. axial strain

FIG.10 TRIAXIAL TEST RESULTS FOR TEST SAND

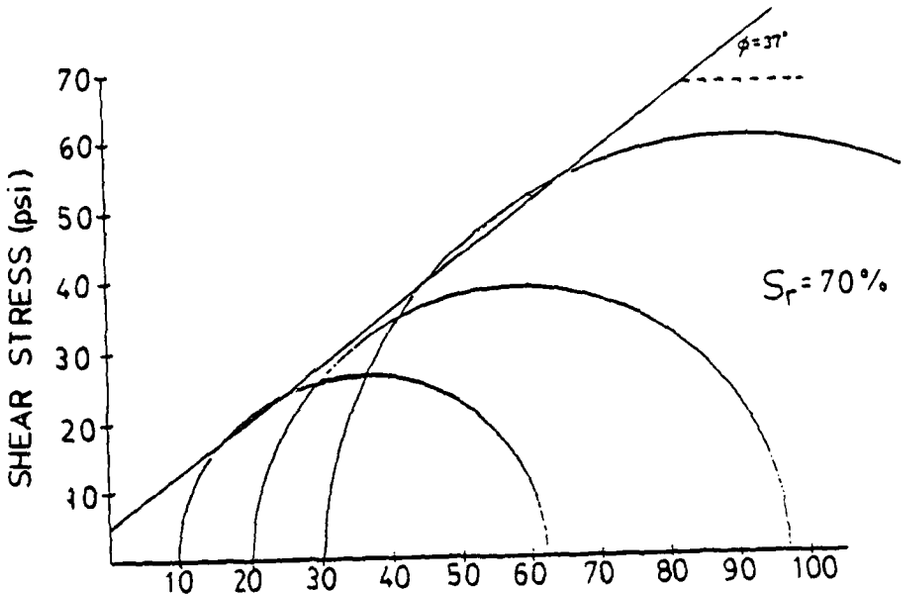

a.) dense unsaturated samples

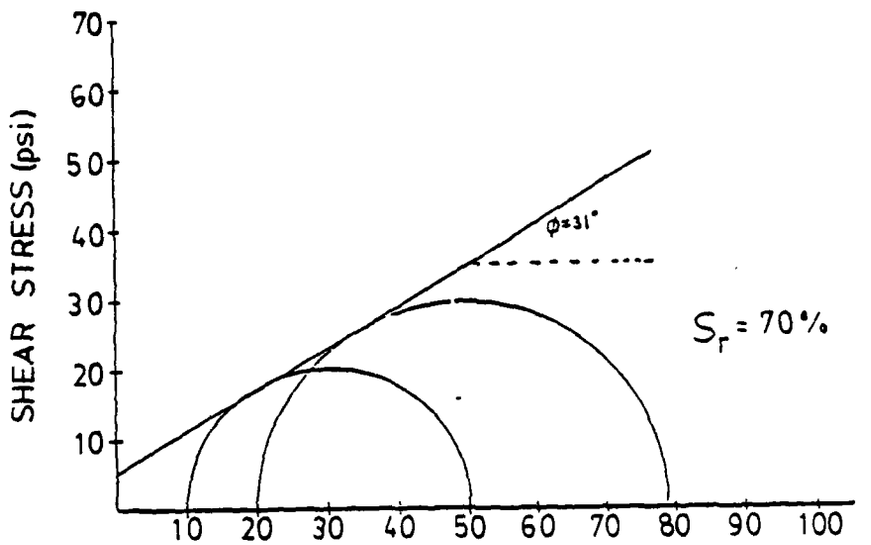

b.) loose unsaturated samples

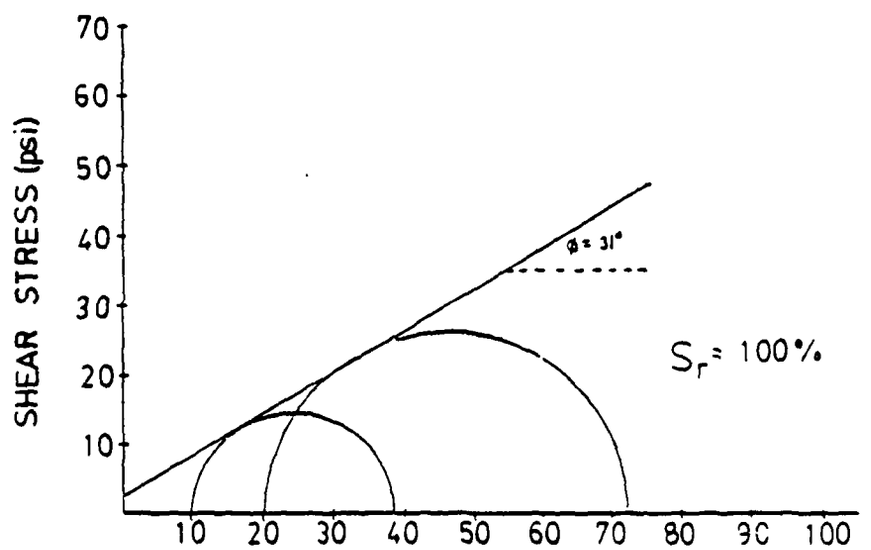

c.) loose saturated samples

FIG.11 MOHR CIRCLE DIAGRAMS OF TEST RESULTS

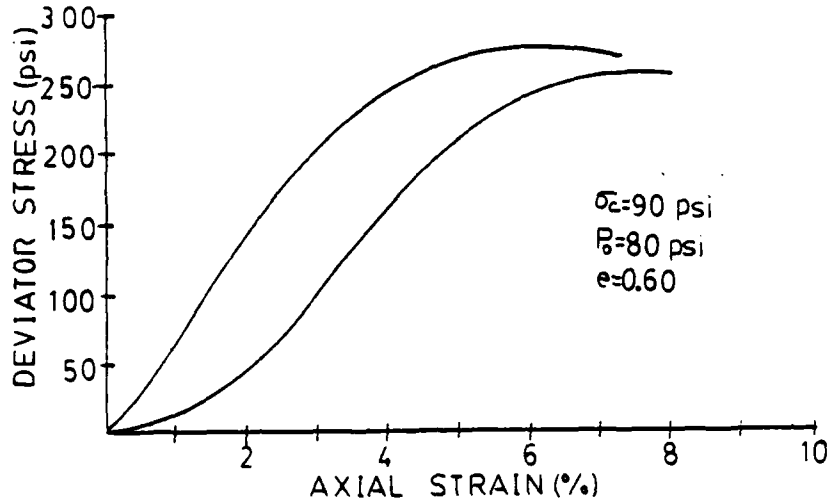

a.) high range

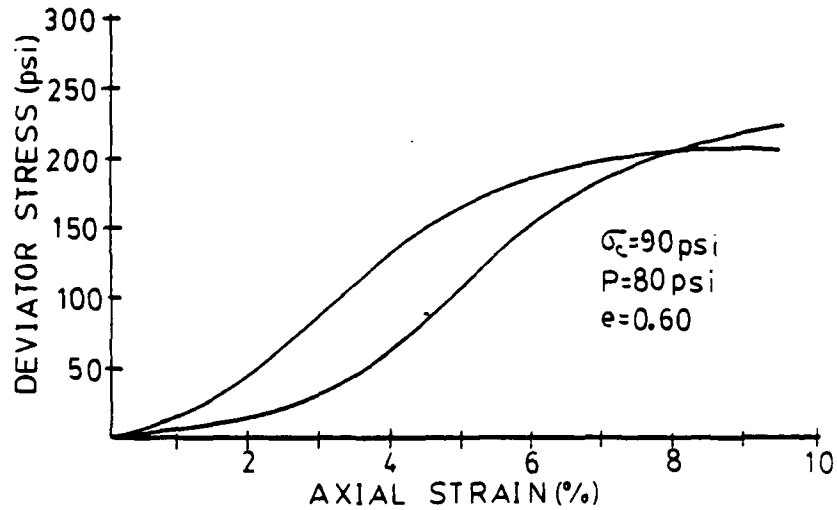

b.) mid range

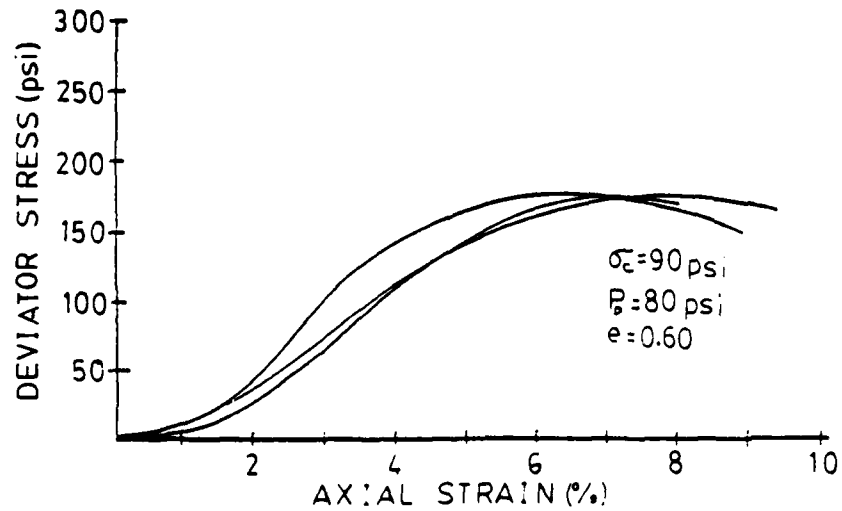

c) low range

FIG.12 STRESS-STRAIN CURVES FOR SATURATED SAMPLES

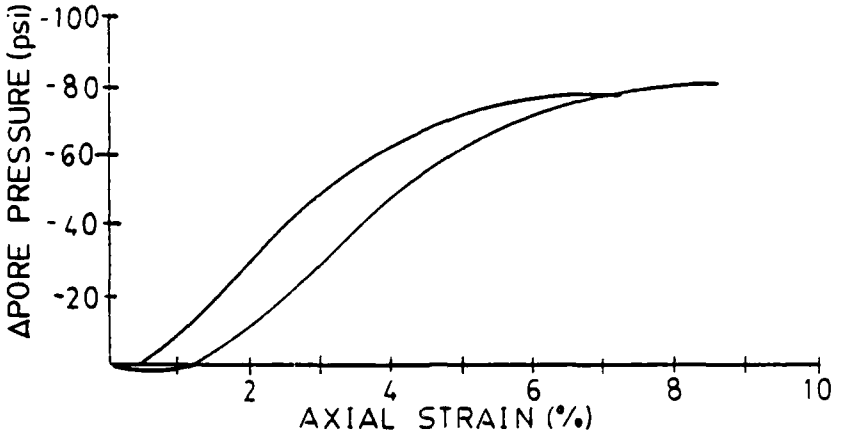

a.) high range

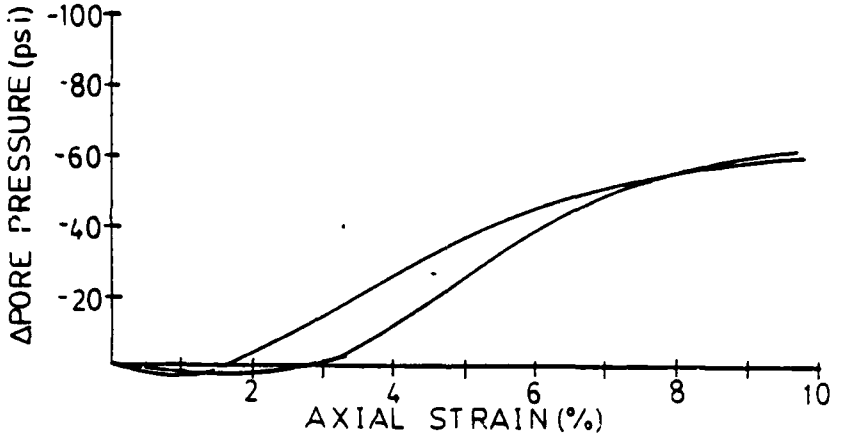

b.) mid range

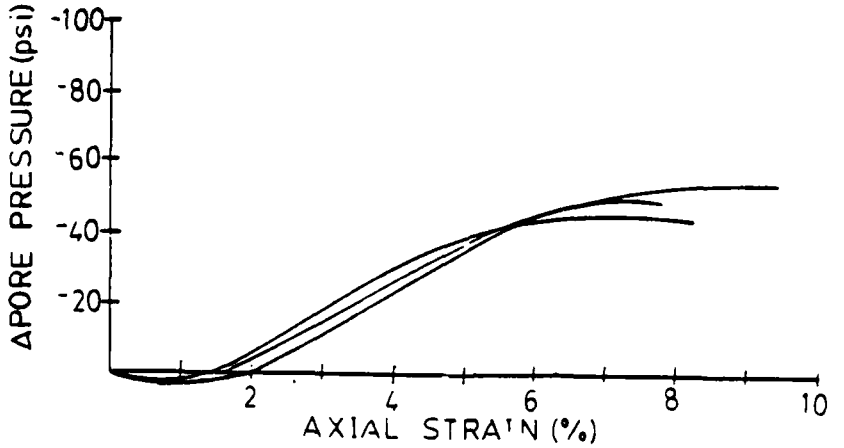

c.) low range

FIG.13 CHANGE IN PORE PRESSURES VS. AXIAL STRAIN FOR SATURATED SAMPLES

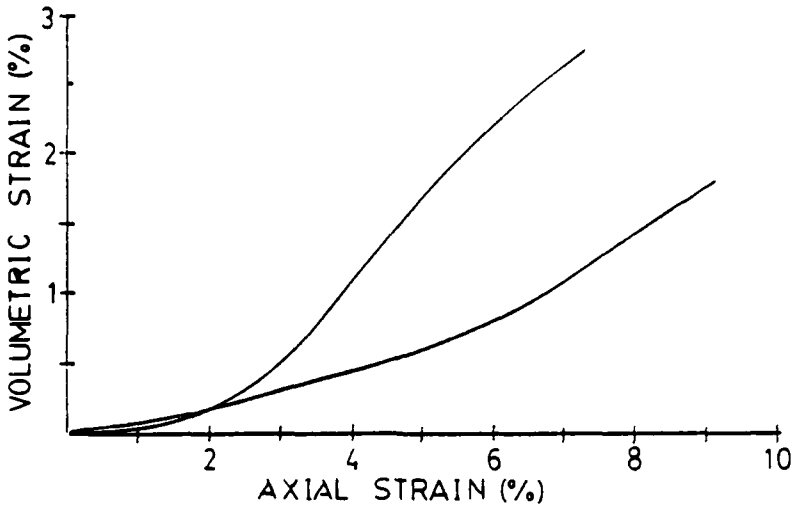

a.) high range

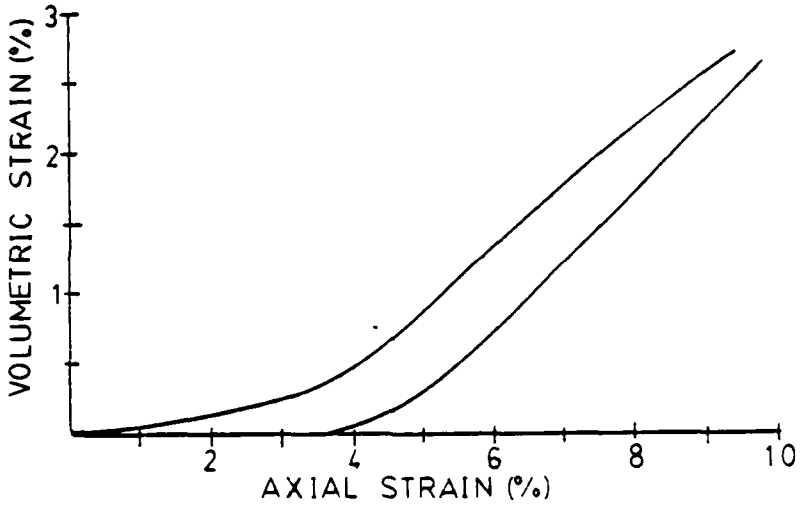

b.) mid range

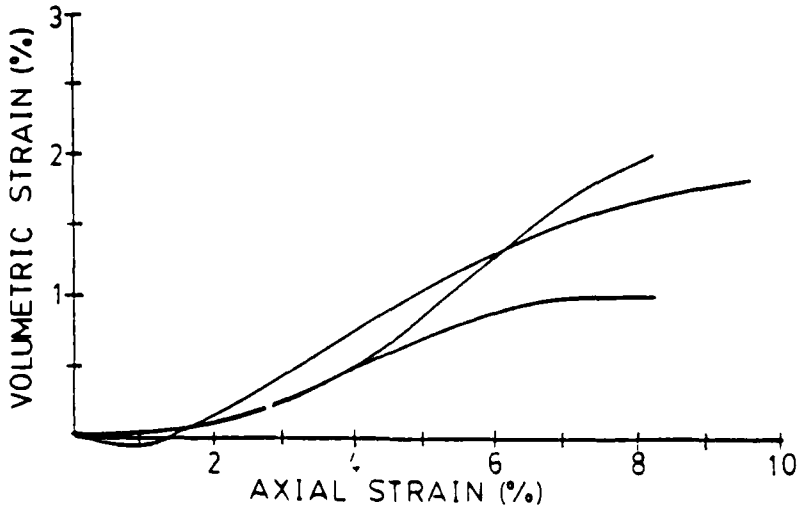

c.) low range

FIG.14 VOLUMETRIC STRAIN VS. AXIAL STRAIN FOR SATURATED SAMPLES

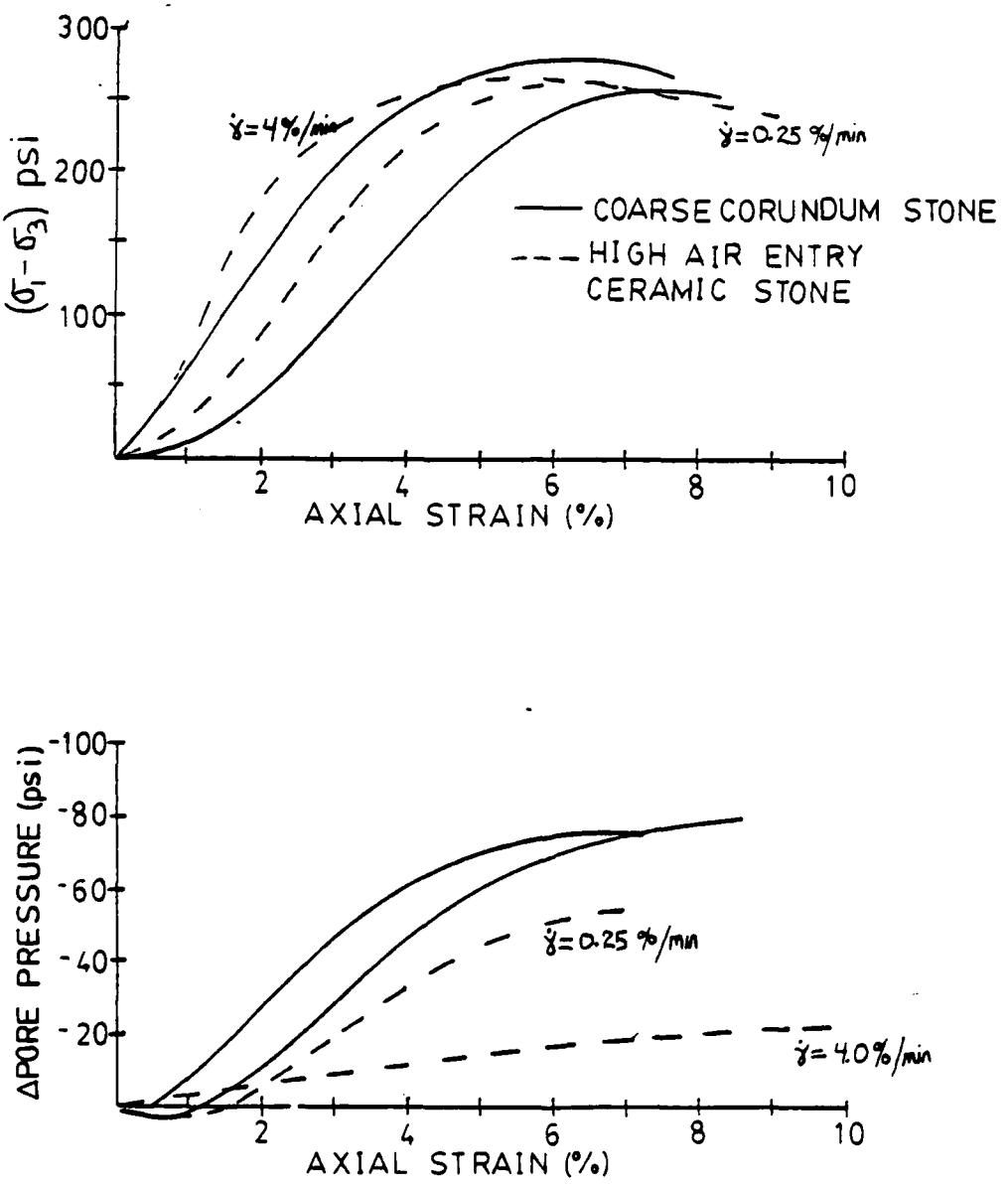

FIG. 15 EVALUATION OF CERAMIC STONE WITH REGARDS TO PORE PRESSURE RESPONSE (high range)

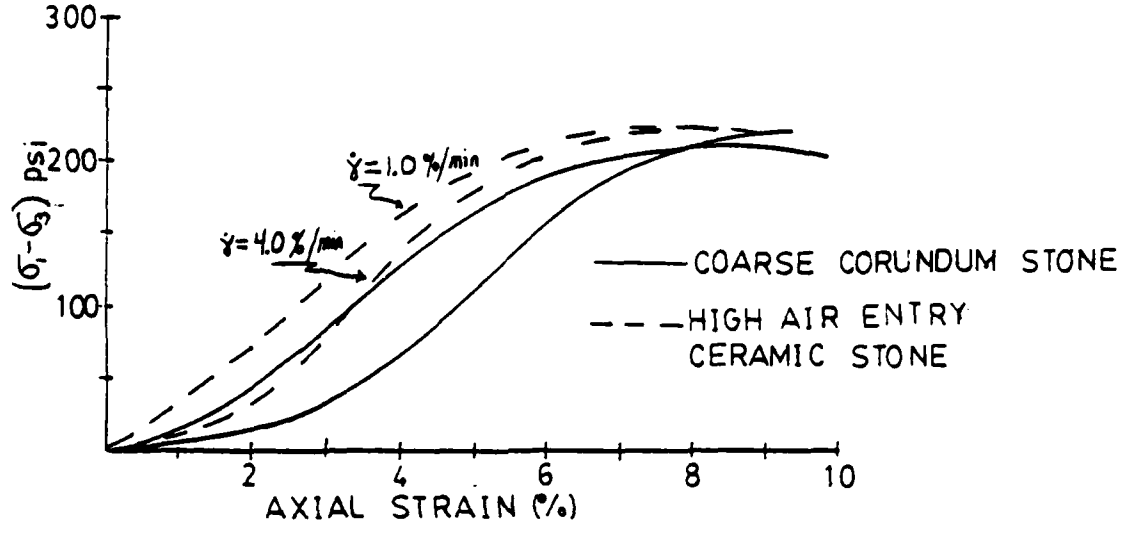

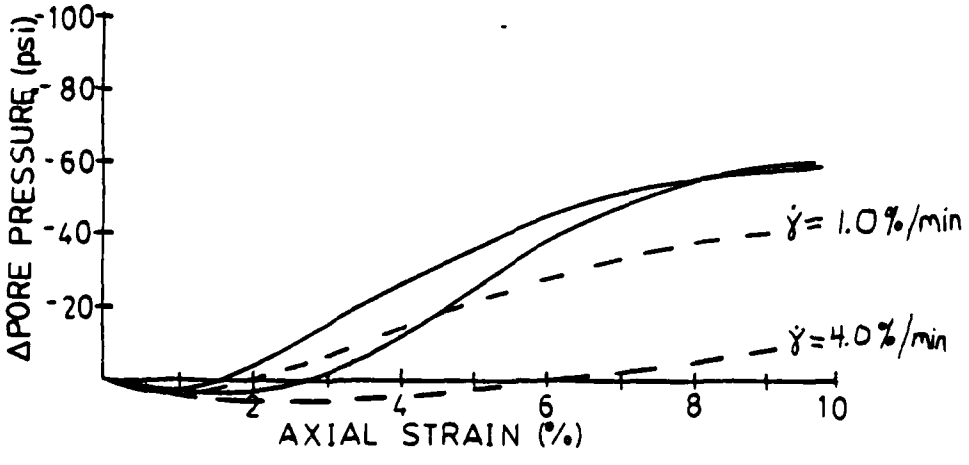

FIG.16 EVALUATION OF CERAMIC STONE WITH REGARDS TO PORE PRESSURE RESPONSE (low range)

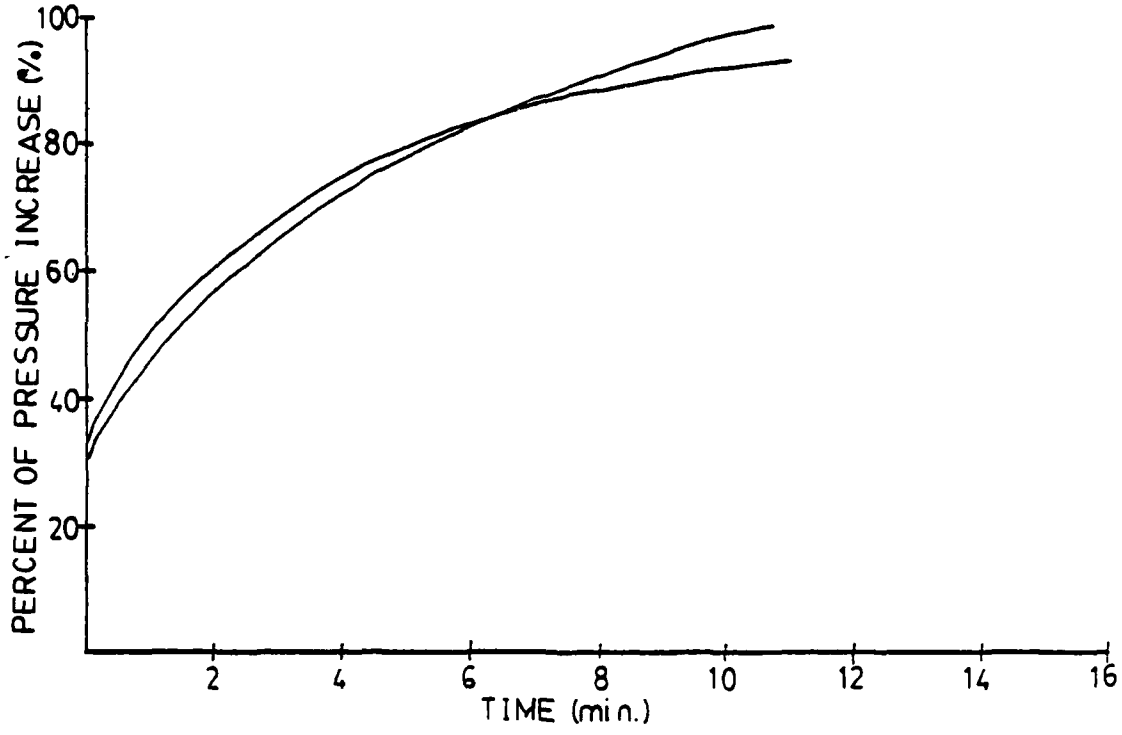

a.) change in pressure equals 1.0 psi

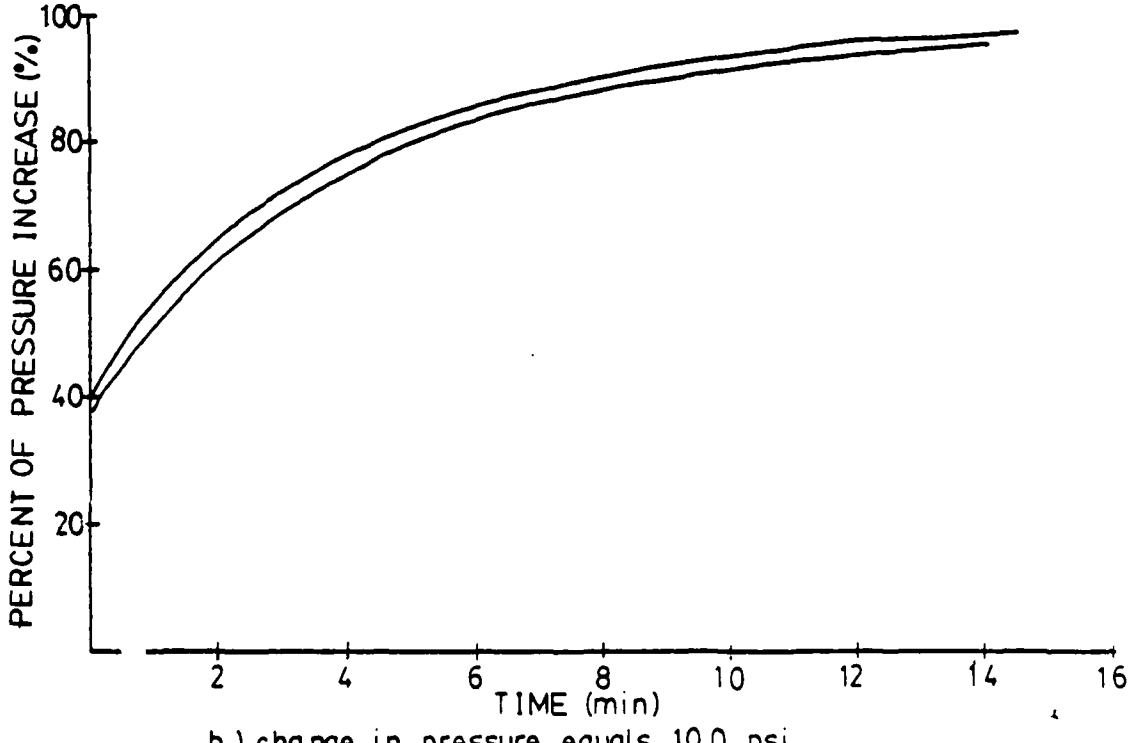

b.) change in pressure equals 10.0 psi

FIG.17 LAG TIME IN PRESSURE RESPONSE WITH CERAMIC STONE

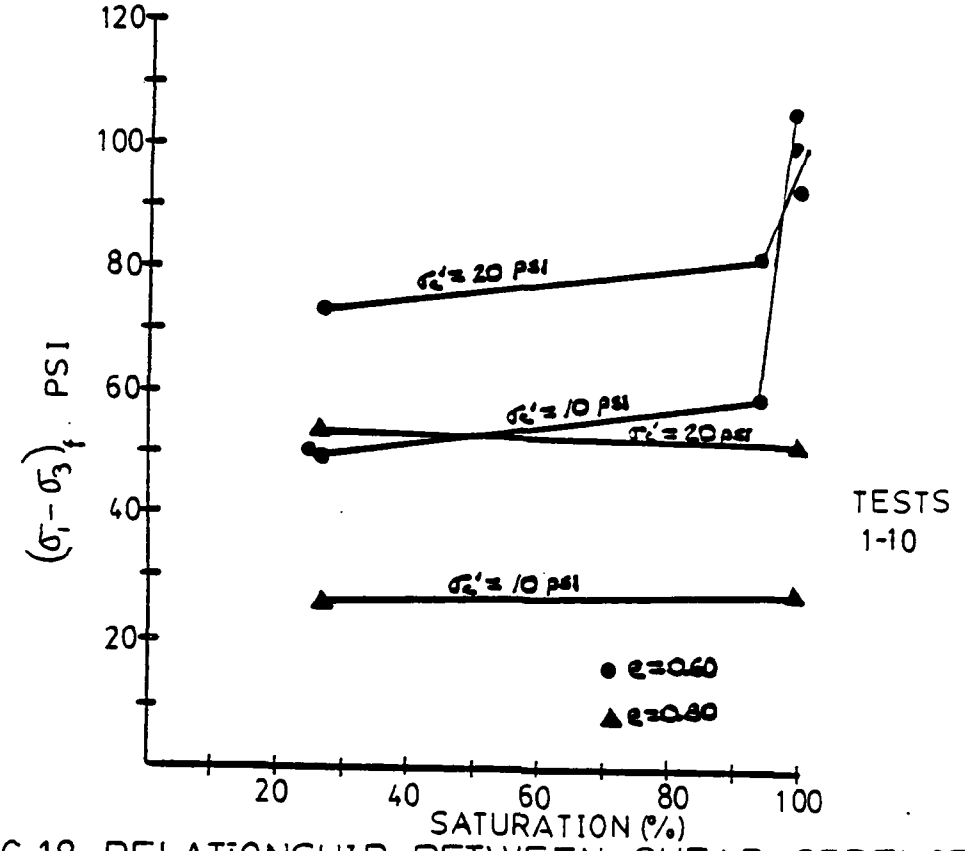

FIG. 18 RELATIONSHIP BETWEEN SHEAR STRENGTH AND SATURATION LEVEL (undrained)

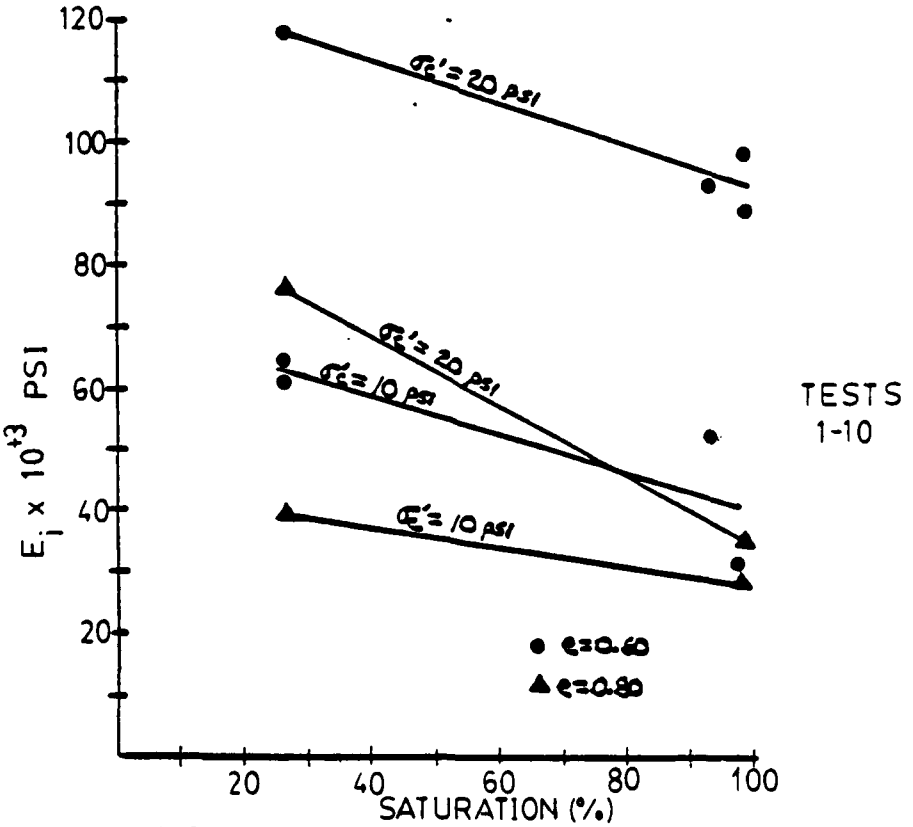

FIG. 19 RELATIONSHIP BETWEEN INITIAL TANGENT MODULUS AND SATURATION LEVEL (undrained)

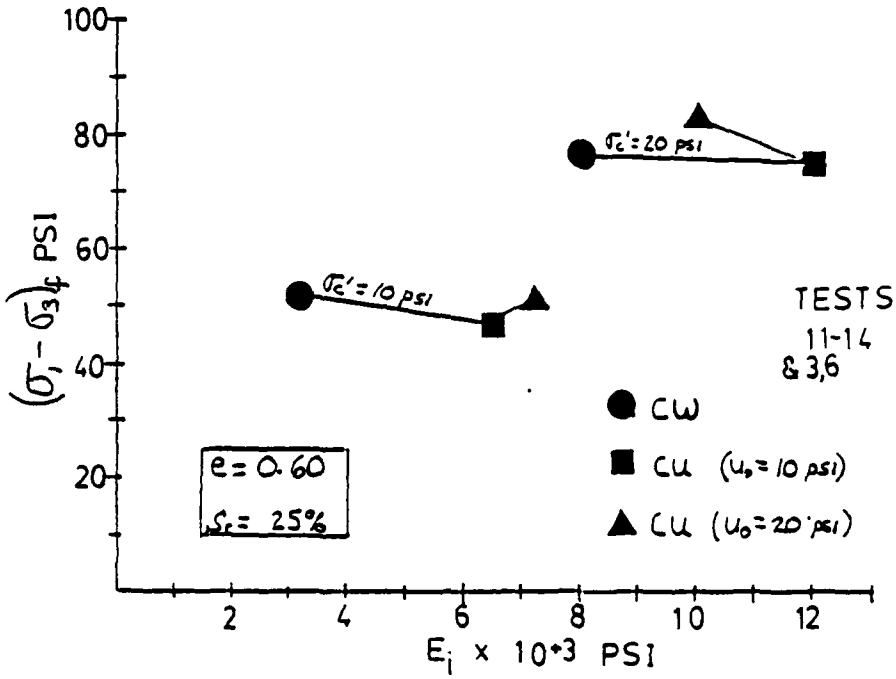

FIG. 20 COMPARISON BETWEEN CONSTANT WATER AND UNDRAINED TRIAXIAL TEST RESULTS

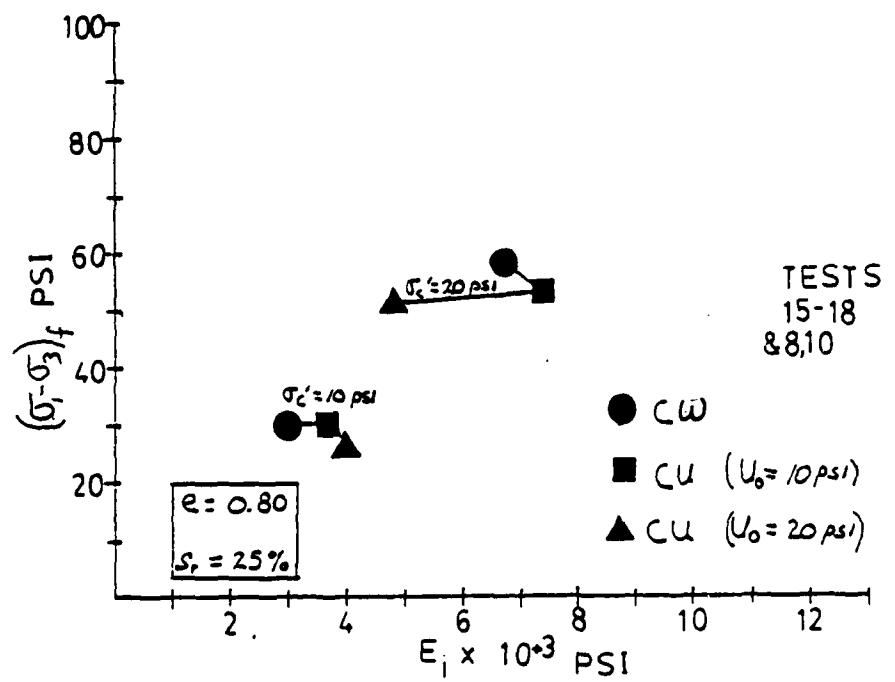

FIG. 21 COMPARISON BETWEEN CONSTANT WATER AND UNDRAINED TRIAXIAL TEST RESULTS

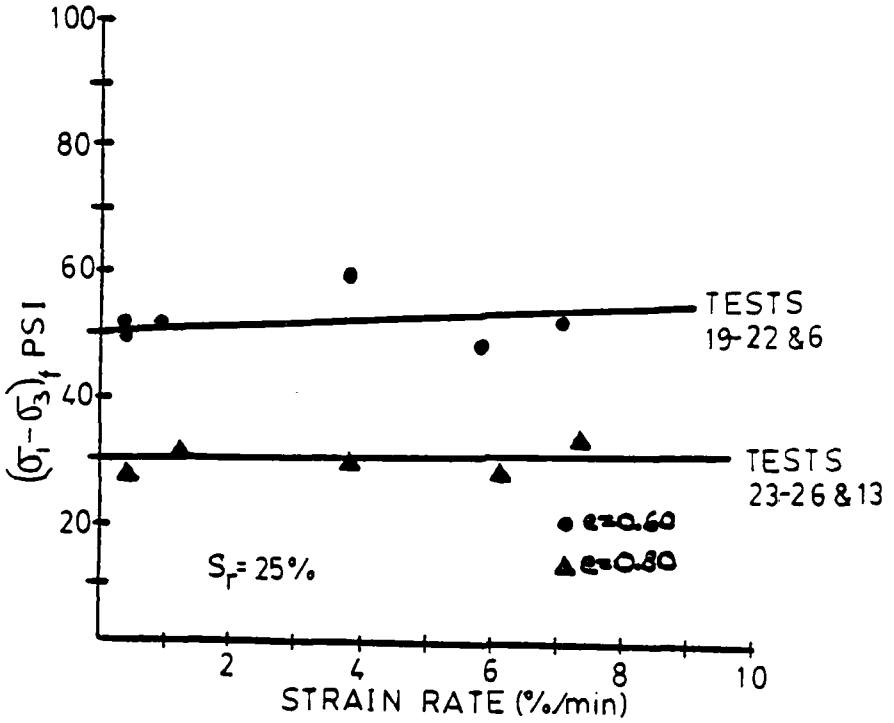

FIG. 22 RELATIONSHIP BETWEEN SHEAR STRENGTH AND STRAIN RATE (undained)

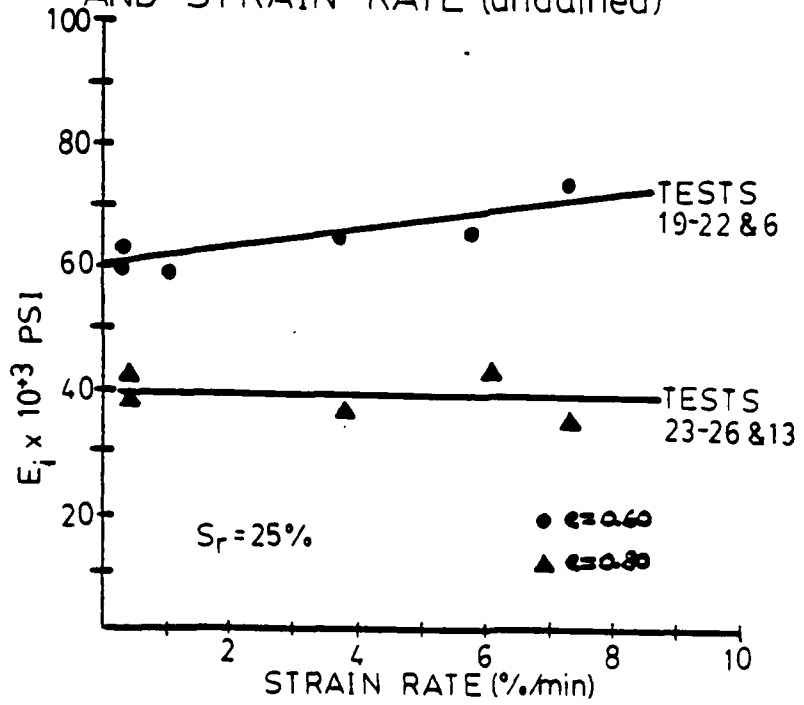

FIG. 23 RELATIONSHIP BETWEEN INITIAL TANGENT MODULUS AND STRAIN RATE (undrained)

APPENDIX

Stress-Strain Curves

TEST 1A

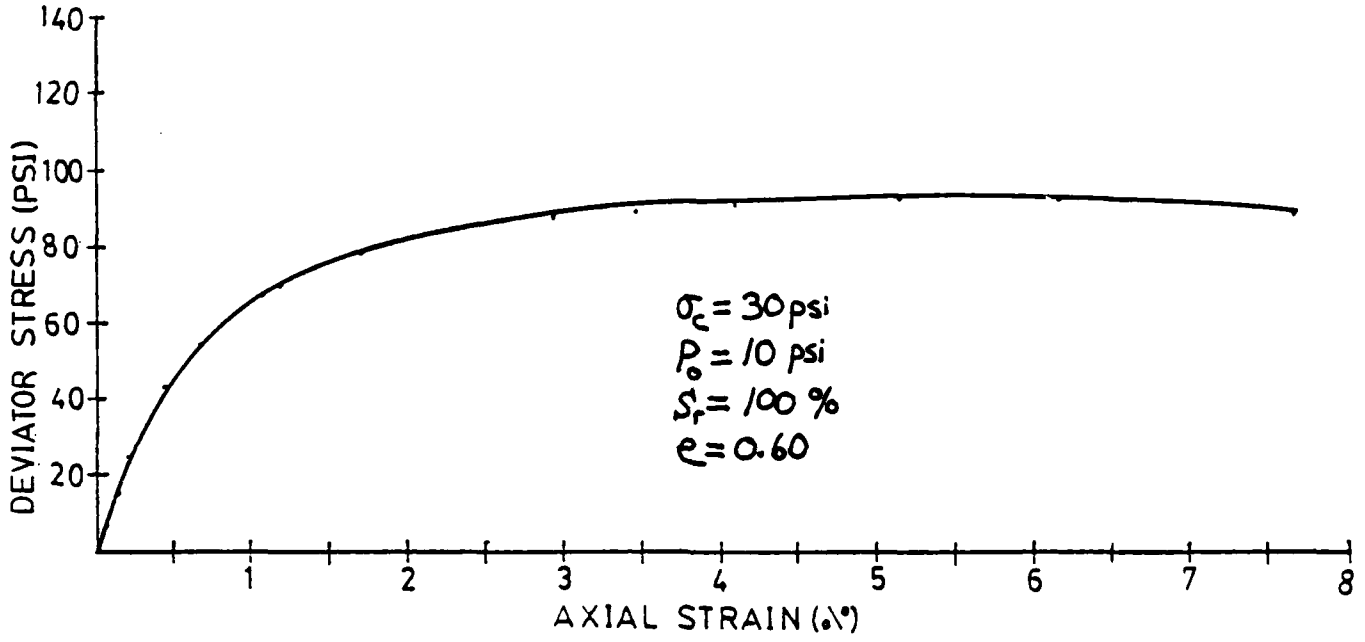
DEVIATOR STRESS (PSI)
140
120
100
80
60
40
20
1
2
3
4
5
6
7
8
AXIAL STRAIN (%)
σ_c = 30 psi
P_o = 10 psi
S_r = 100 %
e = 0.60

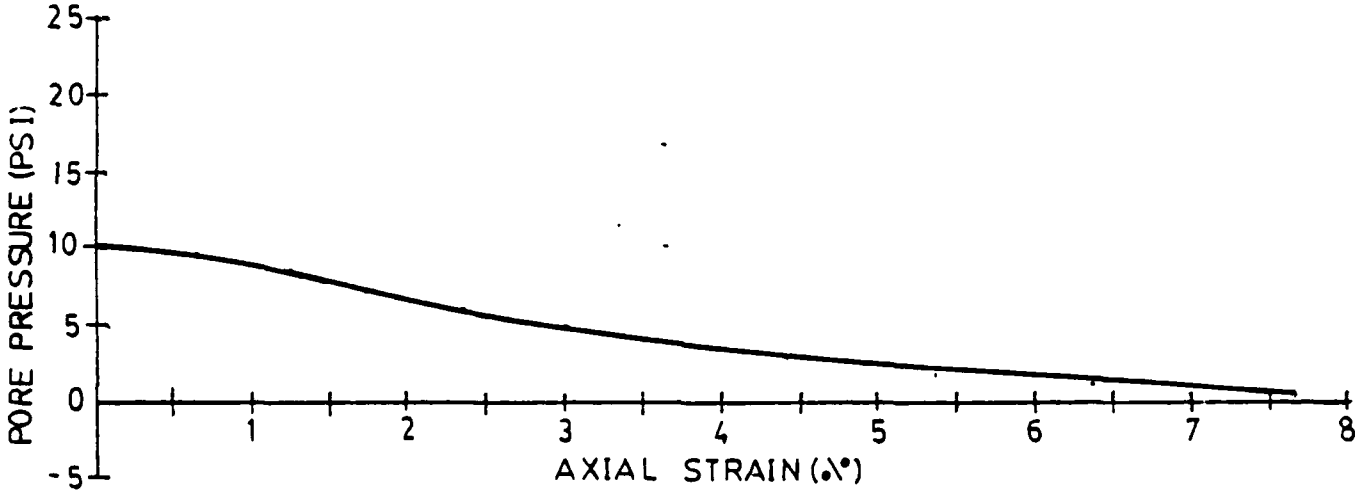
PORE PRESSURE (PSI)
25
20
15
10
5
0
-5
1
2
3
4
5
6
7
8
AXIAL STRAIN (%)

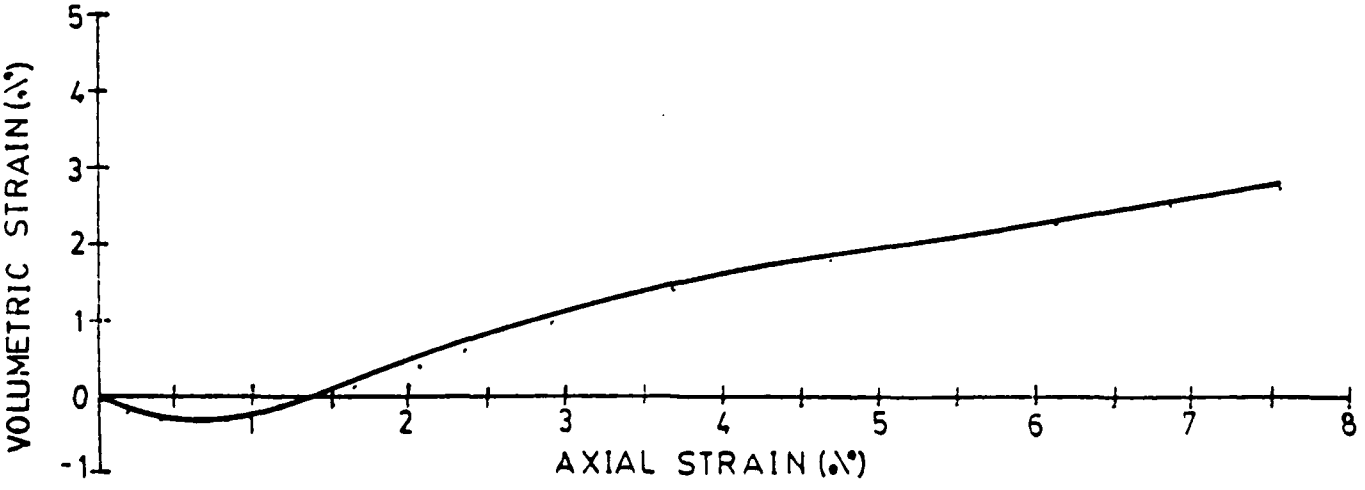
VOLUMETRIC STRAIN (%)
5
4
3
2
1
0
-1
2
3
4
5
6
7
8
AXIAL STRAIN (%)

TEST 1.B

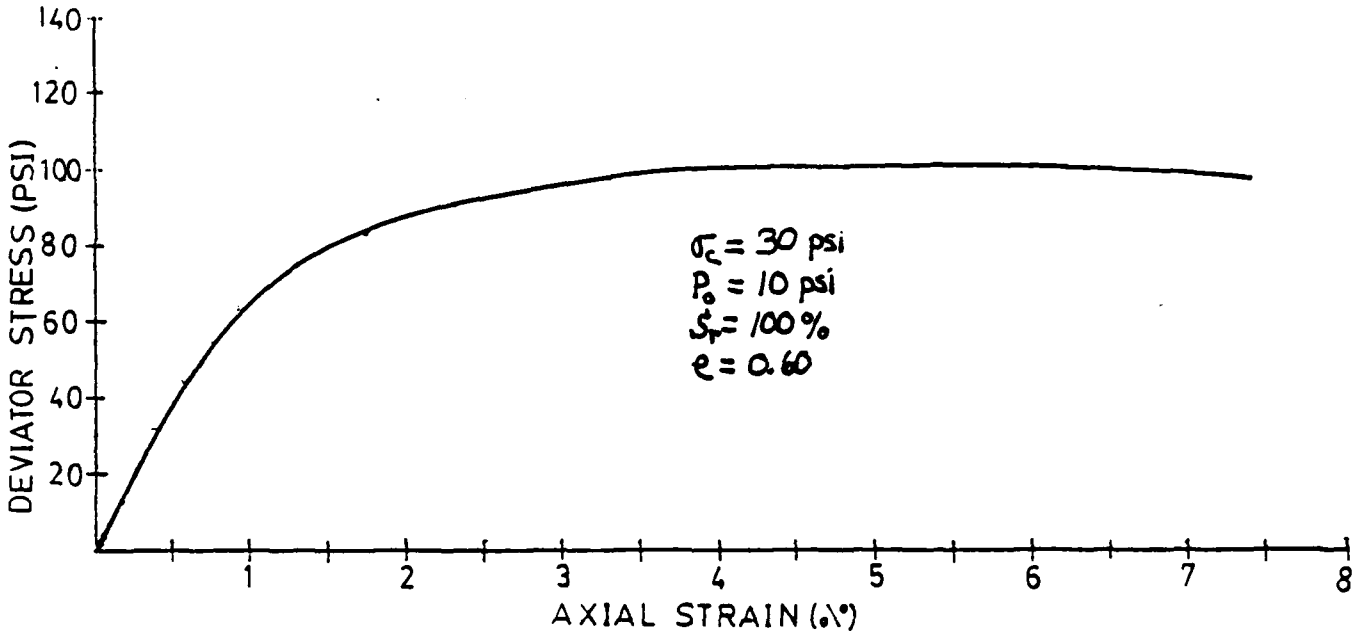
DEVIATOR STRESS (PSI)
140
120
100
80
60
40
20
1
2
3
4
5
6
7
8
AXIAL STRAIN (%)
σ_c = 30 psi
P_o = 10 psi
S_r = 100%
e = 0.60

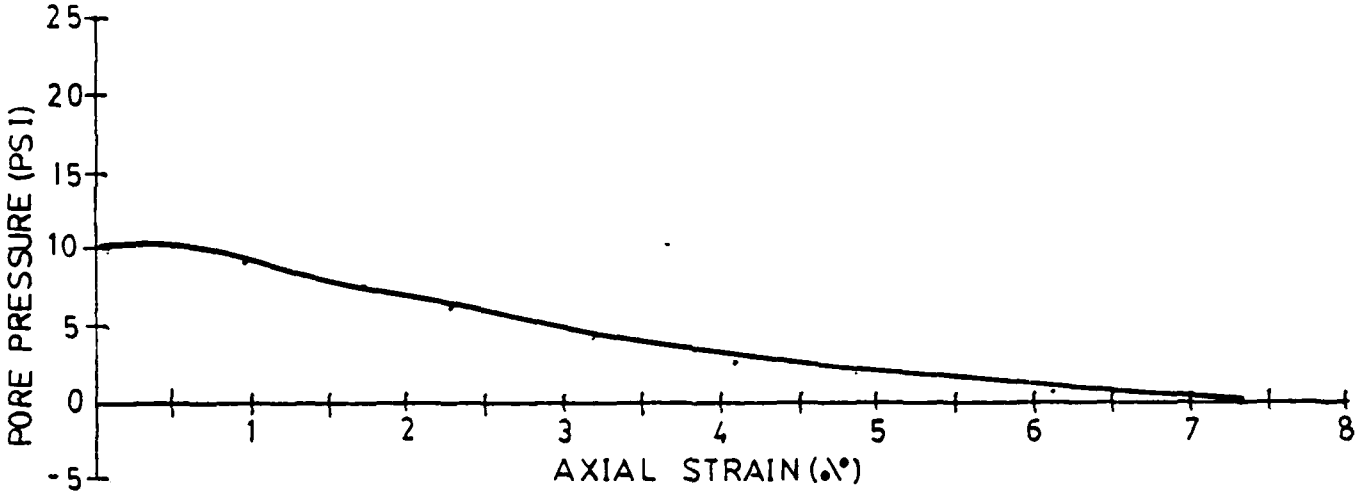
PORE PRESSURE (PSI)
25
20
15
10
5
0
-5
1
2
3
4
5
6
7
8
AXIAL STRAIN (%)

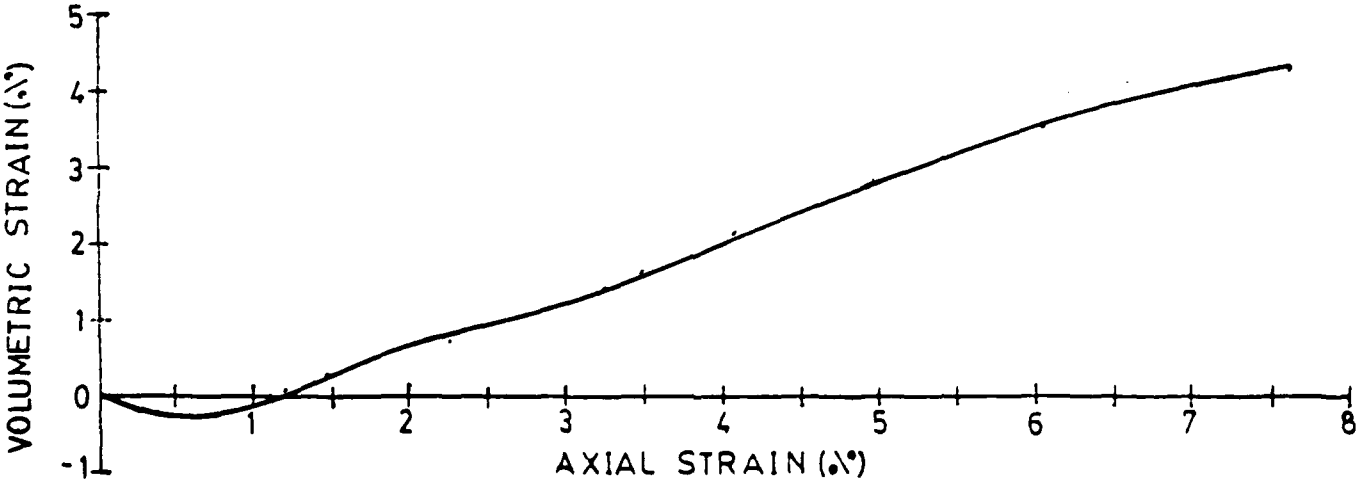
VOLUMETRIC STRAIN (%)
5
4
3
2
1
0
-1
1
2
3
4
5
6
7
8
AXIAL STRAIN (%)

TEST 2

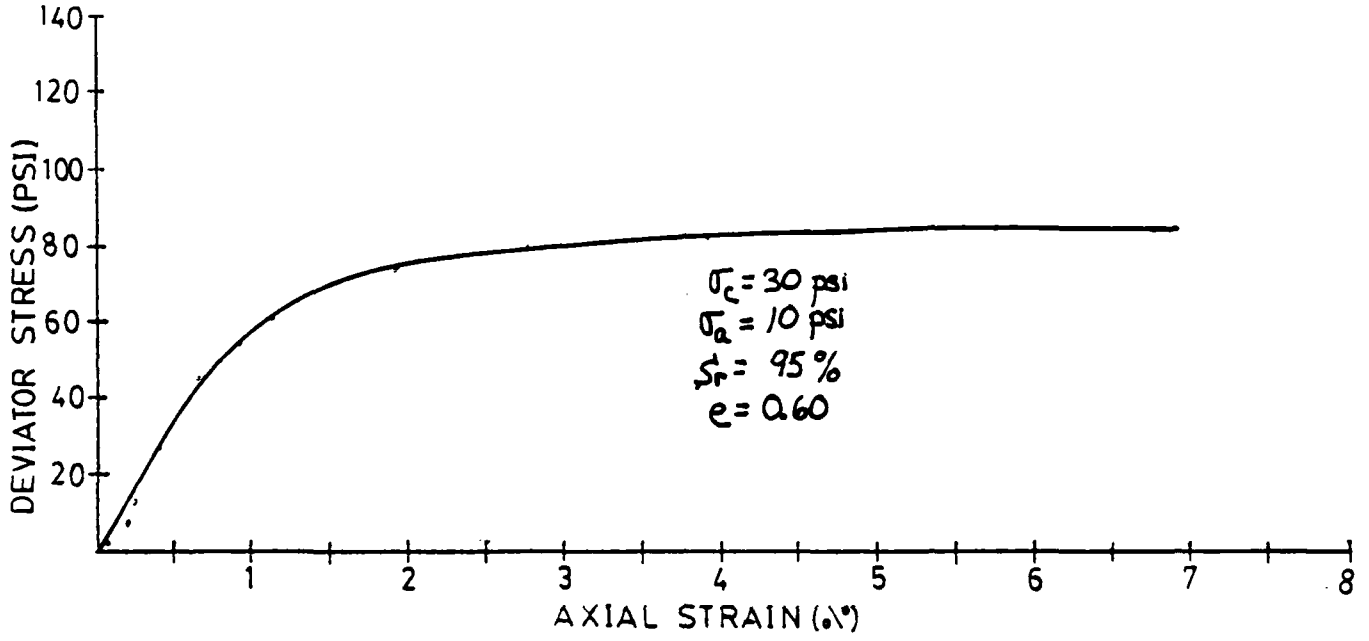
DEVIATOR STRESS (PSI)
140
120
100
80
60
40
20
1
2
3
4
5
6
7
8
AXIAL STRAIN (%)
σ_c = 30 psi
σ_a = 10 psi
S_r = 95 %
e = 0.60

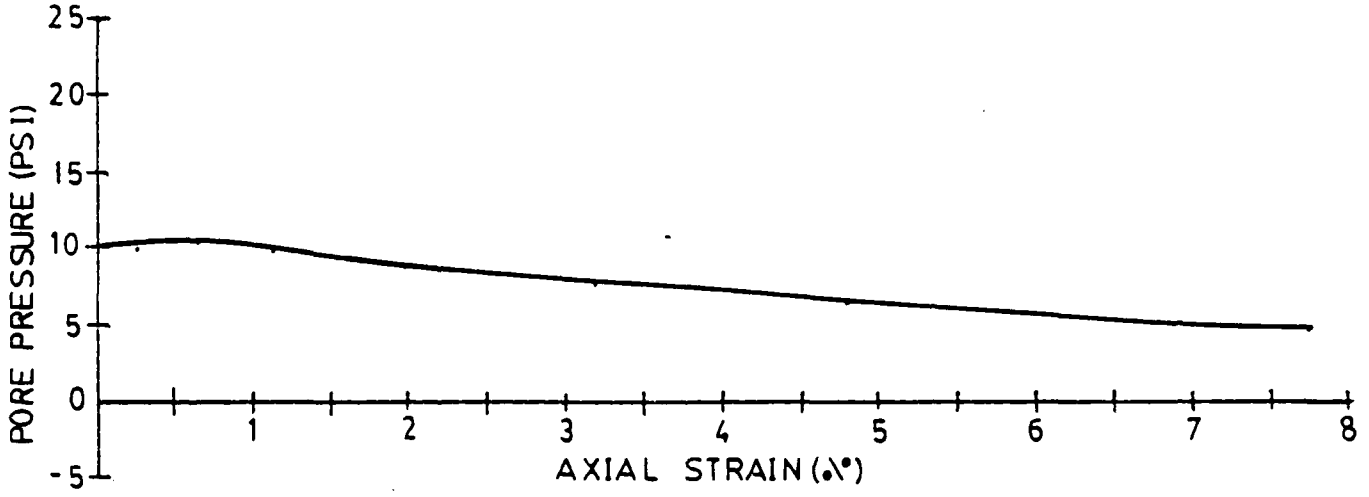
PORE PRESSURE (PSI)
25
20
15
10
5
0
-5
1
2
3
4
5
6
7
8
AXIAL STRAIN (%)

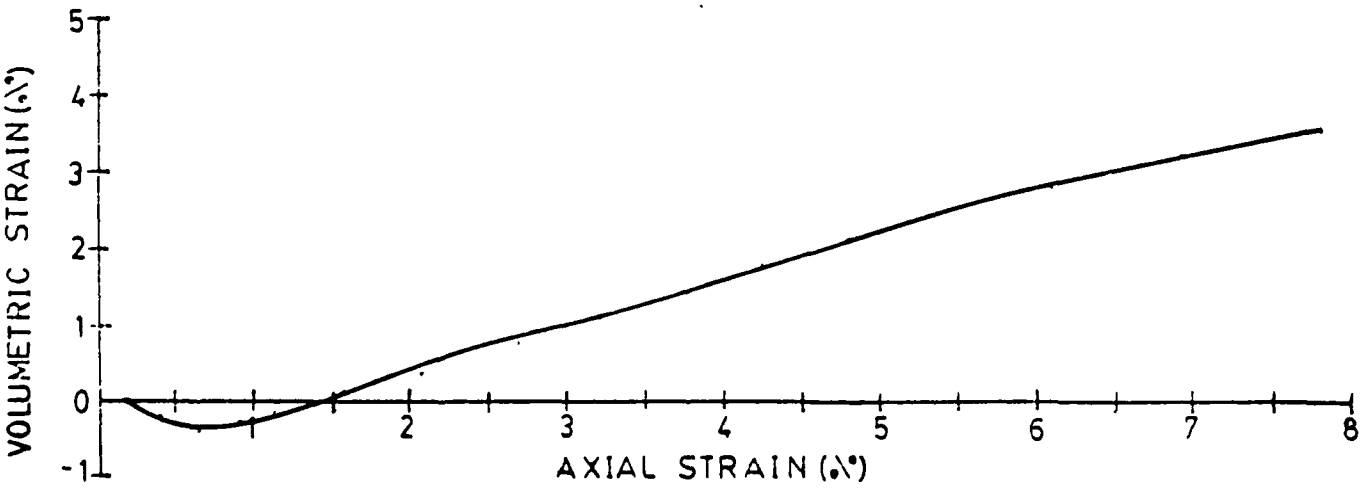
VOLUMETRIC STRAIN (%)
5
4
3
2
1
0
-1
2
3
4
5
6
7
8
AXIAL STRAIN (%)

TEST 3

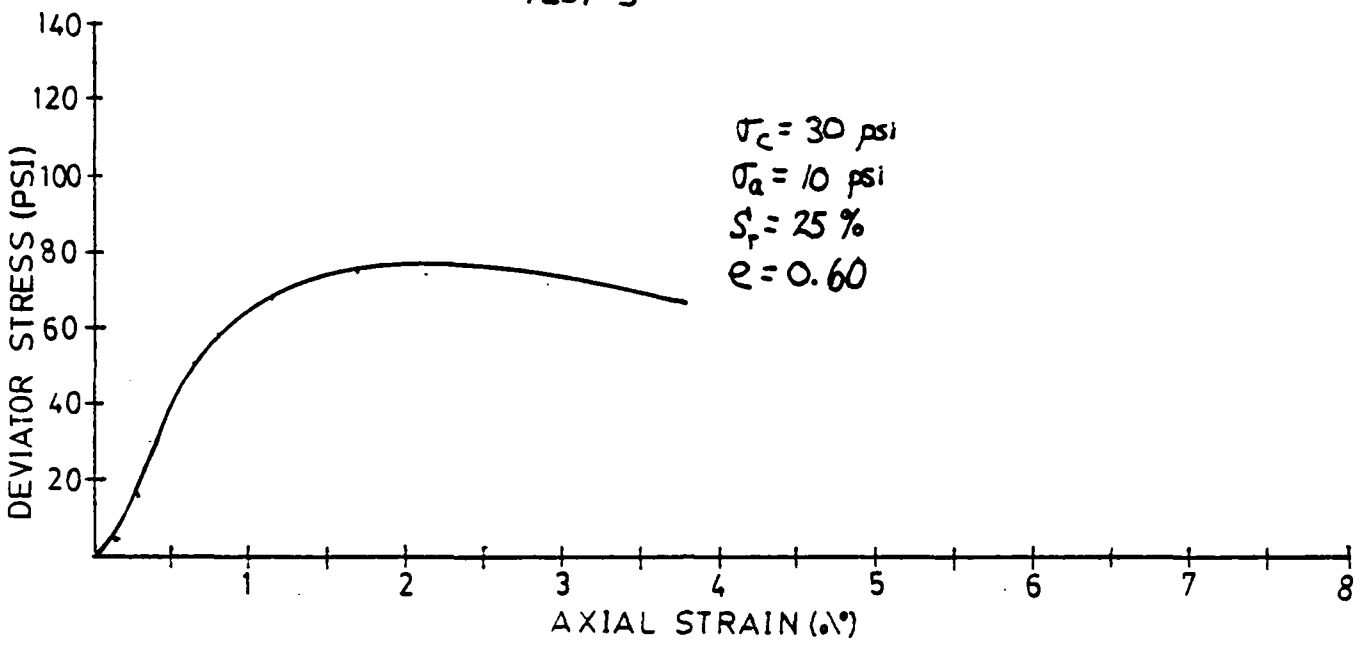
DEVIATOR STRESS (PSI)
140
120
100
80
60
40
20
1
2
3
4
5
6
7
8
AXIAL STRAIN (%)
σ_c = 30 psi
σ_a = 10 psi
S_r = 25 %
e = 0.60

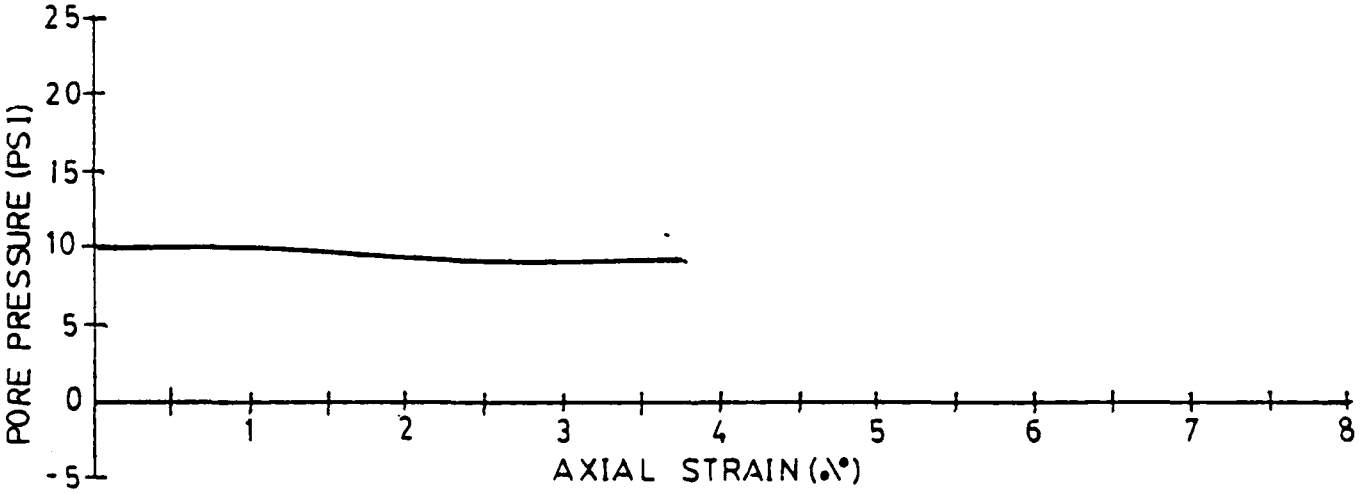
PORE PRESSURE (PSI)
25
20
15
10
5
0
-5
1
2
3
4
5
6
7
8
AXIAL STRAIN (%)

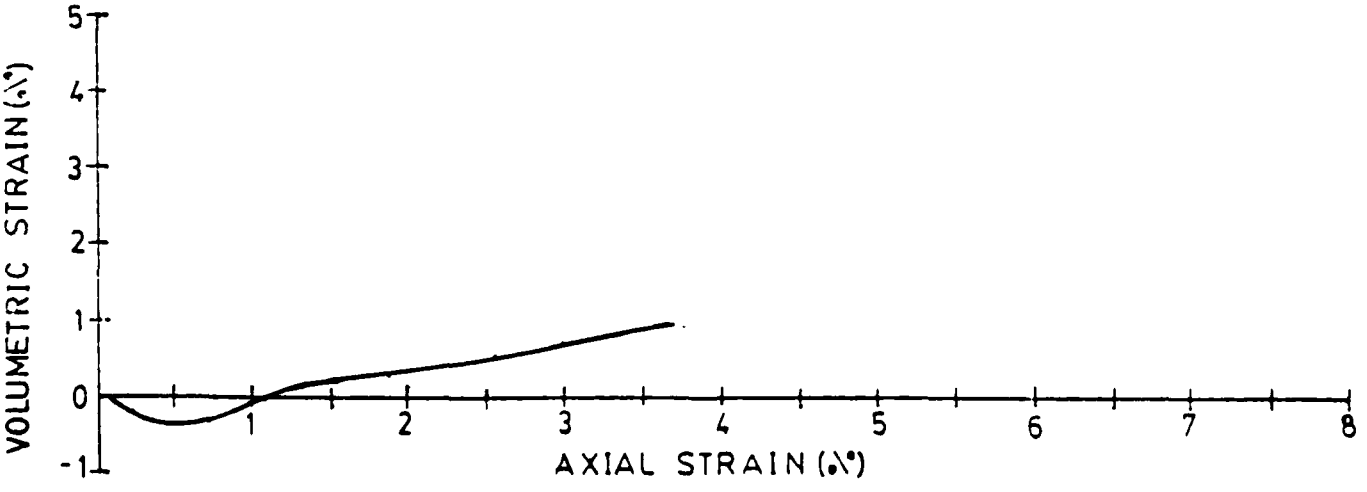
VOLUMETRIC STRAIN (%)
5
4
3
2
1
0
-1
1
2
3
4
5
6
7
8
AXIAL STRAIN (%)

TEST 4

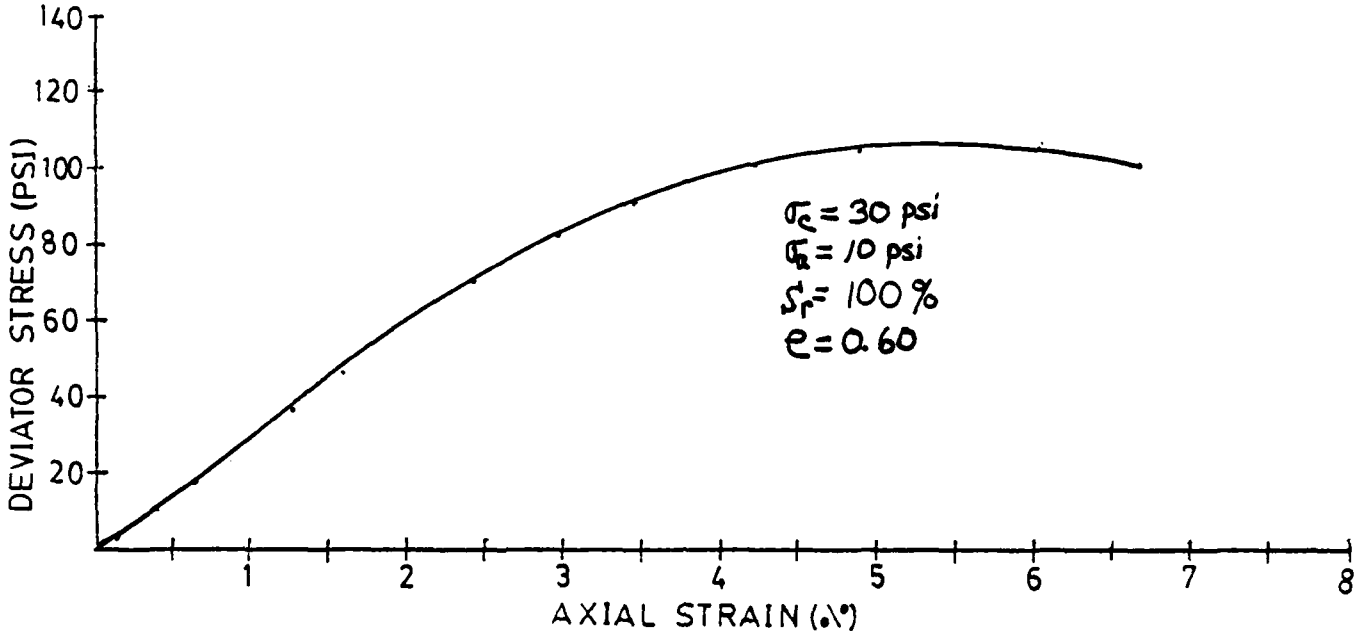
DEVIATOR STRESS (PSI)
140
120
100
80
60
40
20
1
2
3
4
5
6
7
8
AXIAL STRAIN (%)
σ_c = 30 psi
σ_h = 10 psi
S_r = 100 %
e = 0.60

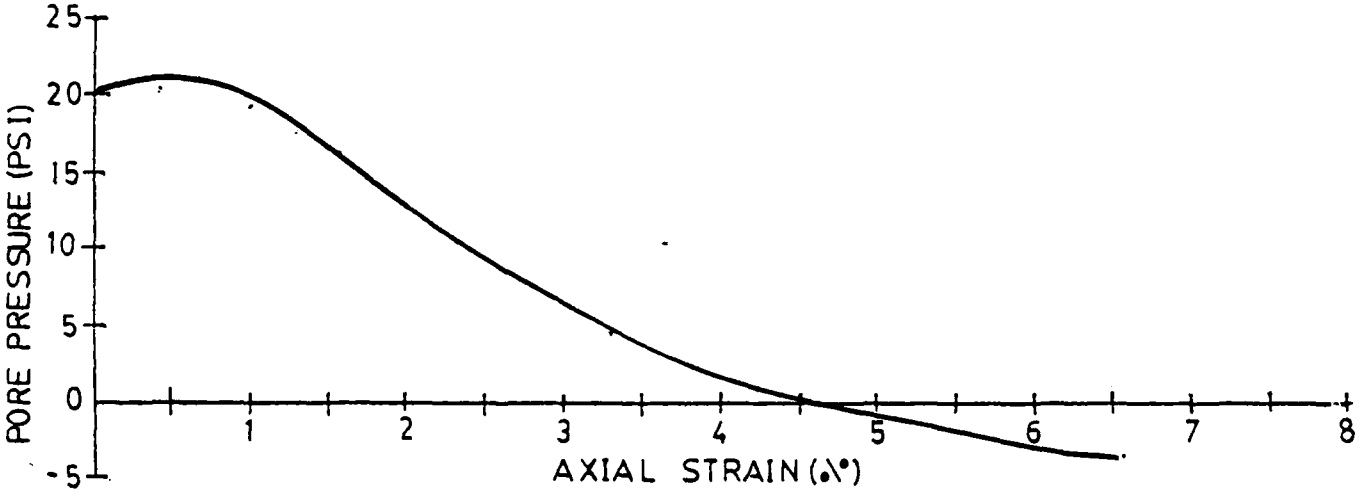
PORE PRESSURE (PSI)
25
20
15
10
5
0
-5
1
2
3
4
5
6
7
8
AXIAL STRAIN (%)

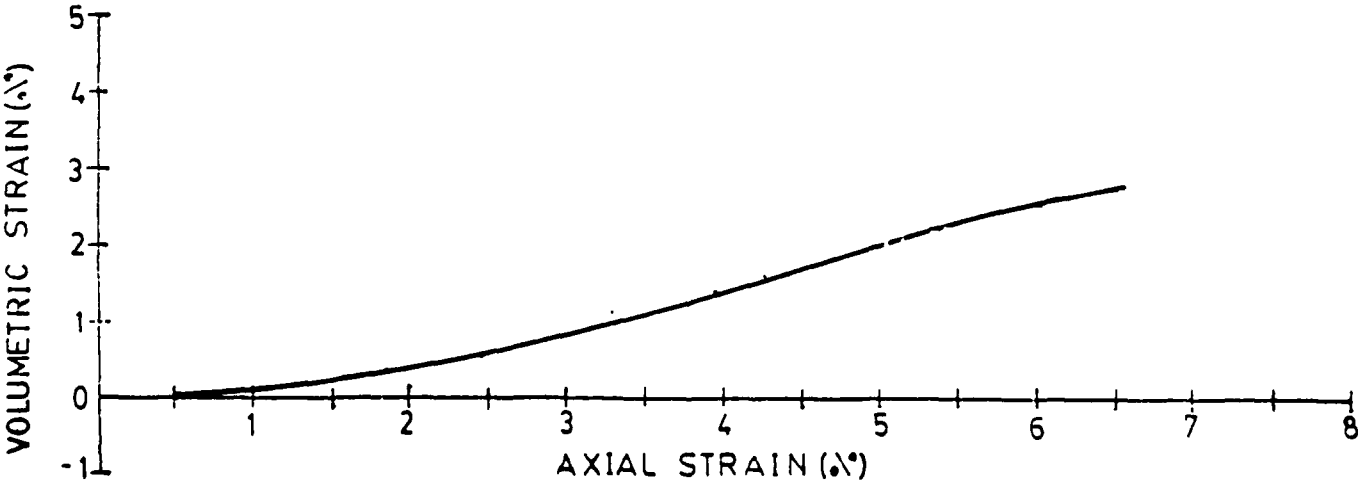
VOLUMETRIC STRAIN (%)
5
4
3
2
1
0
-1
1
2
3
4
5
6
7
8
AXIAL STRAIN (%)

TEST 5

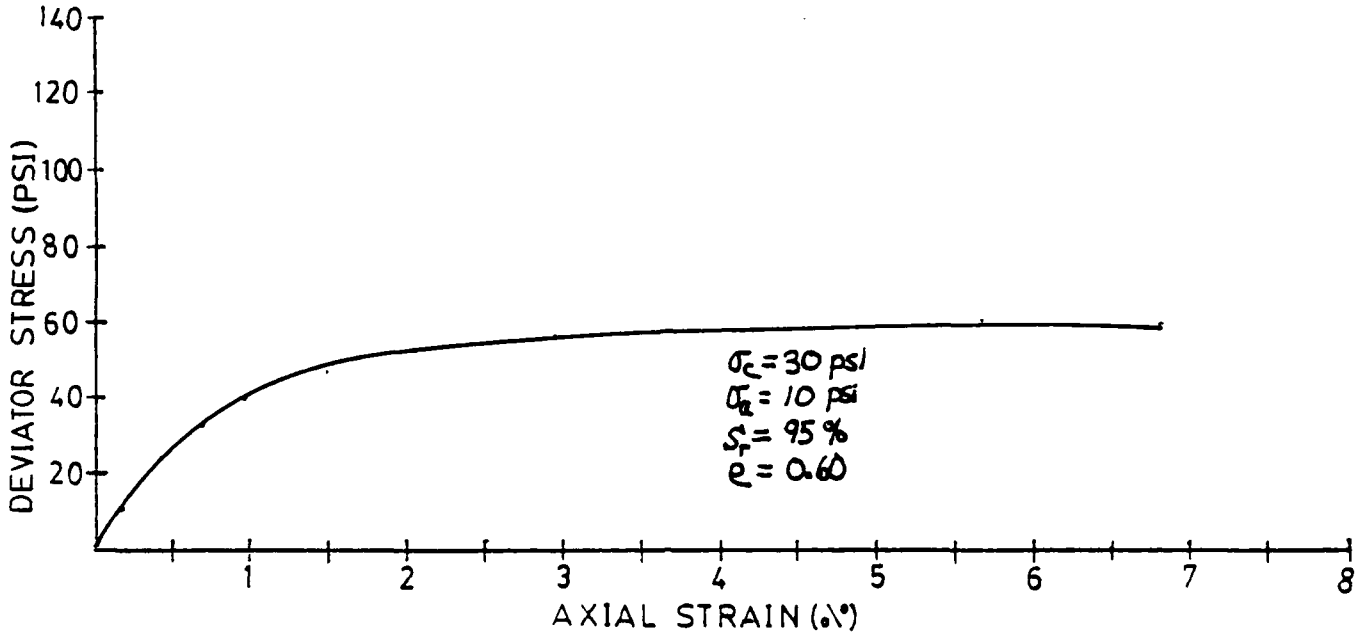
DEVIATOR STRESS (PSI)
140
120
100
80
60
40
20
1
2
3
4
5
6
7
8
AXIAL STRAIN (%)
σ_c = 30 psi
σ_3 = 10 psi
S_r = 95 %
e = 0.60

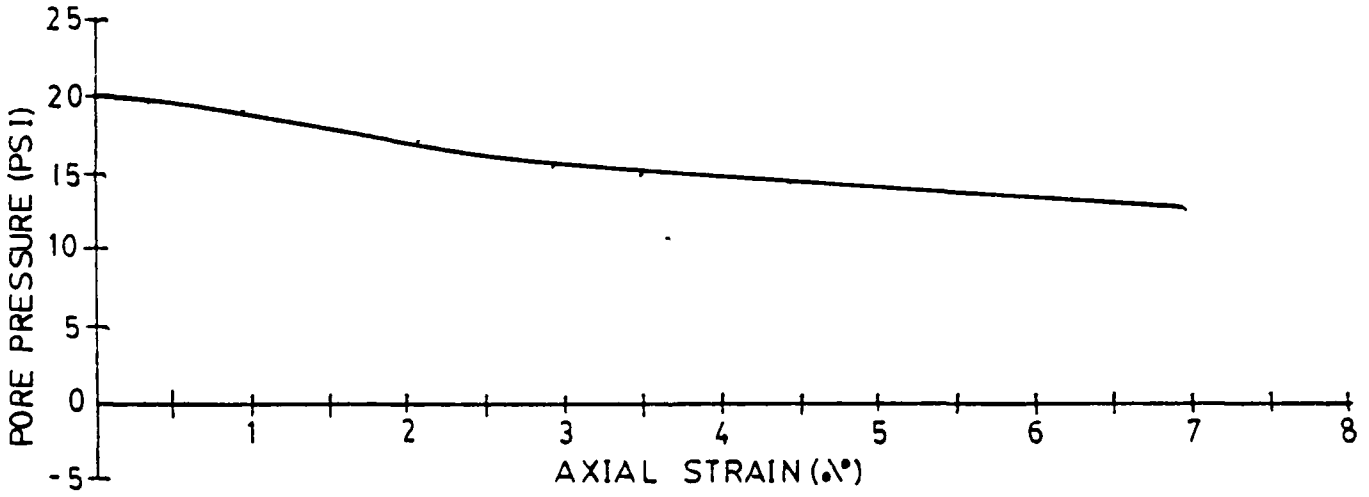
PORE PRESSURE (PSI)
25
20
15
10
5
0
-5
1
2
3
4
5
6
7
8
AXIAL STRAIN (%)

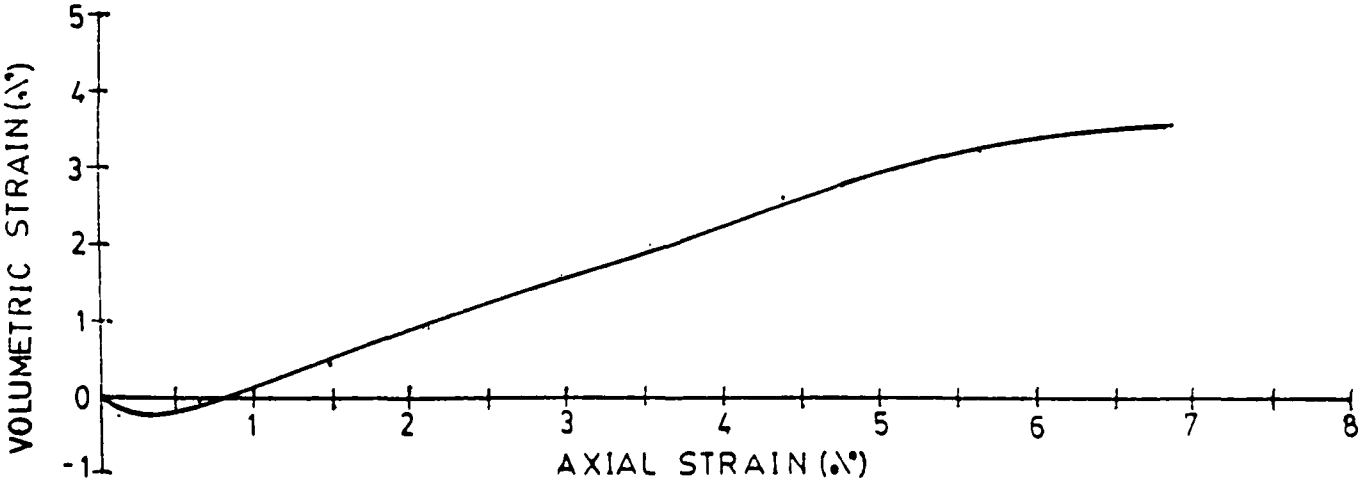
VOLUMETRIC STRAIN (%)
5
4
3
2
1
0
-1
1
2
3
4
5
6
7
8
AXIAL STRAIN (%)

TEST 6A

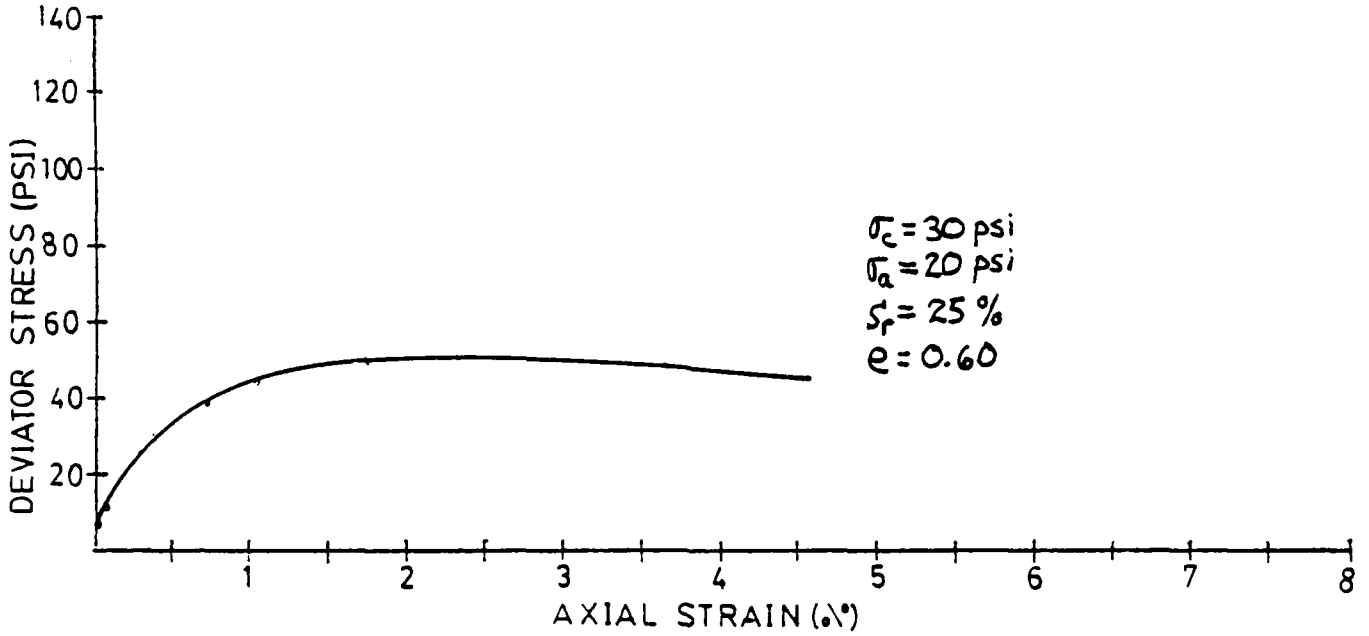
DEVIATOR STRESS (PSI)
140
120
100
80
60
40
20
1
2
3
4
5
6
7
8
AXIAL STRAIN (%)
σ_c = 30 psi
σ_a = 20 psi
S_r = 25 %
e = 0.60

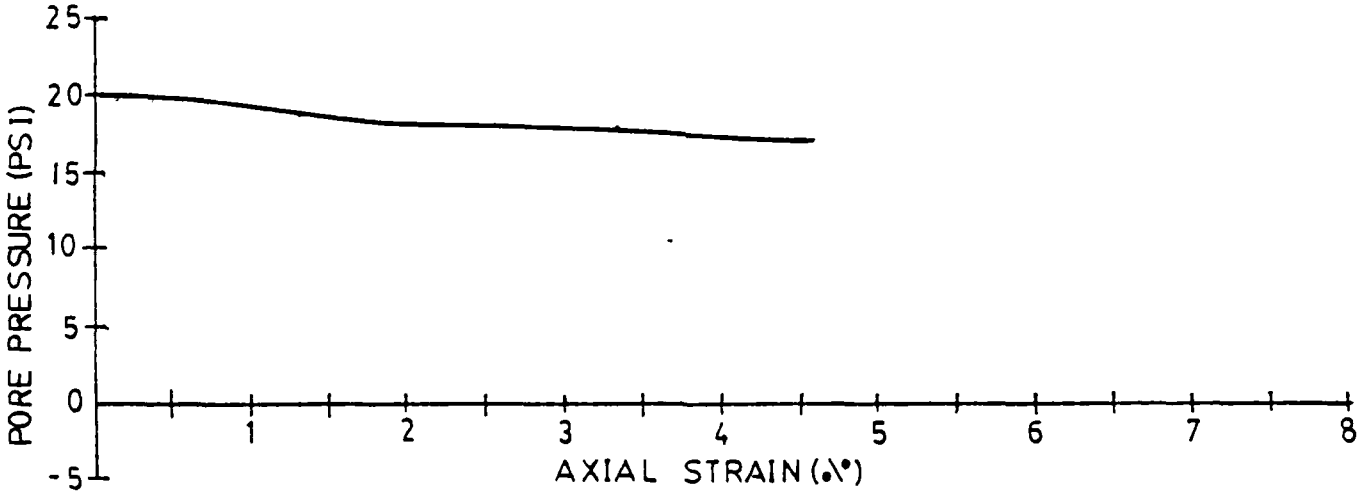
PORE PRESSURE (PSI)
25
20
15
10
5
0
-5
1
2
3
4
5
6
7
8
AXIAL STRAIN (%)

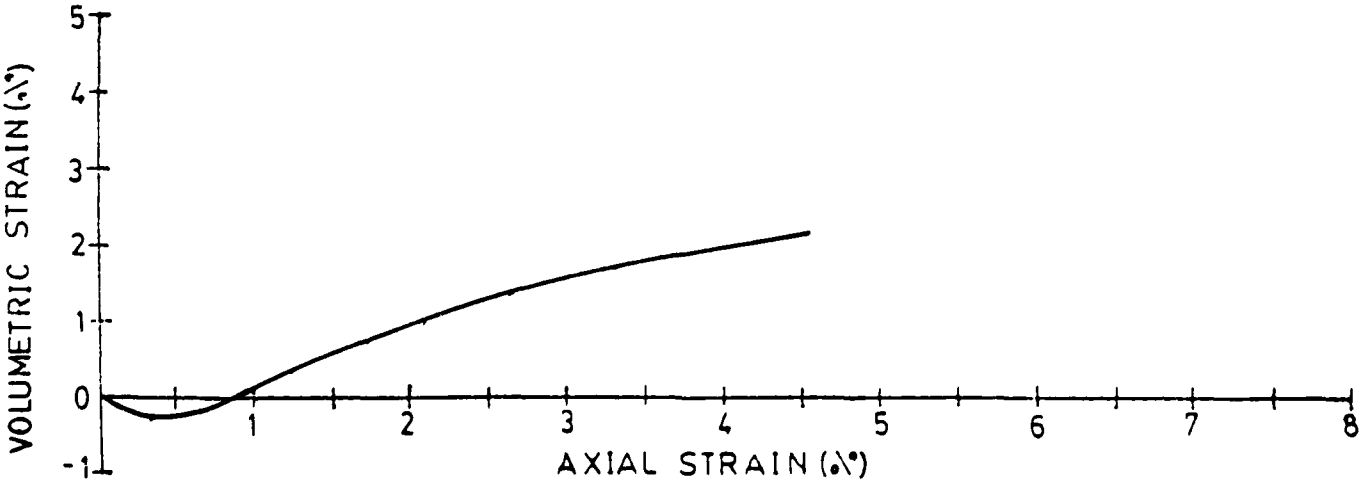
VOLUMETRIC STRAIN (%)
5
4
3
2
1
0
-1
1
2
3
4
5
6
7
8
AXIAL STRAIN (%)

TEST 6.B

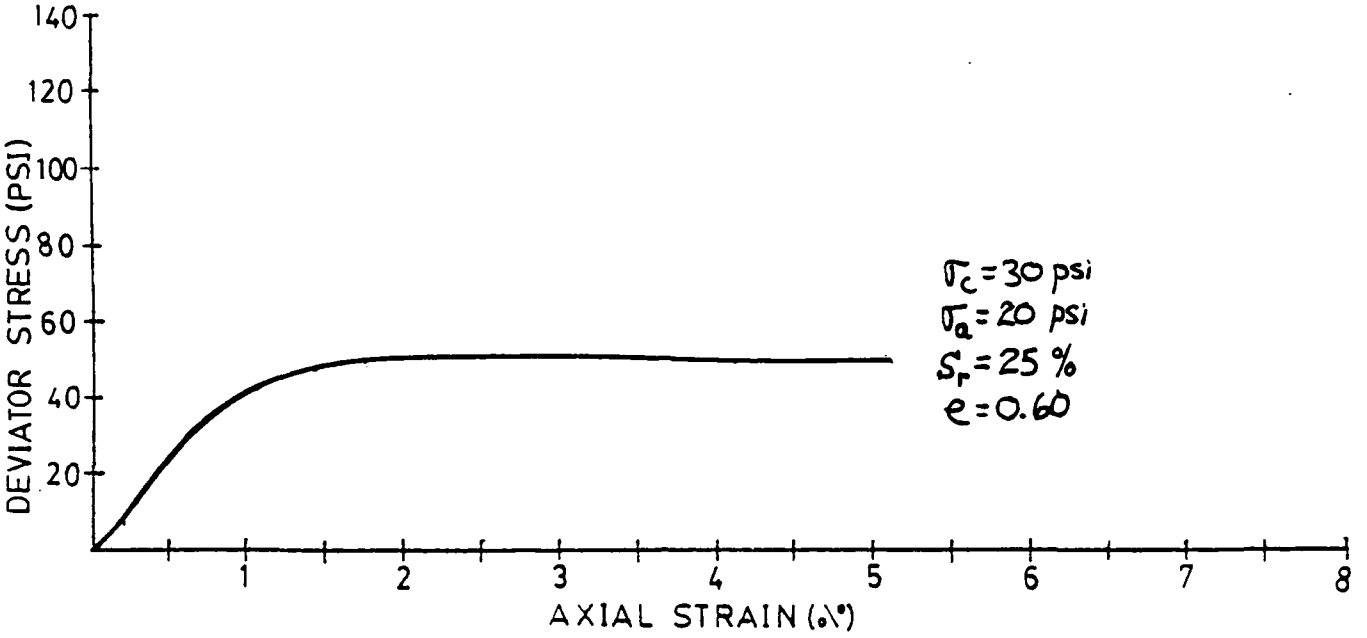
DEVIATOR STRESS (PSI)
140
120
100
80
60
40
20
1
2
3
4
5
6
7
8
AXIAL STRAIN (%)
σ_c = 30 psi
σ_a = 20 psi
S_r = 25 %
e = 0.60

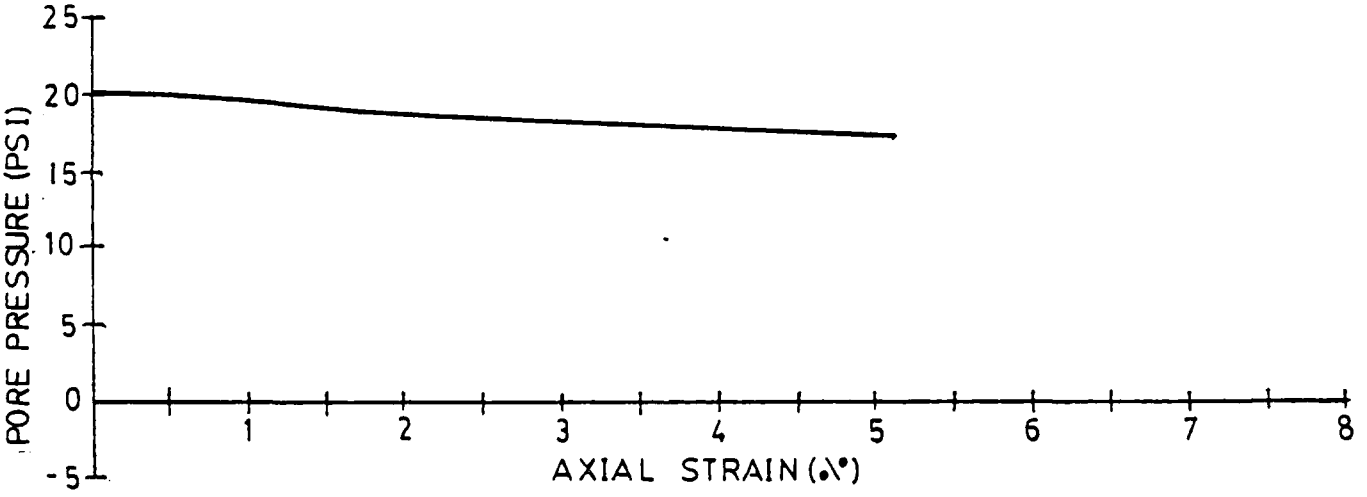
PORE PRESSURE (PSI)
25
20
15
10
5
0
-5
1
2
3
4
5
6
7
8
AXIAL STRAIN (%)

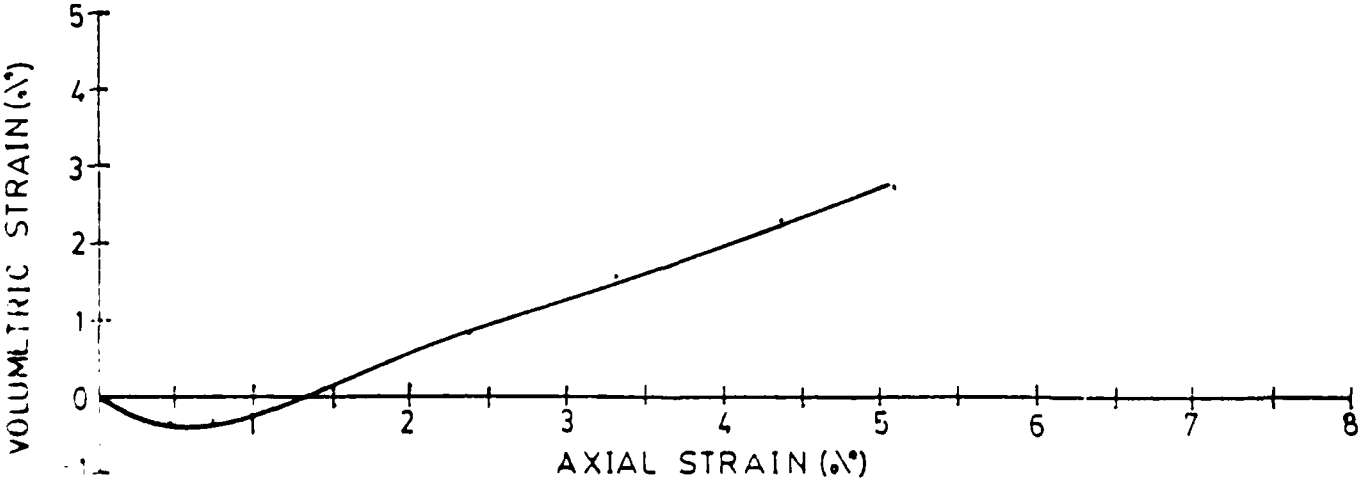
VOLUMETRIC STRAIN (%)
5
4
3
2
1
0
2
3
4
5
6
7
8
AXIAL STRAIN (%)

TEST 7

$\sigma_c = 30$ psi
$\sigma_a = 10$ psi
$S_r = 100\%$
$e = 0.80$

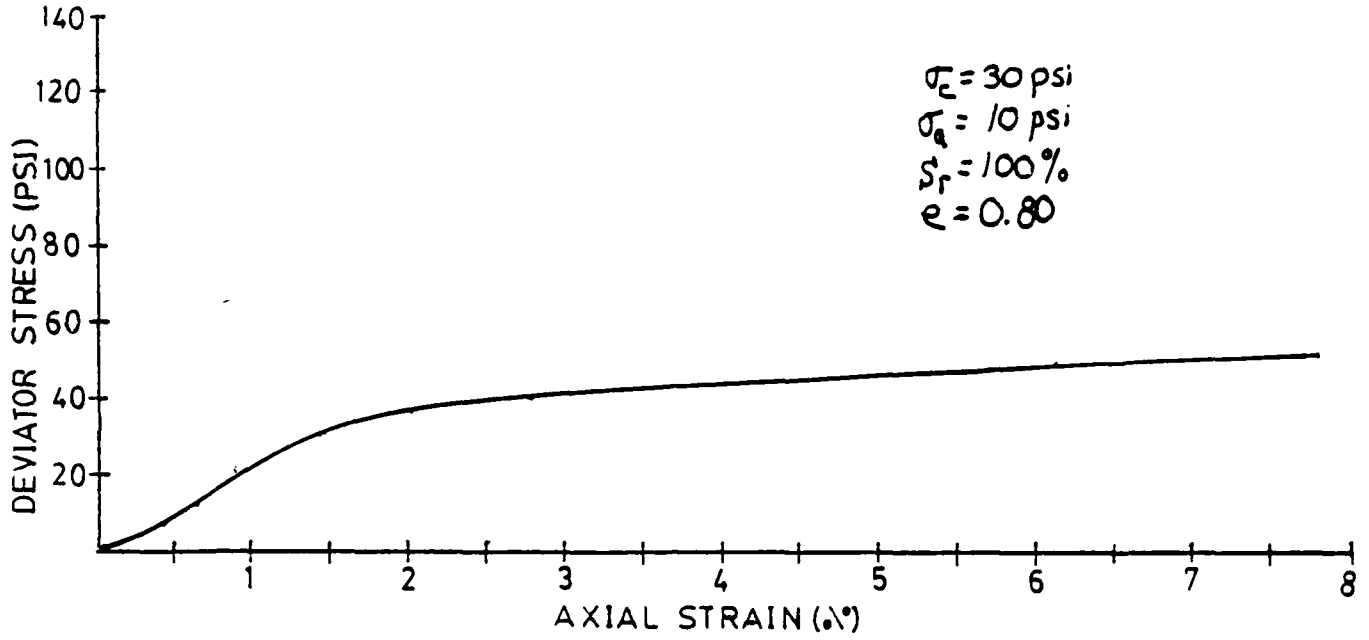

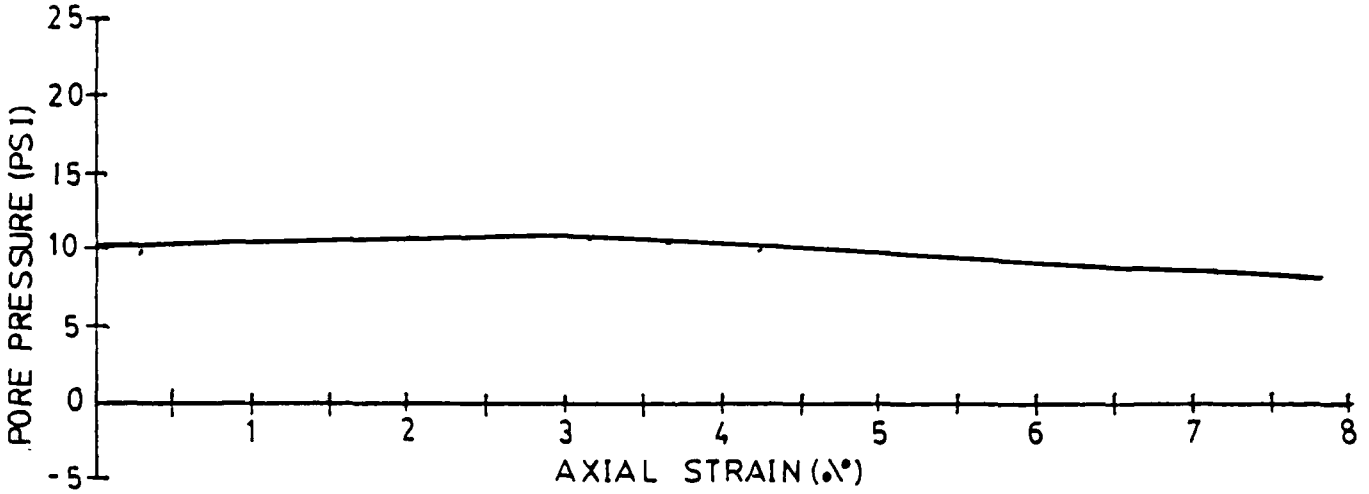

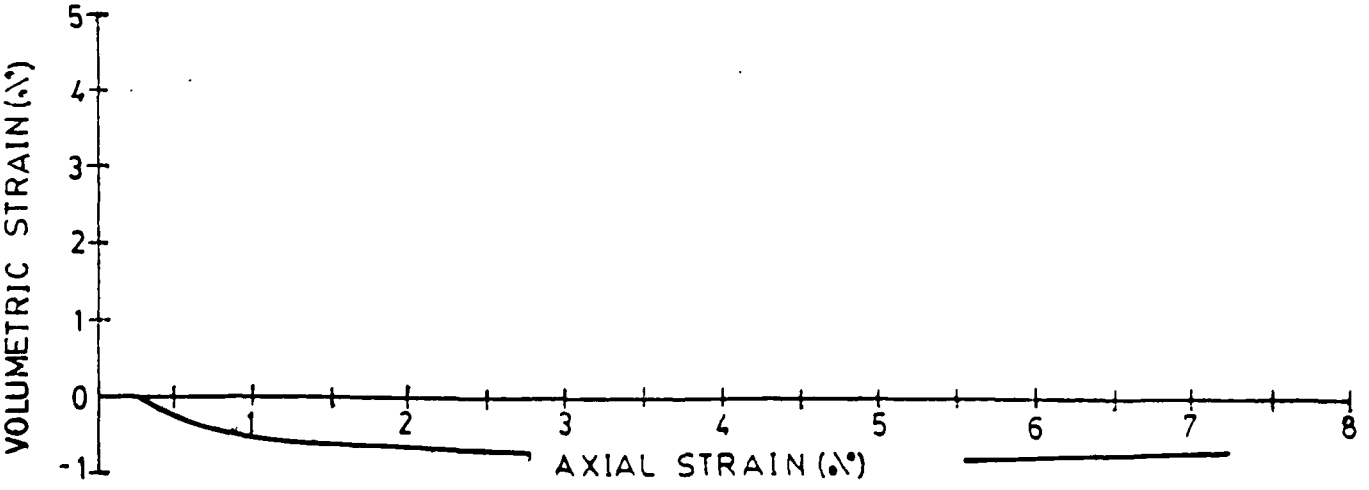

TEST 8

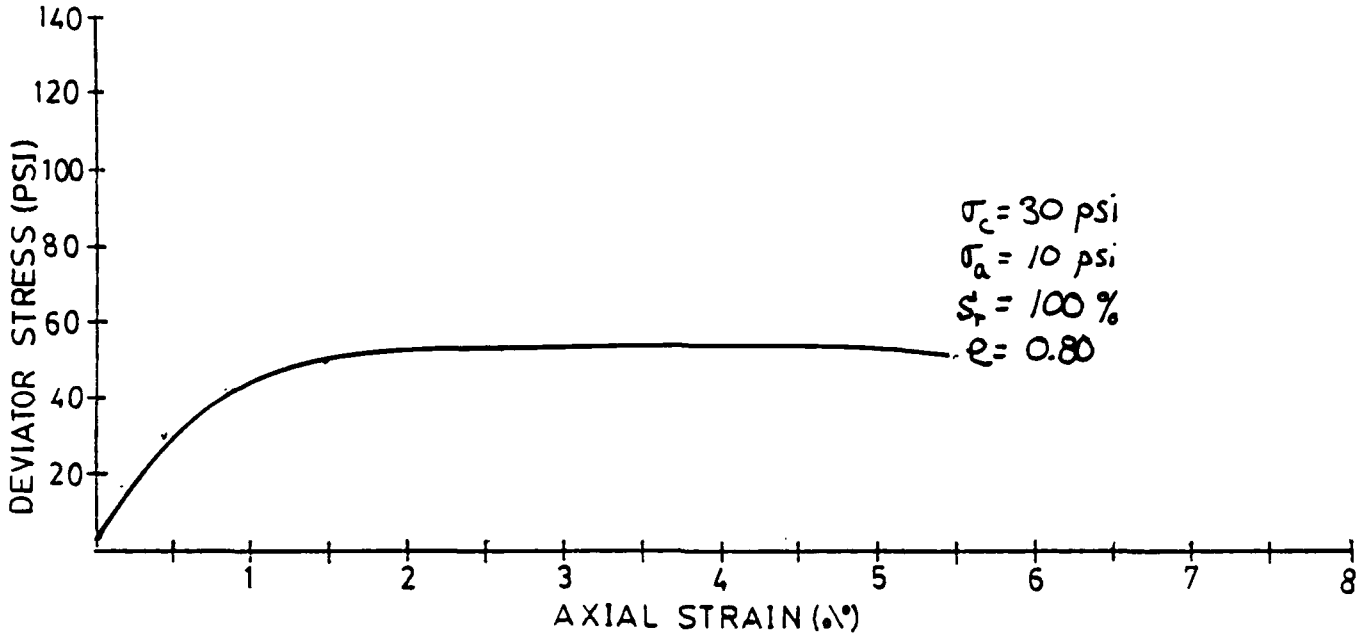
DEVIATOR STRESS (PSI)
140
120
100
80
60
40
20
1
2
3
4
5
6
7
8
AXIAL STRAIN (%)
σ_c = 30 psi
σ_a = 10 psi
S_r = 100 %
e = 0.80

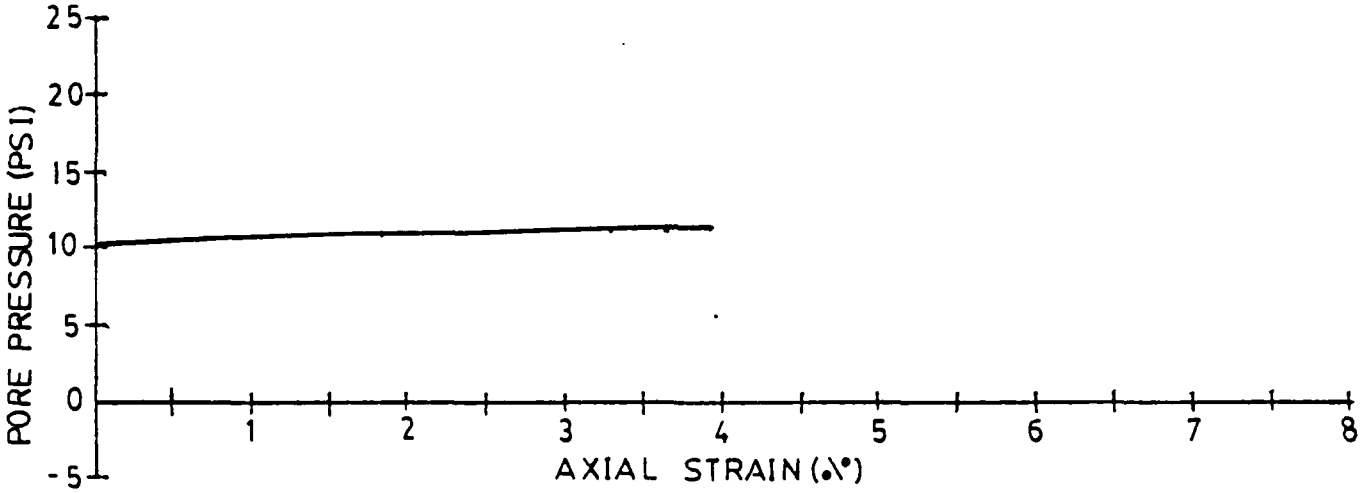
PORE PRESSURE (PSI)
25
20
15
10
5
0
-5
1
2
3
4
5
6
7
8
AXIAL STRAIN (%)

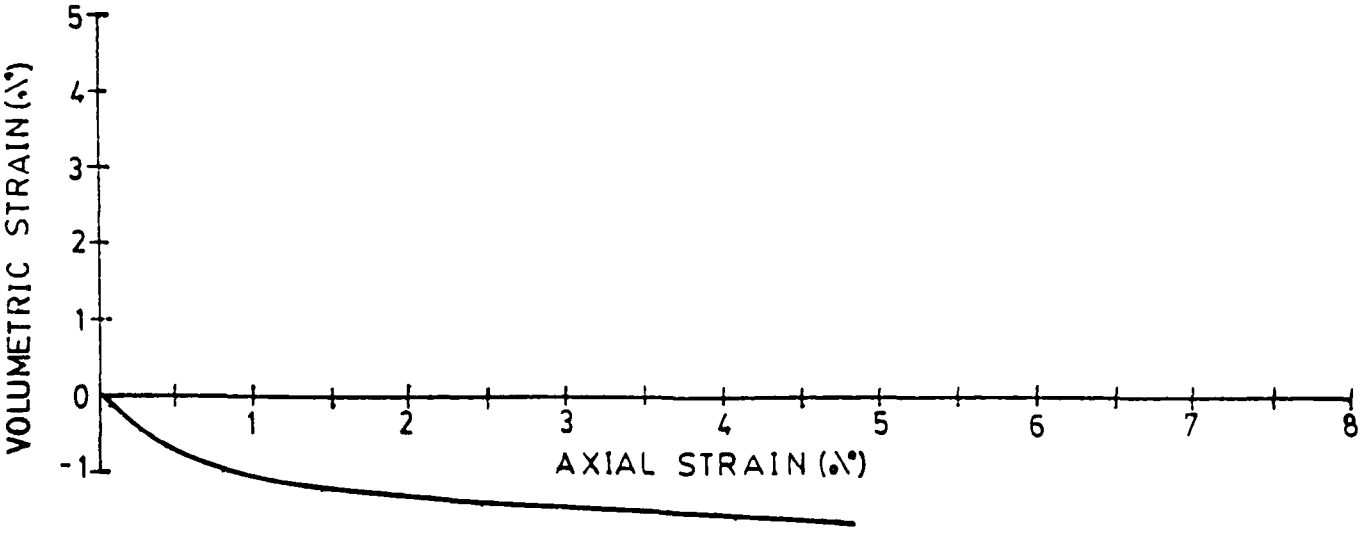
VOLUMETRIC STRAIN (%)
5
4
3
2
1
0
-1
1
2
3
4
5
6
7
8
AXIAL STRAIN (%)

TEST 9

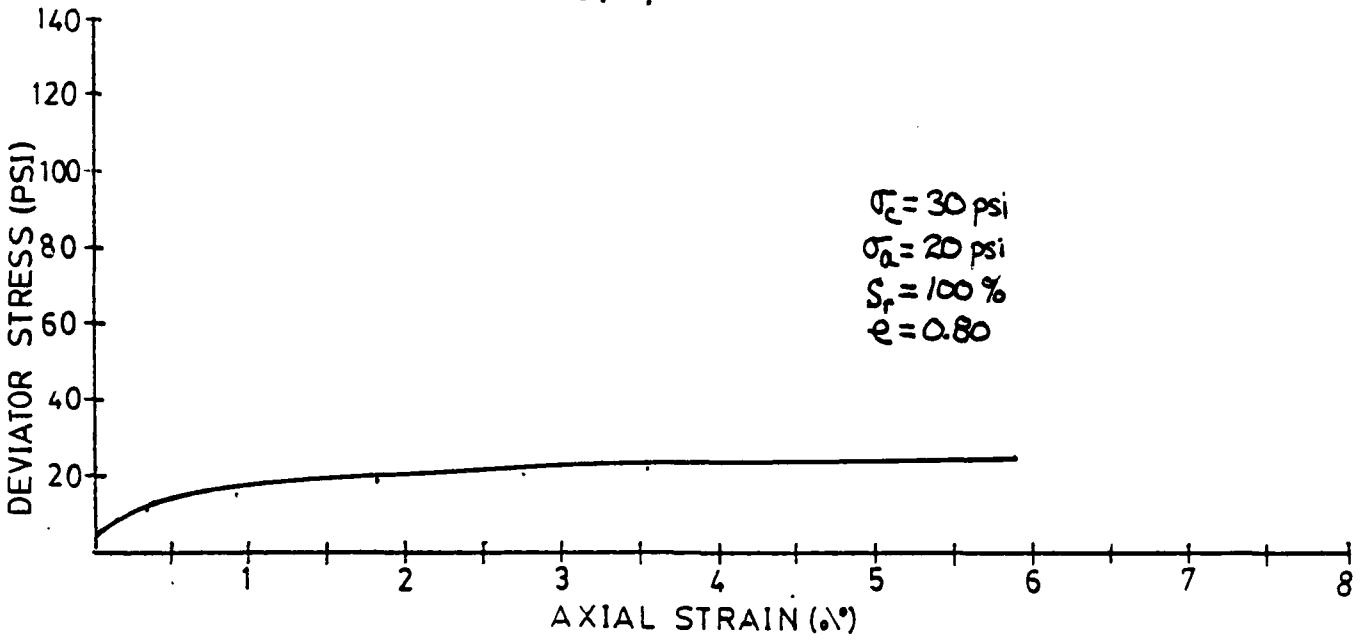
DEVIATOR STRESS (PSI)
140
120
100
80
60
40
20
1
2
3
4
5
6
7
8
AXIAL STRAIN (%)
σ_c = 30 psi
σ_a = 20 psi
S_r = 100 %
e = 0.80

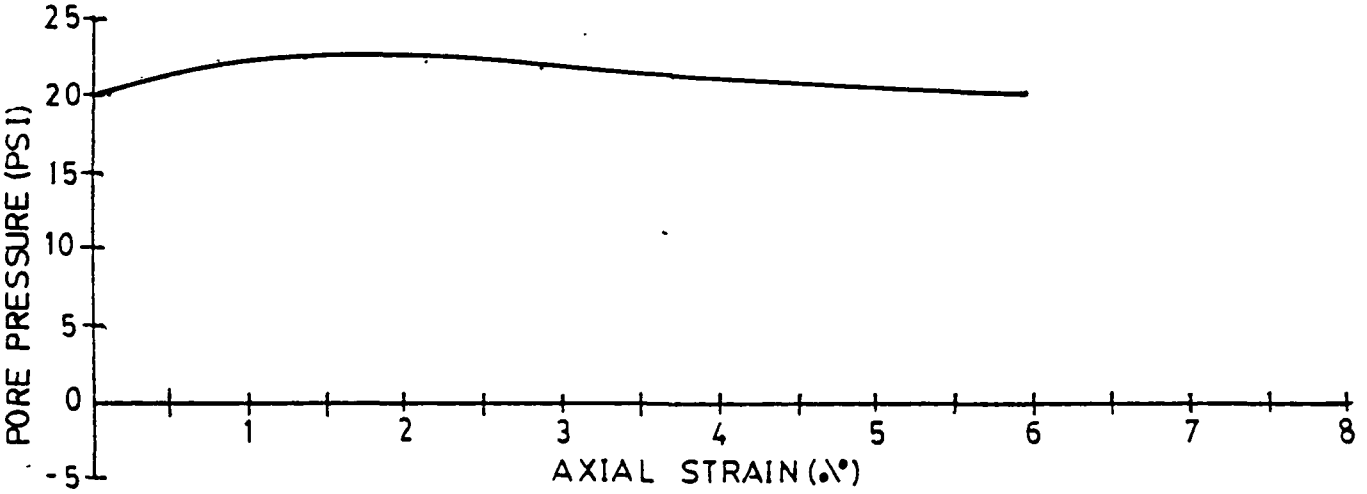
PORE PRESSURE (PSI)
25
20
15
10
5
0
-5
1
2
3
4
5
6
7
8
AXIAL STRAIN (%)

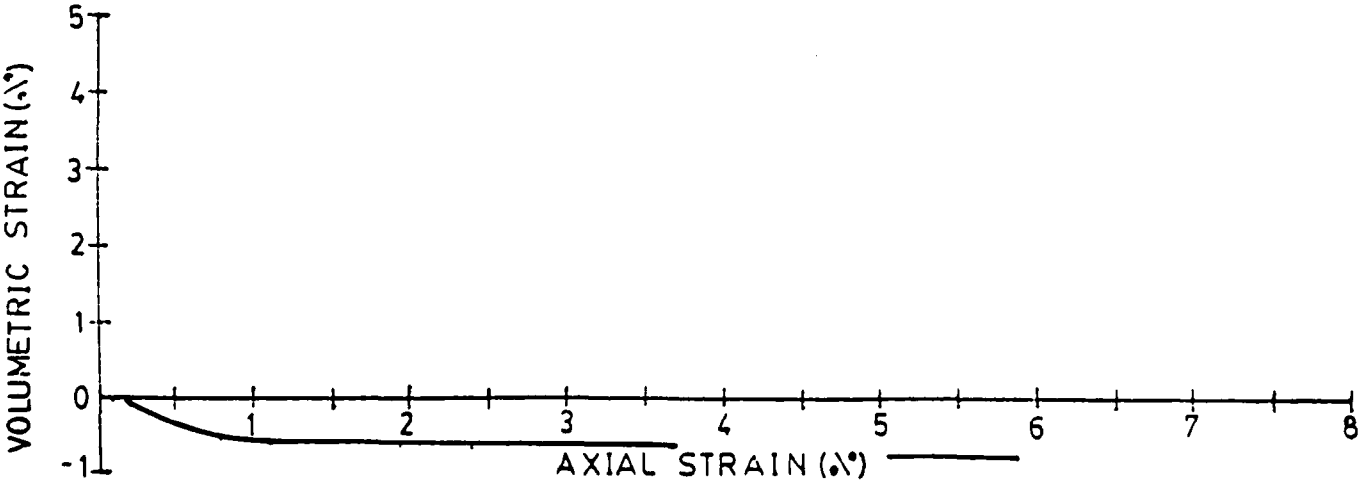
VOLUMETRIC STRAIN (%)
5
4
3
2
1
0
-1
1
2
3
4
5
6
7
8
AXIAL STRAIN (%)

TEST 10

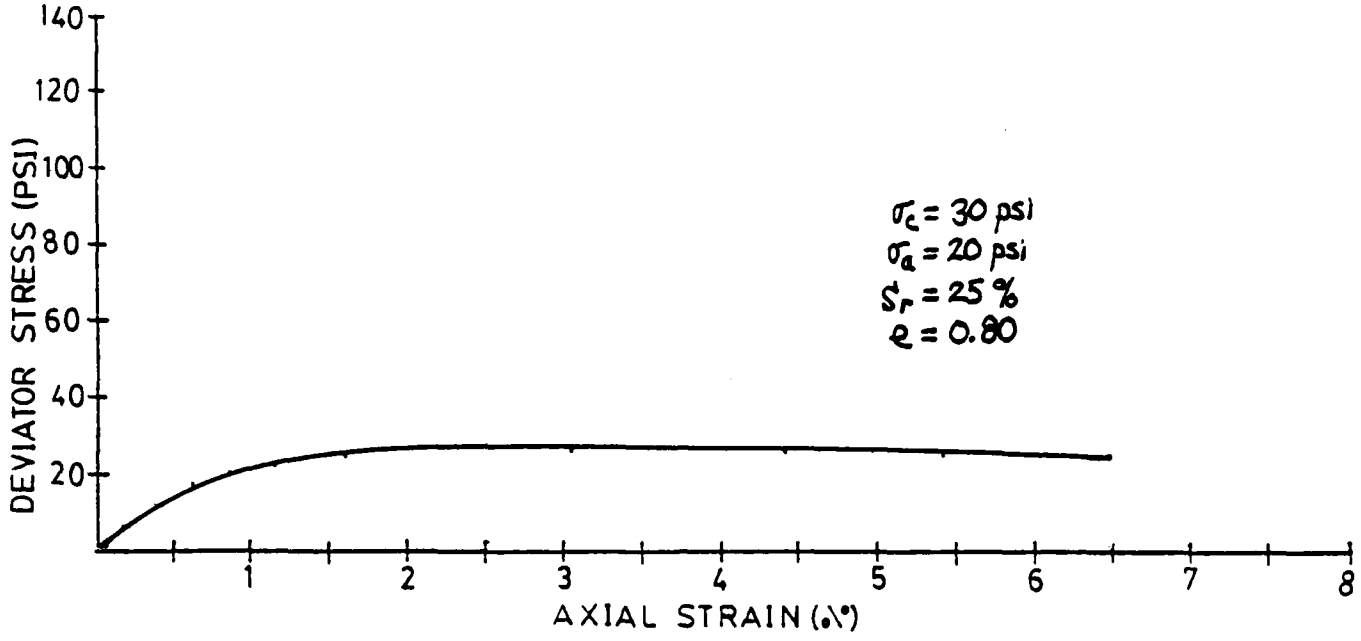
DEVIATOR STRESS (PSI)
140
120
100
80
60
40
20
1
2
3
4
5
6
7
8
AXIAL STRAIN (%)
σ_c = 30 psi
σ_d = 20 psi
S_r = 25 %
e = 0.80

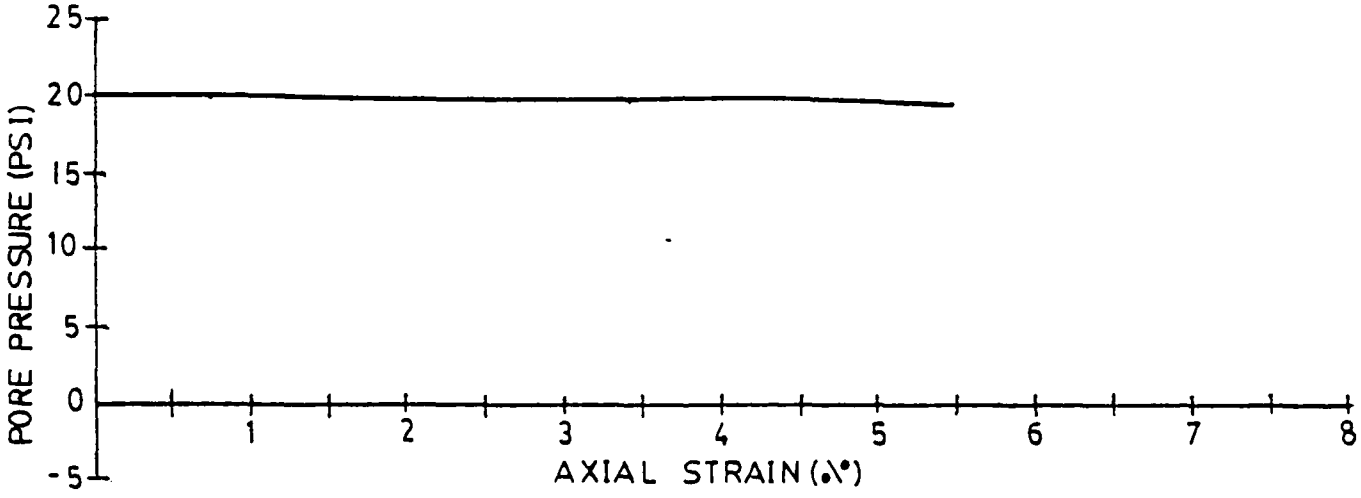
PORE PRESSURE (PSI)
25
20
15
10
5
0
-5
1
2
3
4
5
6
7
8
AXIAL STRAIN (%)

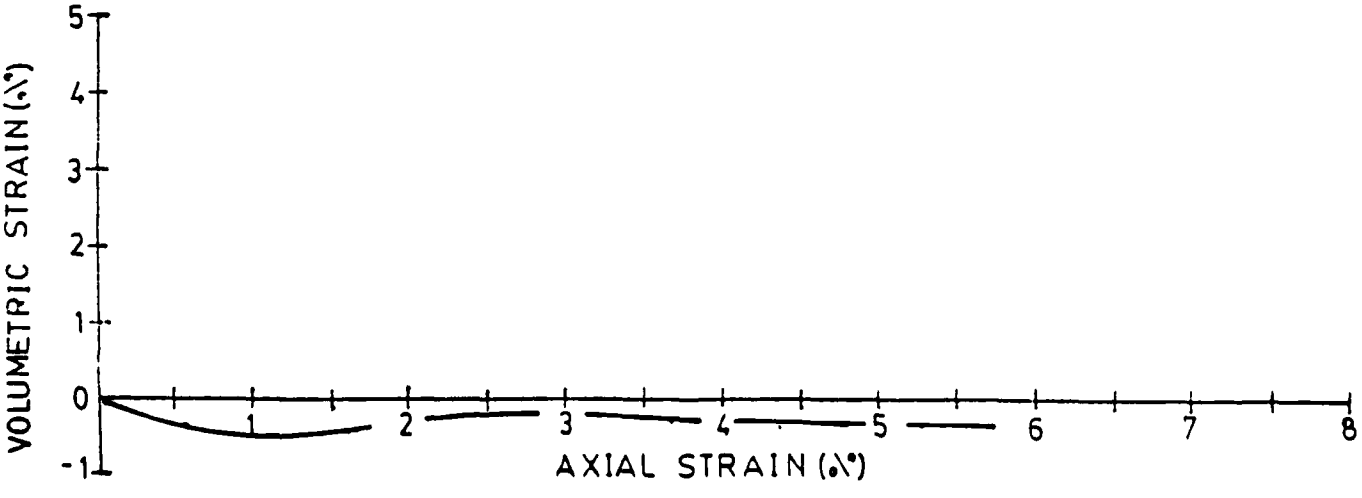
VOLUMETRIC STRAIN (%)
5
4
3
2
1
0
-1
1
2
3
4
5
6
7
8
AXIAL STRAIN (%)

TEST 11

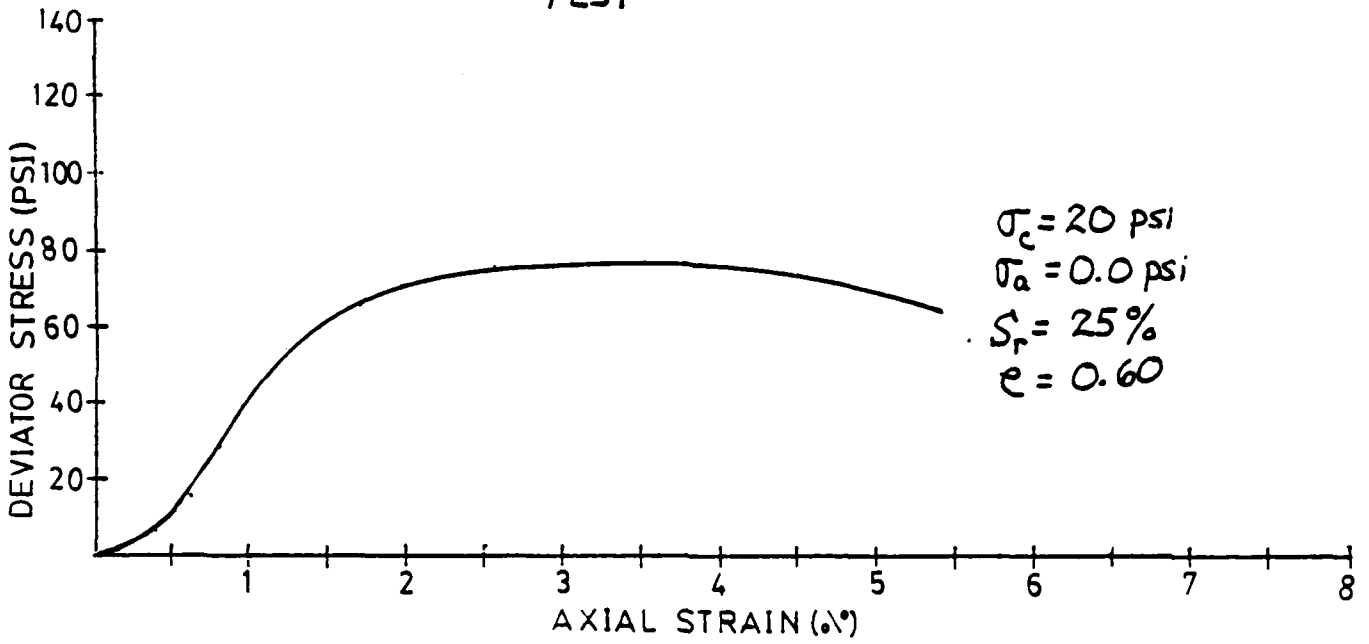
DEVIATOR STRESS (PSI)
140
120
100
80
60
40
20
1
2
3
4
5
6
7
8
AXIAL STRAIN (%)
σ_c = 20 psi
σ_a = 0.0 psi
S_r = 25%
e = 0.60

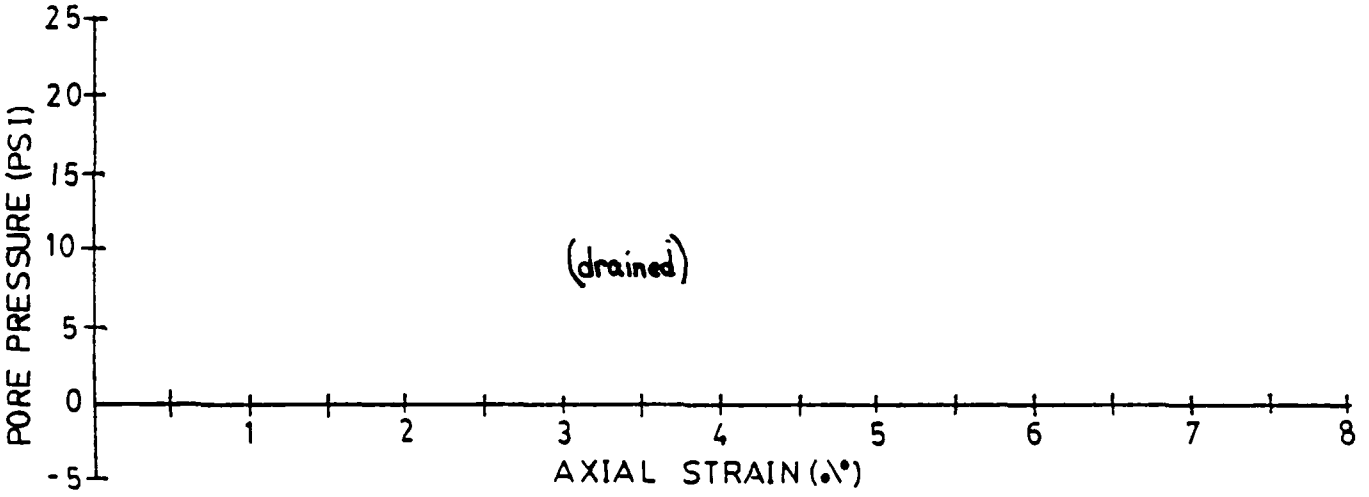
PORE PRESSURE (PSI)
25
20
15
10
5
0
-5
1
2
3
4
5
6
7
8
AXIAL STRAIN (%)
(drained)

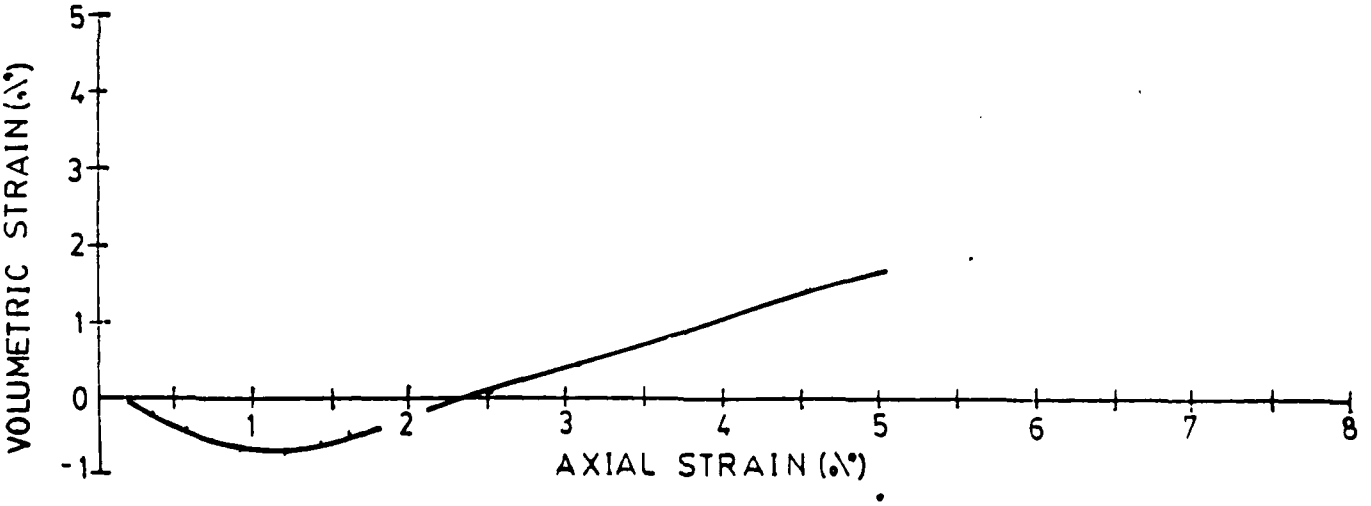
VOLUMETRIC STRAIN (%)
5
4
3
2
1
0
-1
1
2
3
4
5
6
7
8
AXIAL STRAIN (%)

TEST 12

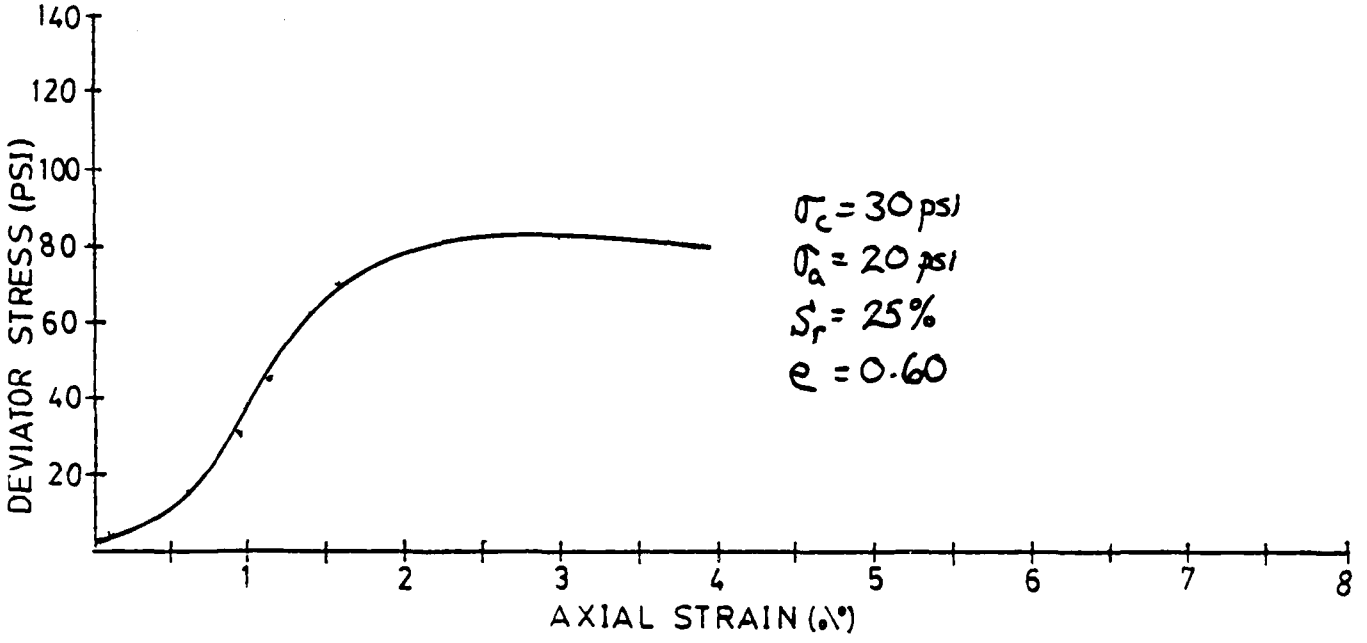
DEVIATOR STRESS (PSI)
140
120
100
80
60
40
20
1
2
3
4
5
6
7
8
AXIAL STRAIN (%)
σ_c = 30 psi
σ_a = 20 psi
S_r = 25%
e = 0.60

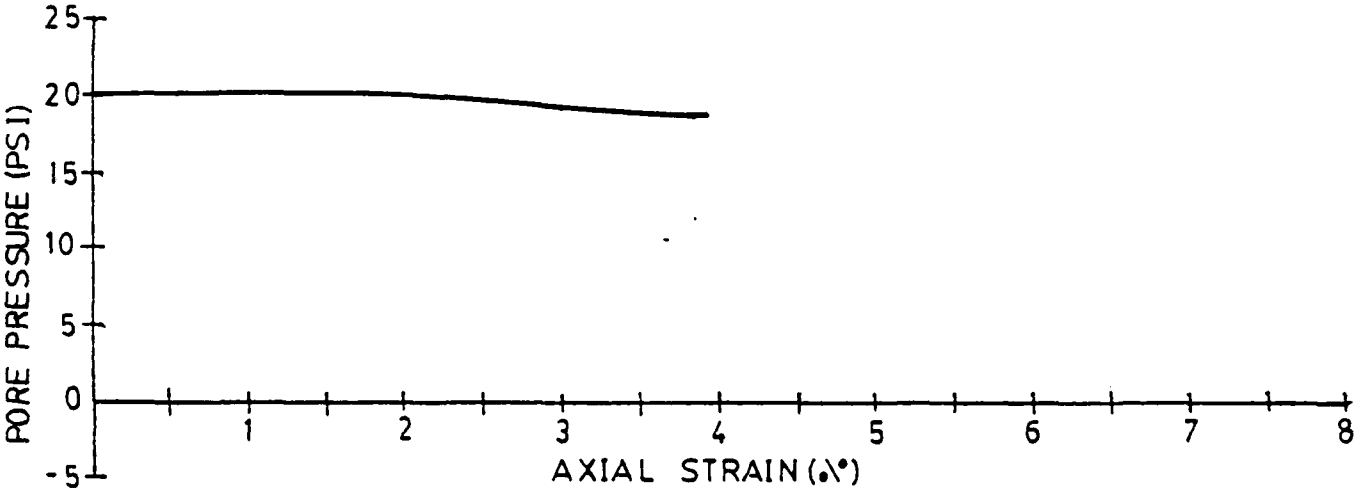
PORE PRESSURE (PSI)
25
20
15
10
5
0
-5
1
2
3
4
5
6
7
8
AXIAL STRAIN (%)

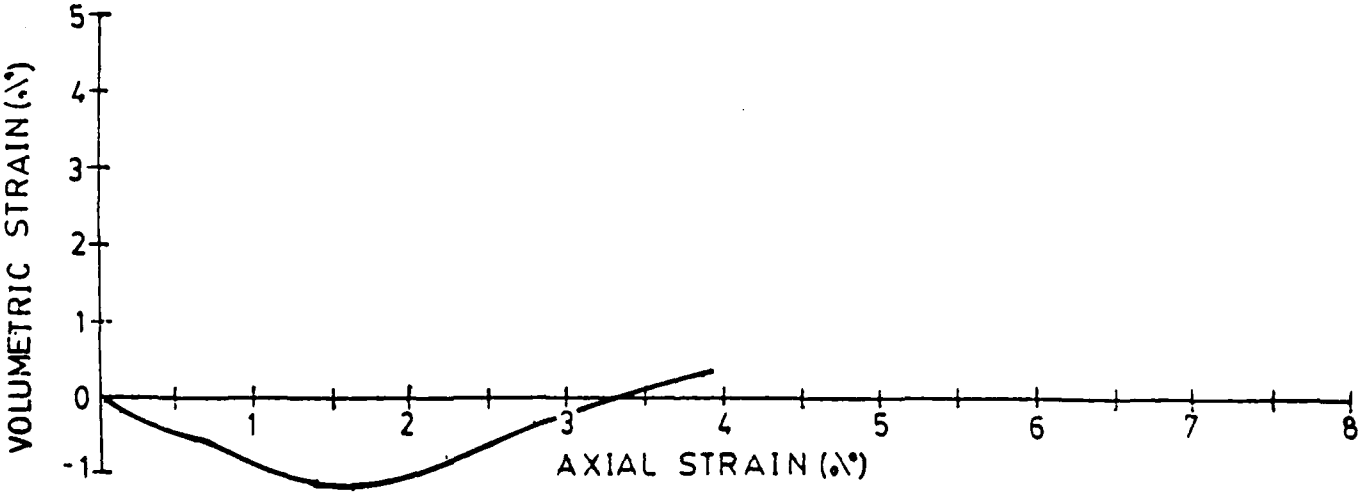
VOLUMETRIC STRAIN (%)
5
4
3
2
1
0
-1
1
2
3
4
5
6
7
8
AXIAL STRAIN (%)

TEST 13

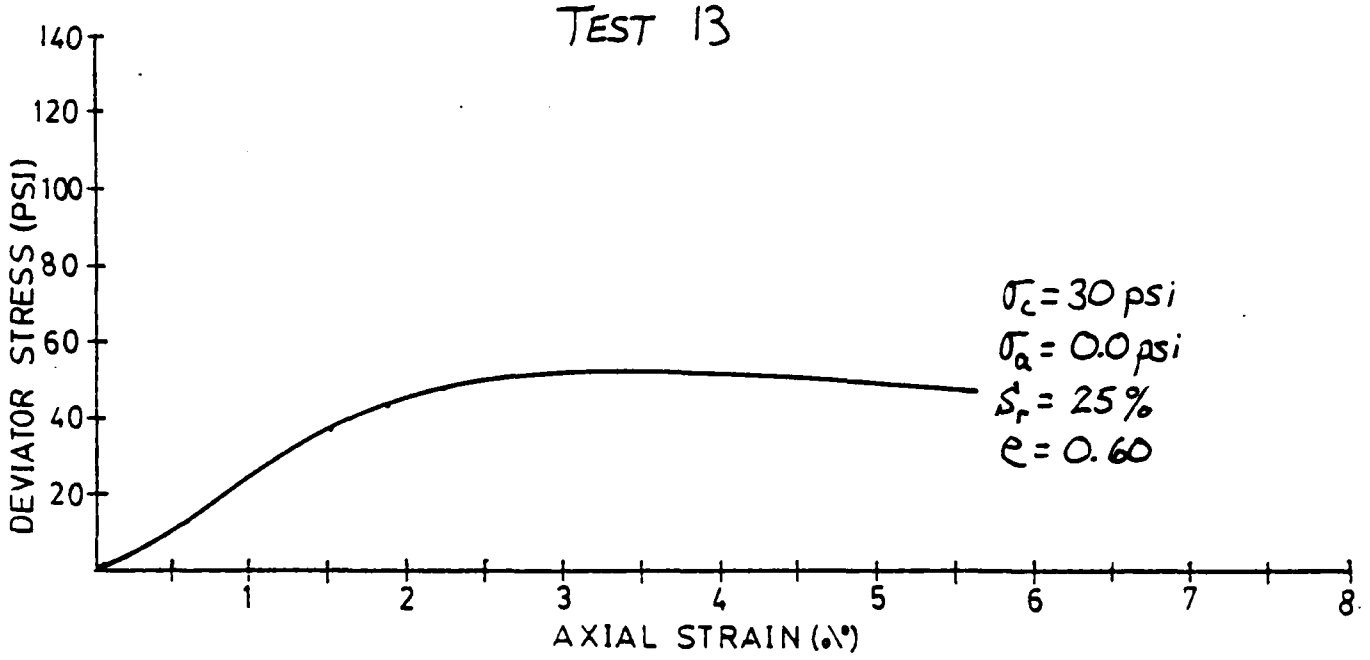
DEVIATOR STRESS (PSI)
140
120
100
80
60
40
20
1
2
3
4
5
6
7
8
AXIAL STRAIN (%)
$\sigma_c = 30$ psi
$\sigma_a = 0.0$ psi
$\varepsilon_r = 25\%$
$e = 0.60$

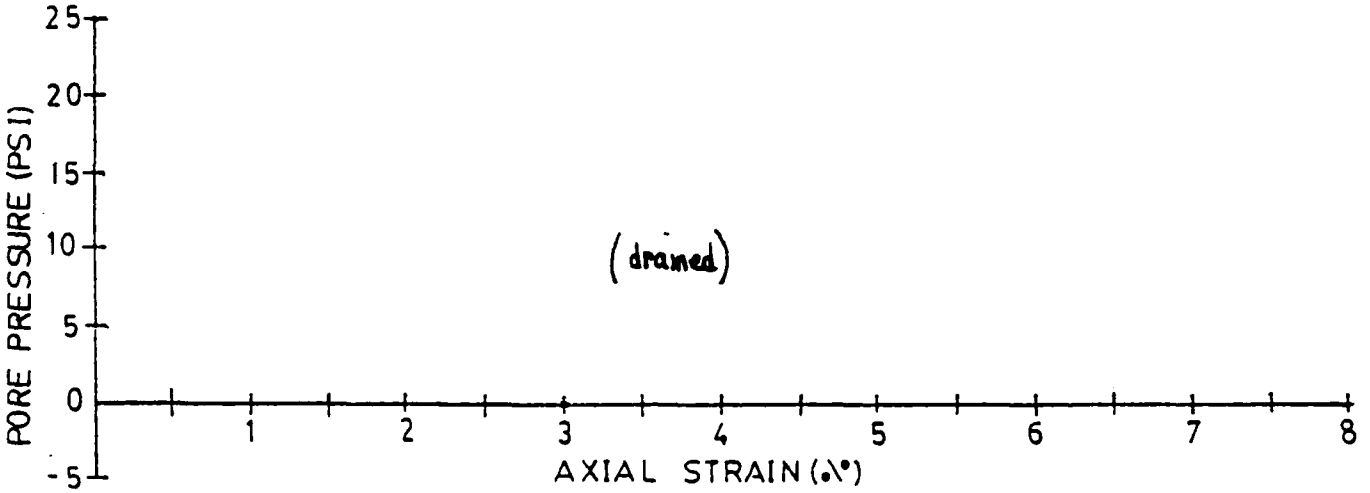
PORE PRESSURE (PSI)
25
20
15
10
5
0
-5
1
2
3
4
5
6
7
8
AXIAL STRAIN (%)
(drained)

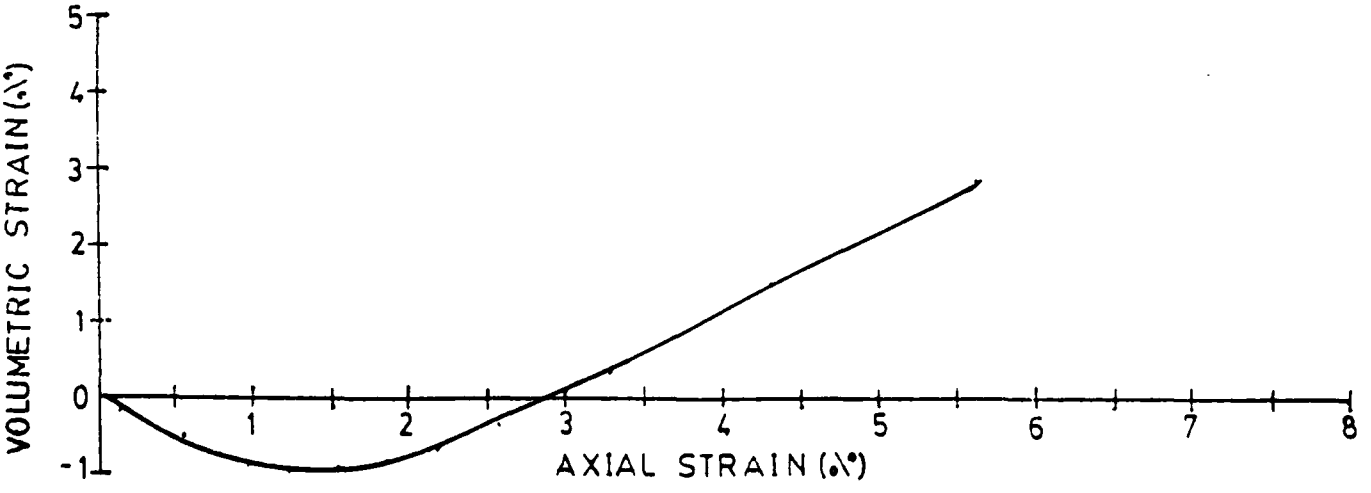
VOLUMETRIC STRAIN (%)
5
4
3
2
1
0
-1
1
2
3
4
5
6
7
8
AXIAL STRAIN (%)

TEST 14

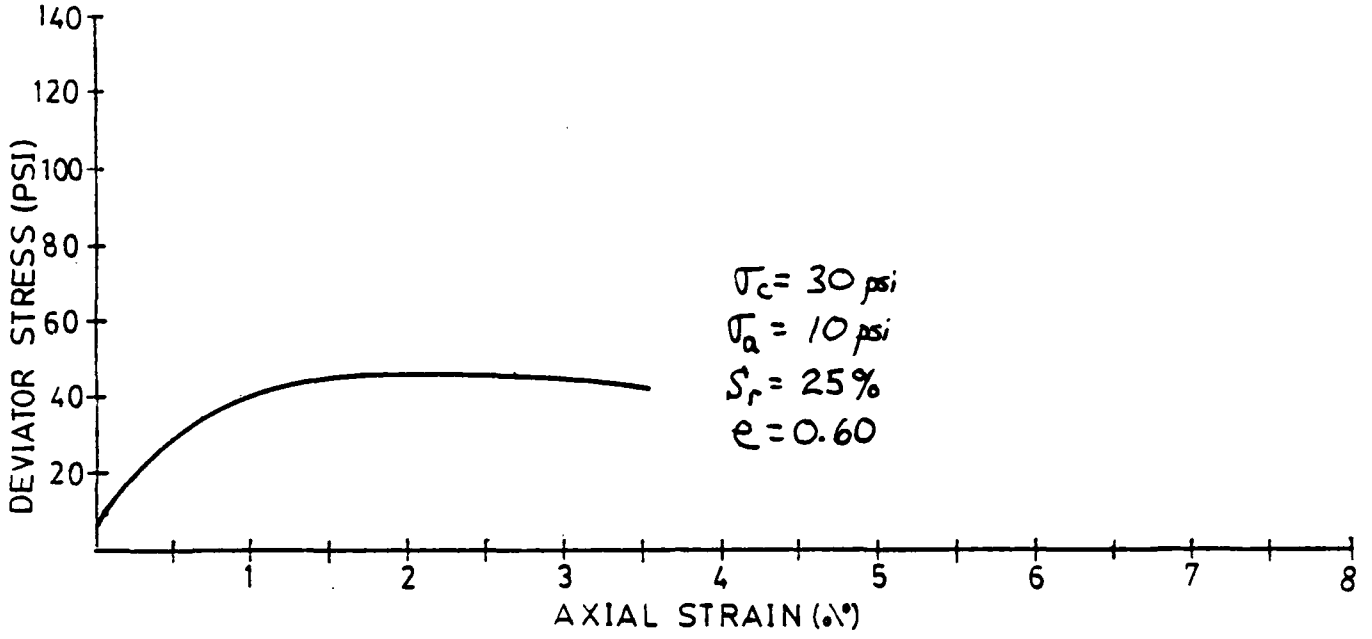
DEVIATOR STRESS (PSI)
140
120
100
80
60
40
20
1
2
3
4
5
6
7
8
AXIAL STRAIN (%)
σ_c = 30 psi
σ_a = 10 psi
S_r = 25%
e = 0.60

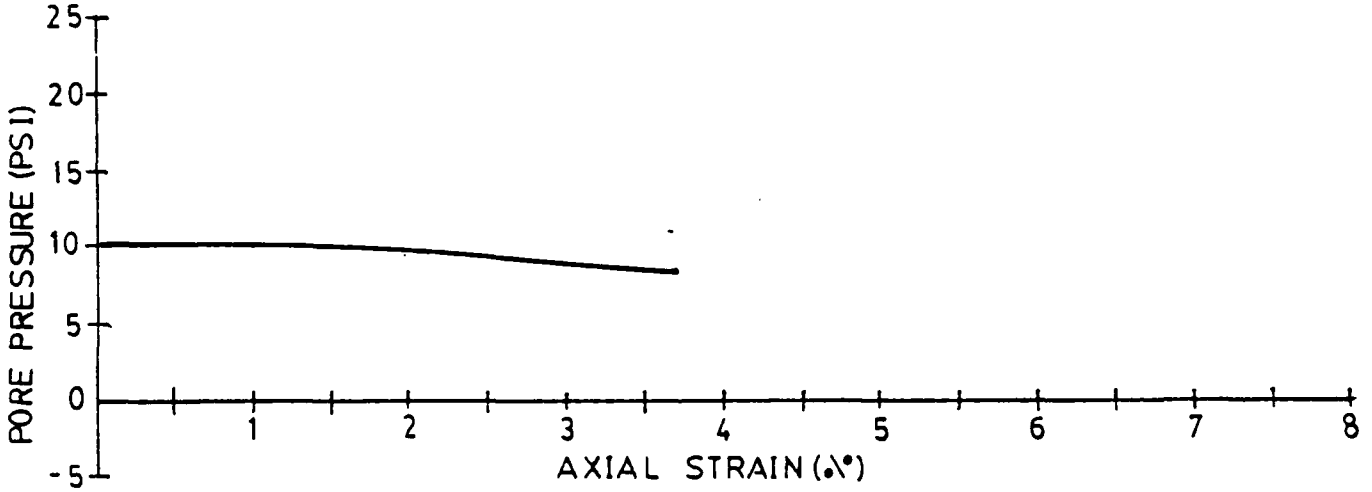
PORE PRESSURE (PSI)
25
20
15
10
5
0
-5
1
2
3
4
5
6
7
8
AXIAL STRAIN (%)

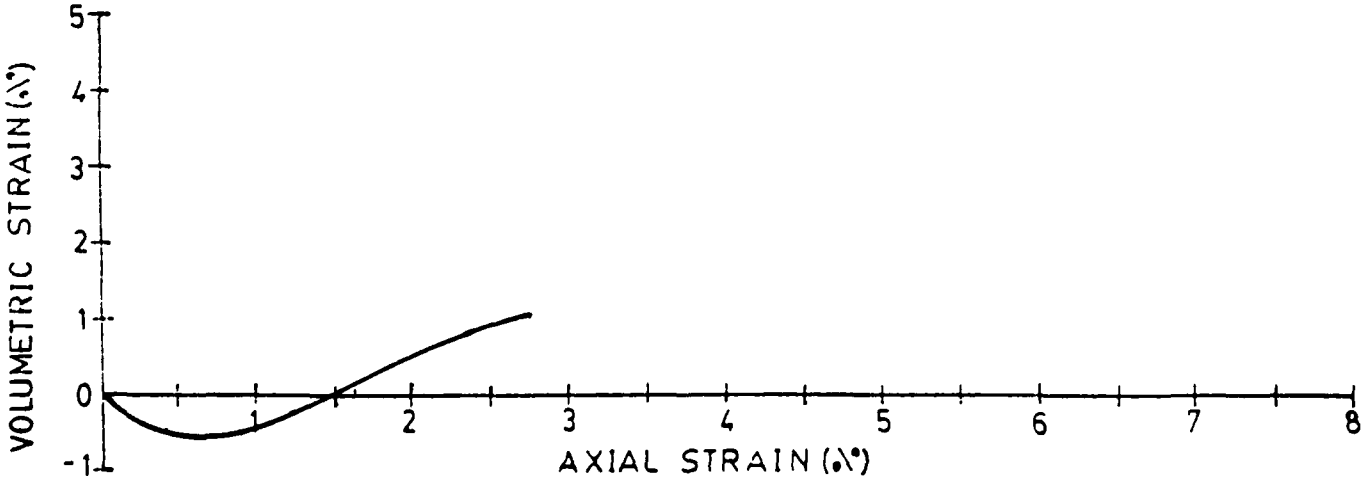
VOLUMETRIC STRAIN (%)
5
4
3
2
1
0
-1
1
2
3
4
5
6
7
8
AXIAL STRAIN (%)

TEST 15

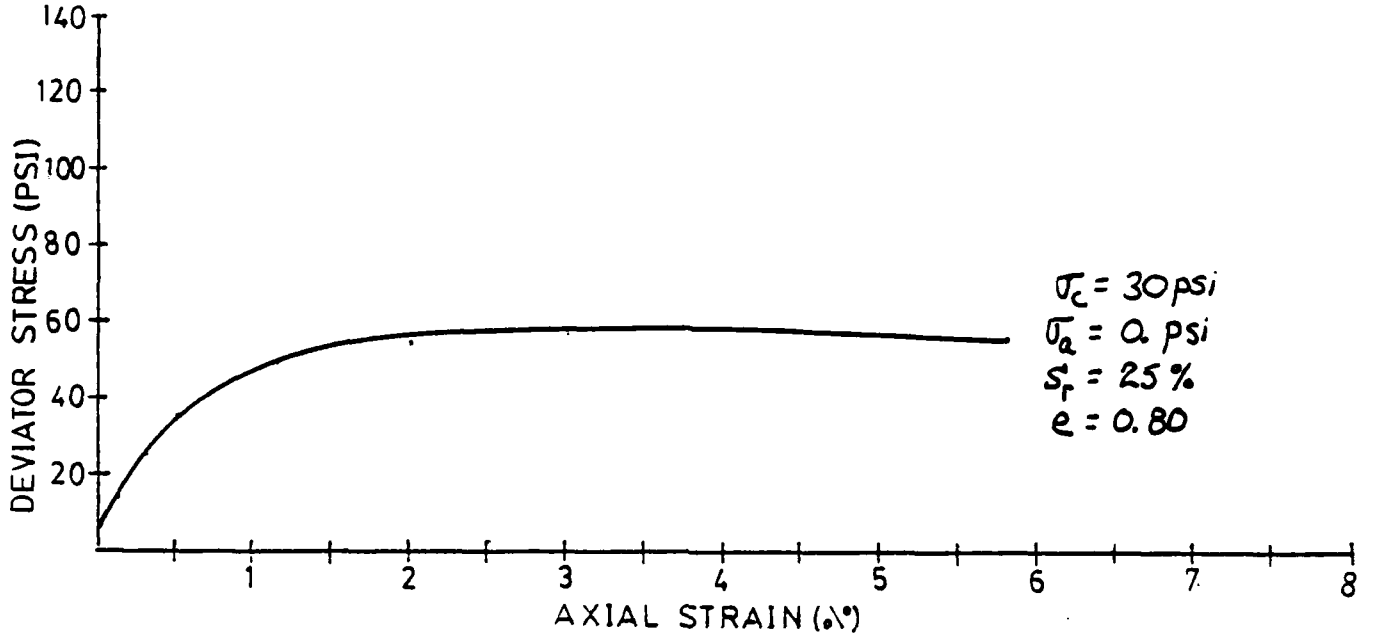
DEVIATOR STRESS (PSI)
140
120
100
80
60
40
20
1
2
3
4
5
6
7
8
AXIAL STRAIN (%)
σ_c = 30 psi
σ_a = 0 psi
S_r = 25 %
e = 0.80

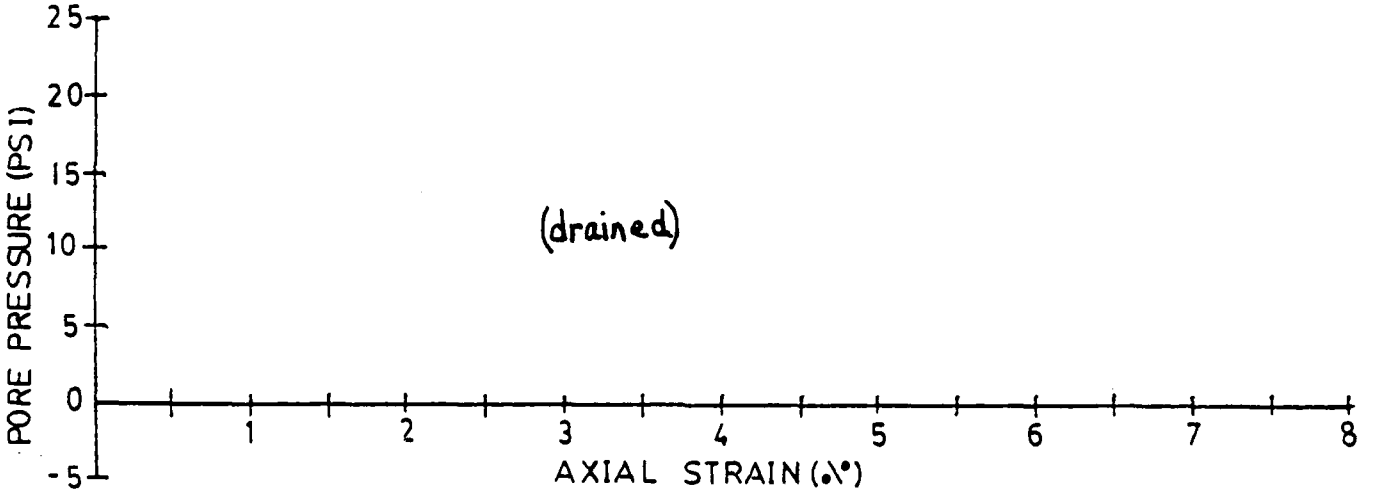
PORE PRESSURE (PSI)
25
20
15
10
5
0
-5
1
2
3
4
5
6
7
8
AXIAL STRAIN (%)
(drained)

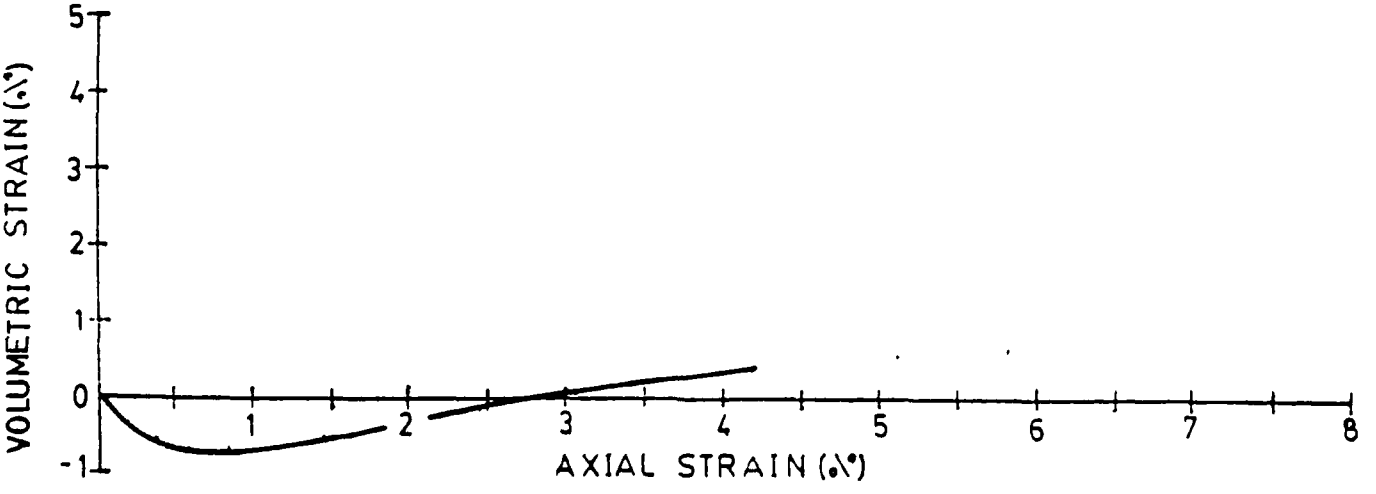
VOLUMETRIC STRAIN (%)
5
4
3
2
1
0
-1
1
2
3
4
5
6
7
8
AXIAL STRAIN (%)

TEST 16

σ_c = 30 psi
σ_a = 20 psi
ε_r = 25 %
e = 0.80

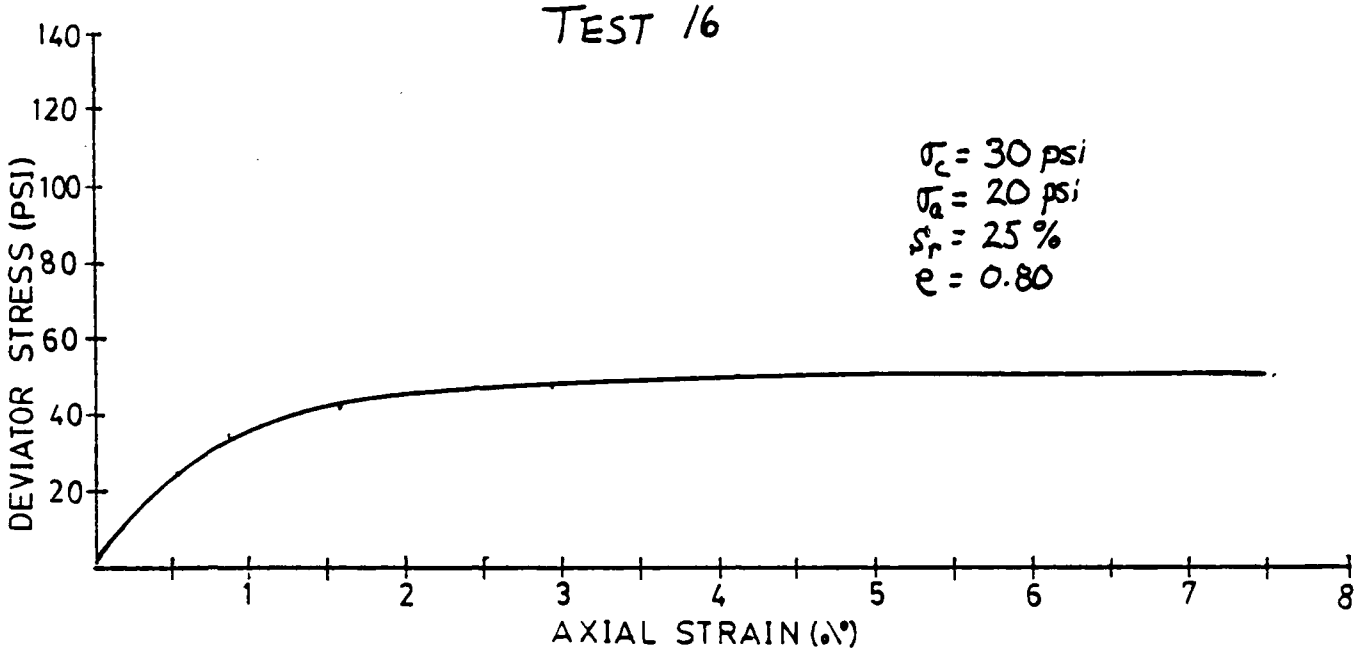

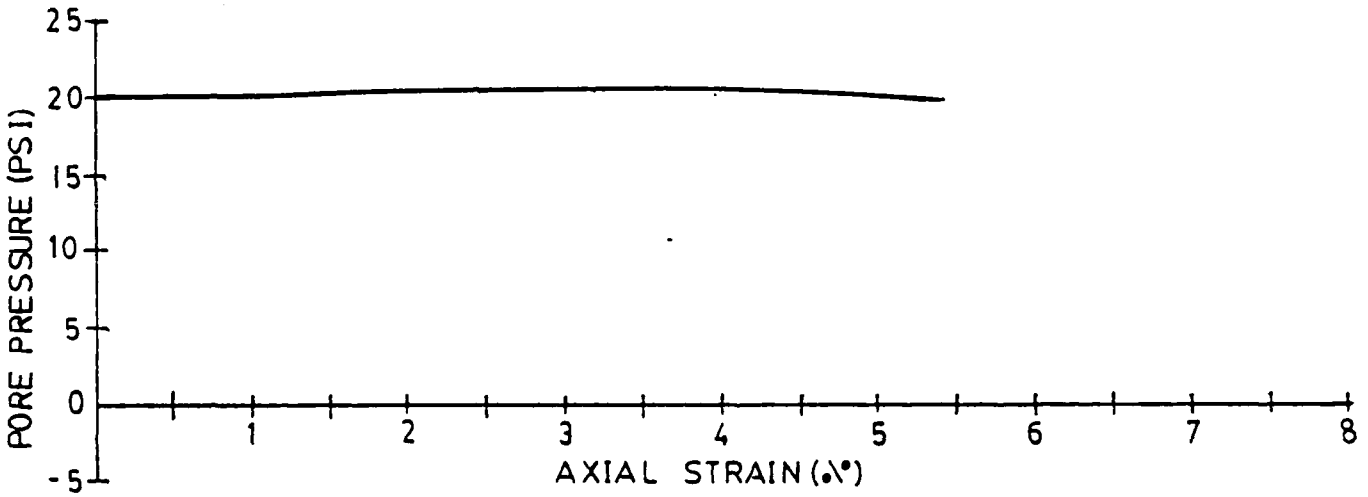

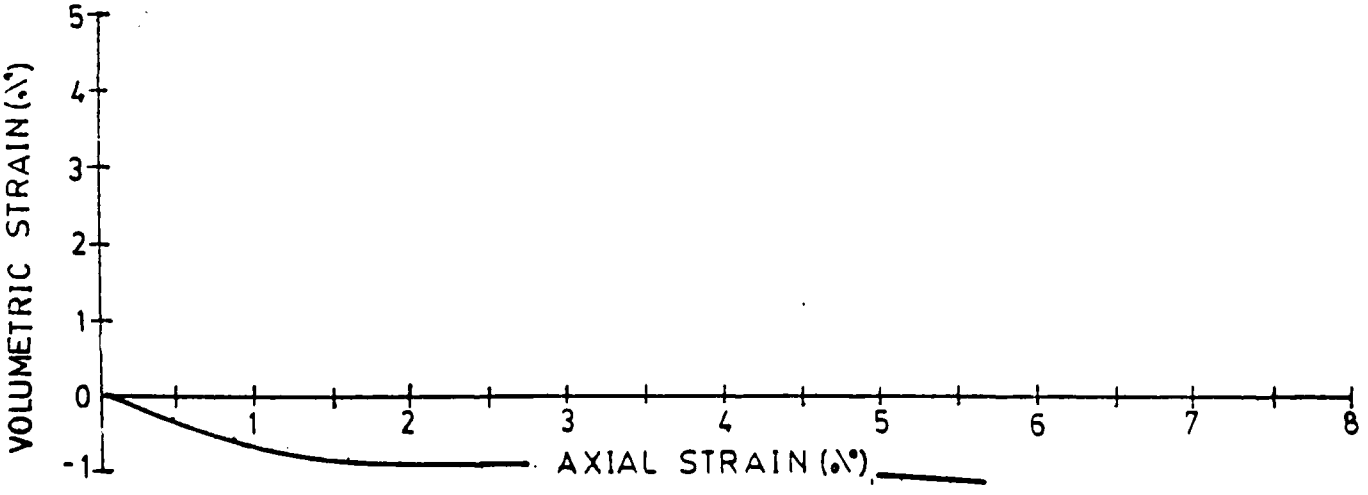

TEST 17

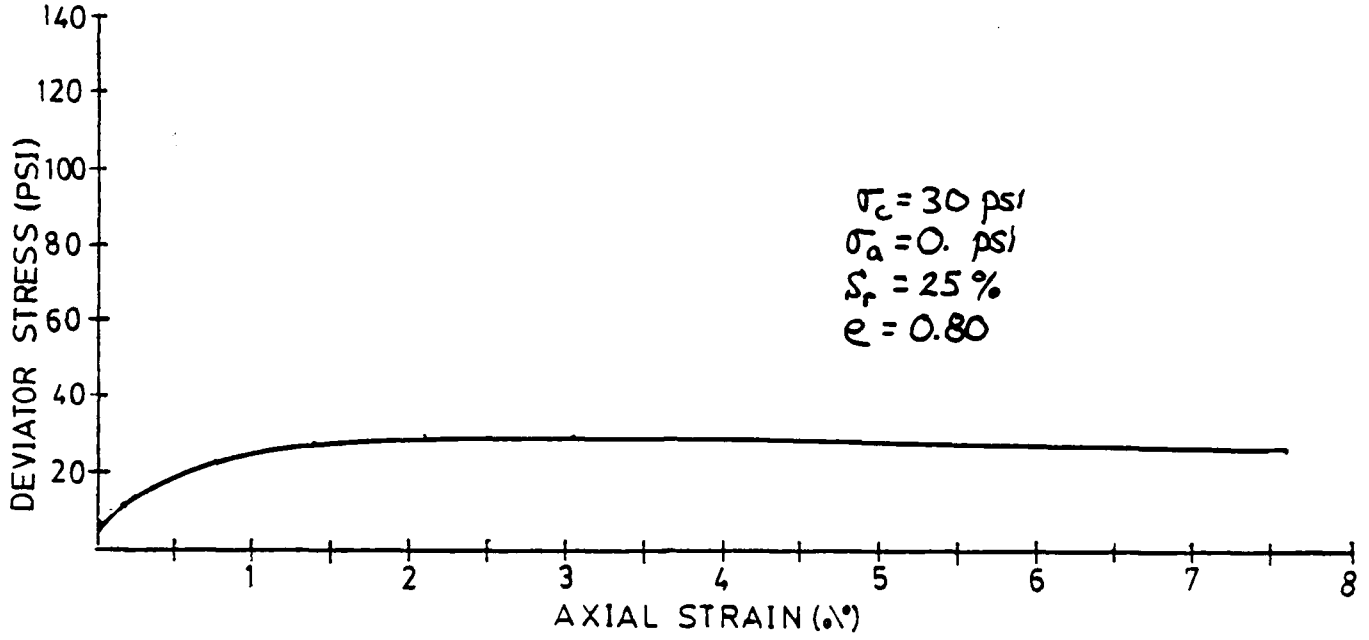
DEVIATOR STRESS (PSI)
140
120
100
80
60
40
20
1
2
3
4
5
6
7
8
AXIAL STRAIN (%)
σ_c = 30 psi
σ_a = 0. psi
S_r = 25 %
e = 0.80

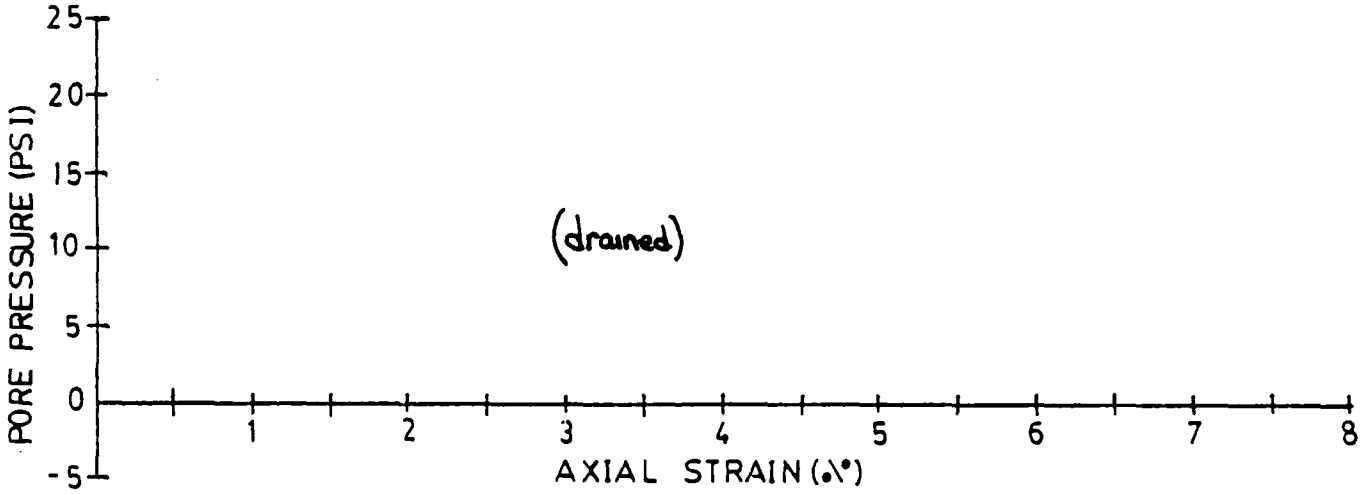
PORE PRESSURE (PSI)
25
20
15
10
5
0
-5
1
2
3
4
5
6
7
8
AXIAL STRAIN (%)
(drained)

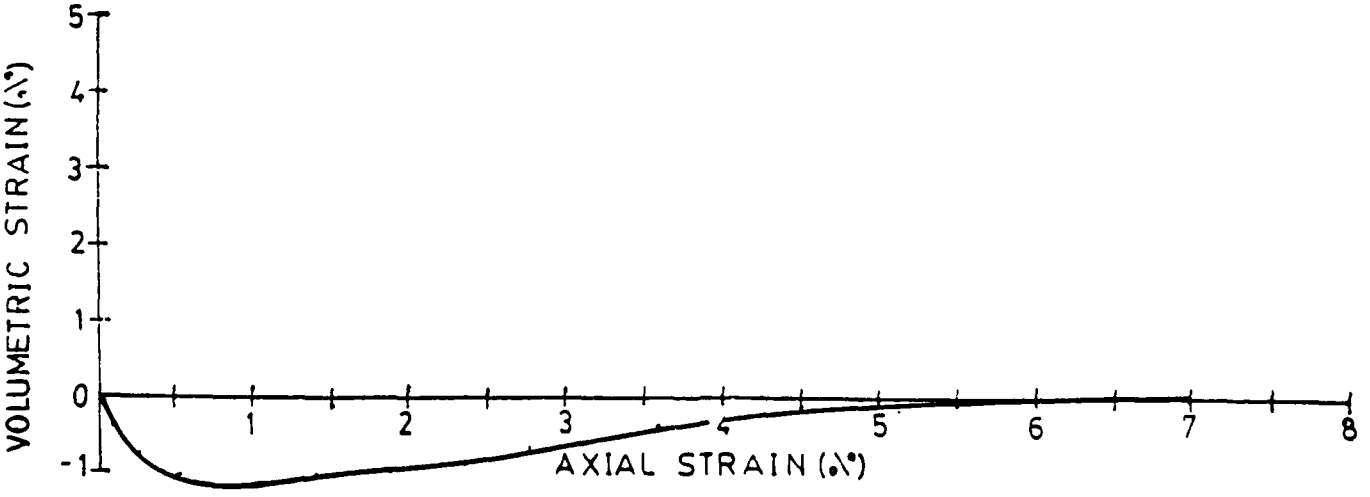
VOLUMETRIC STRAIN (%)
5
4
3
2
1
0
-1
1
2
3
4
5
6
7
8
AXIAL STRAIN (%)

TEST 18

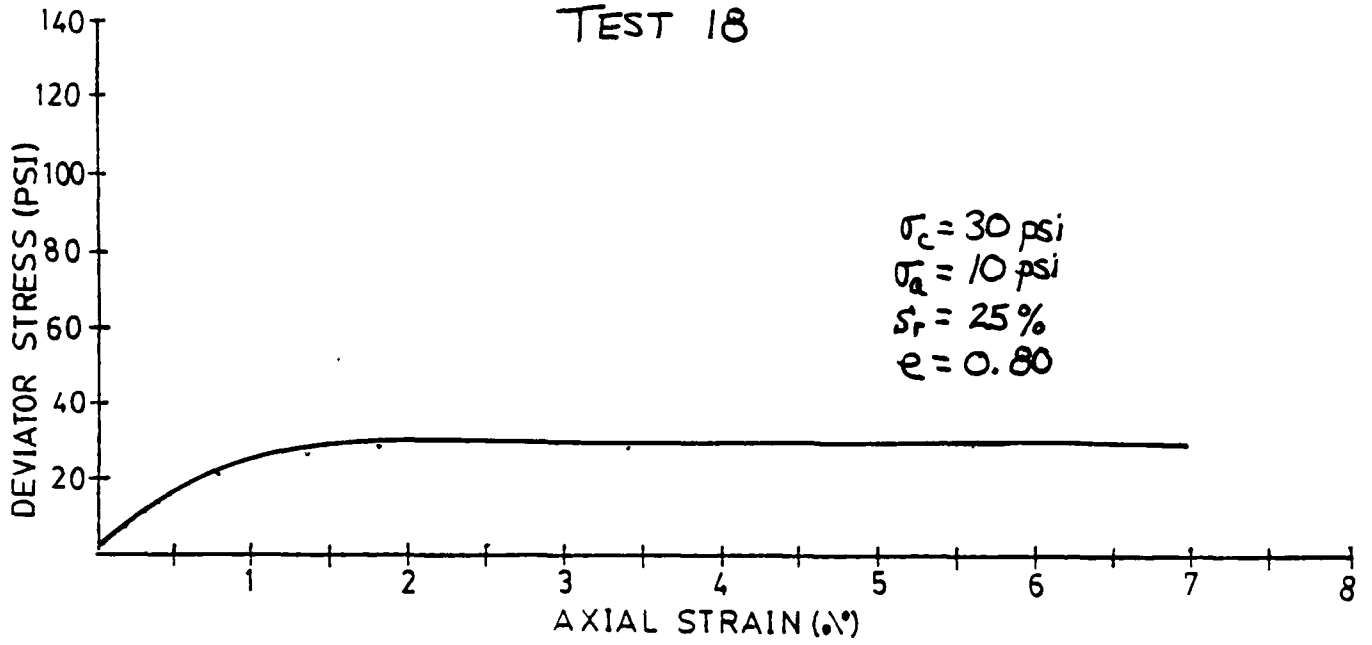
DEVIATOR STRESS (PSI)
140
120
100
80
60
40
20
1
2
3
4
5
6
7
8
AXIAL STRAIN (%)
σ_c = 30 psi
σ_a = 10 psi
ε_r = 25%
e = 0.80

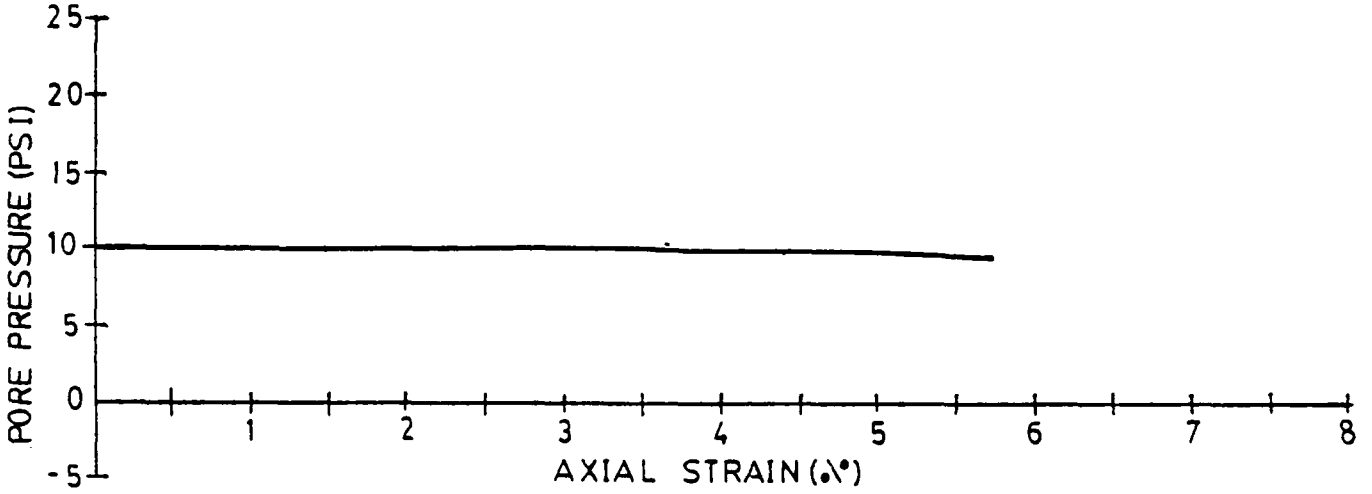
PORE PRESSURE (PSI)
25
20
15
10
5
0
-5
1
2
3
4
5
6
7
8
AXIAL STRAIN (%)

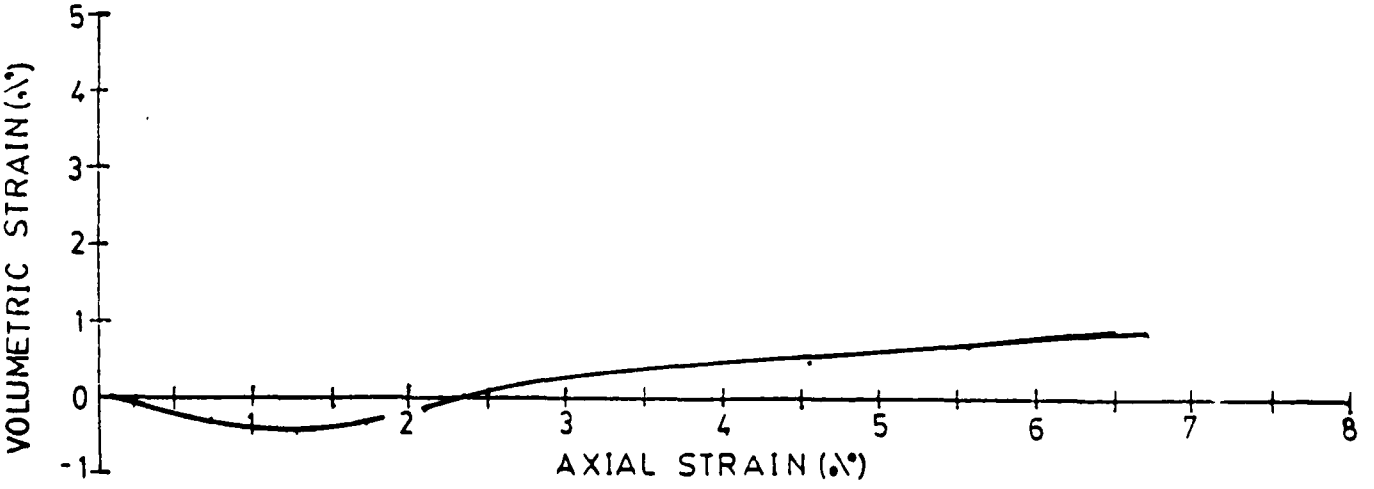
VOLUMETRIC STRAIN (%)
5
4
3
2
1
0
-1
2
3
4
5
6
7
8
AXIAL STRAIN (%)

TEST 19

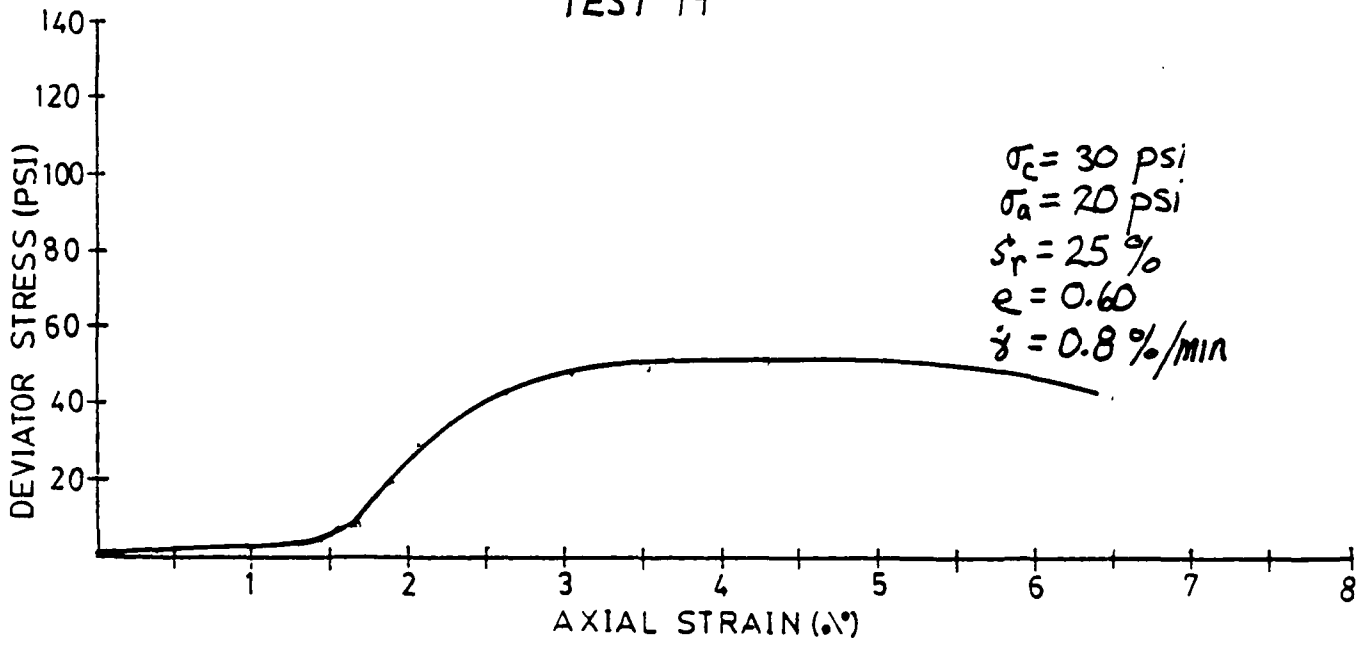
DEVIATOR STRESS (PSI)
140
120
100
80
60
40
20
1
2
3
4
5
6
7
8
AXIAL STRAIN (%)
σ_c = 30 psi
σ_a = 20 psi
S_r = 25 %
e = 0.60
$\dot{\varepsilon}$ = 0.8 %/min

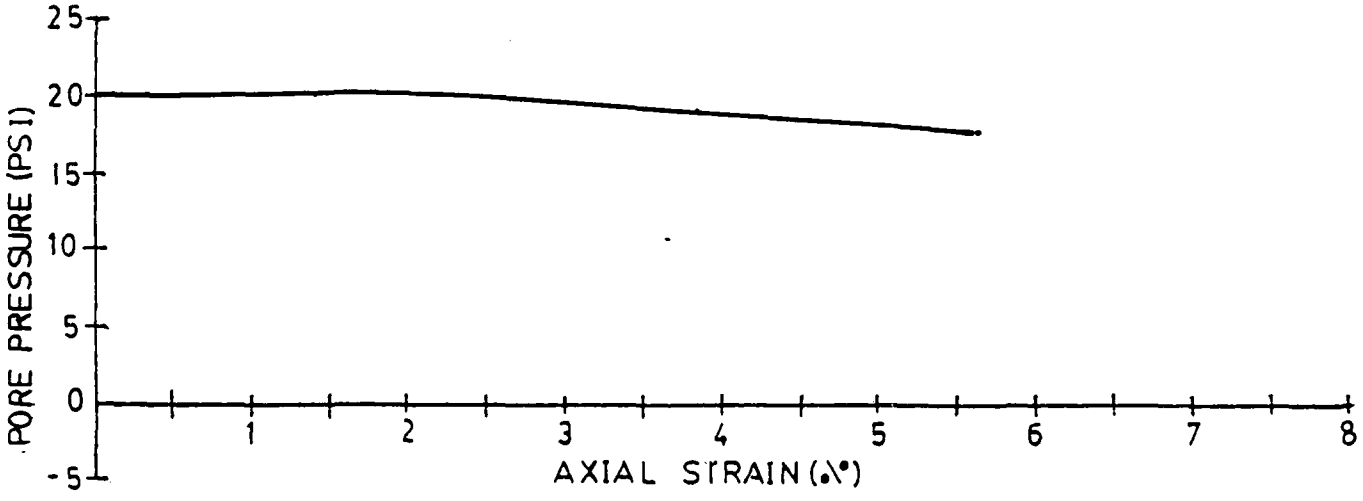
PORE PRESSURE (PSI)
25
20
15
10
5
0
-5
1
2
3
4
5
6
7
8
AXIAL STRAIN (%)

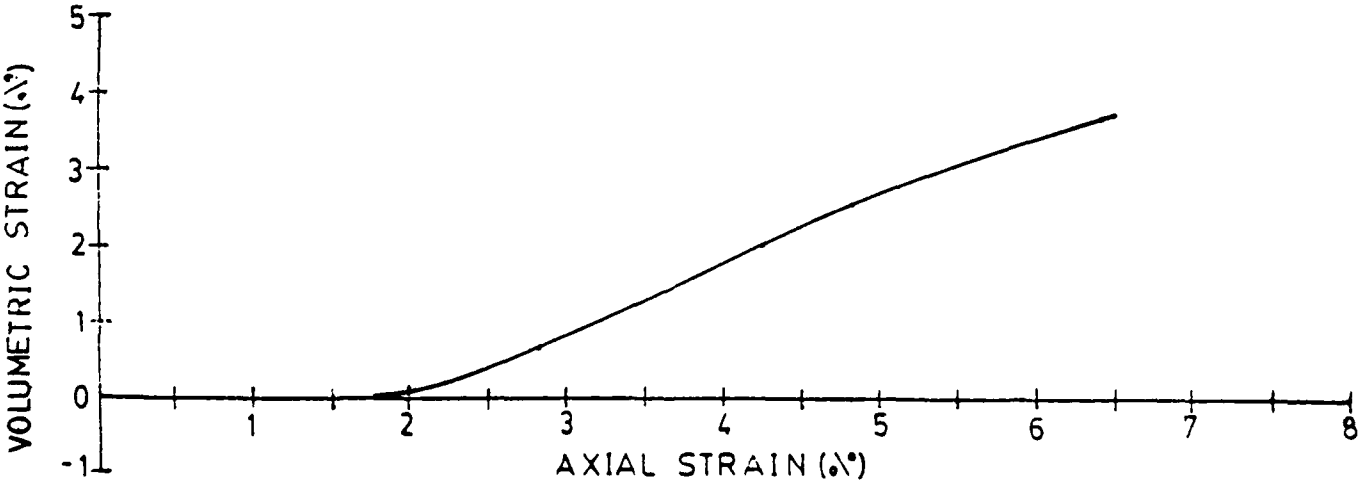
VOLUMETRIC STRAIN (%)
5
4
3
2
1
0
-1
1
2
3
4
5
6
7
8
AXIAL STRAIN (%)

AD-A191 924 UNDRAINED STRESS-STRAIN BEHAVIOR OF UNSATURATED SANDS 2/2
VOLUME 1(U) WISCONSIN UNIV-MADISON R G BOEHM ET AL.
25 JAN 88 AFOSR-TR-88-0155 AFOSR-84-0090

UNCLASSIFIED F/G 8/10 NL

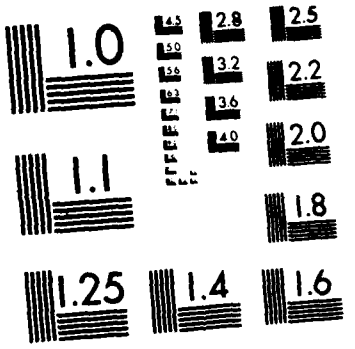

TEST 20

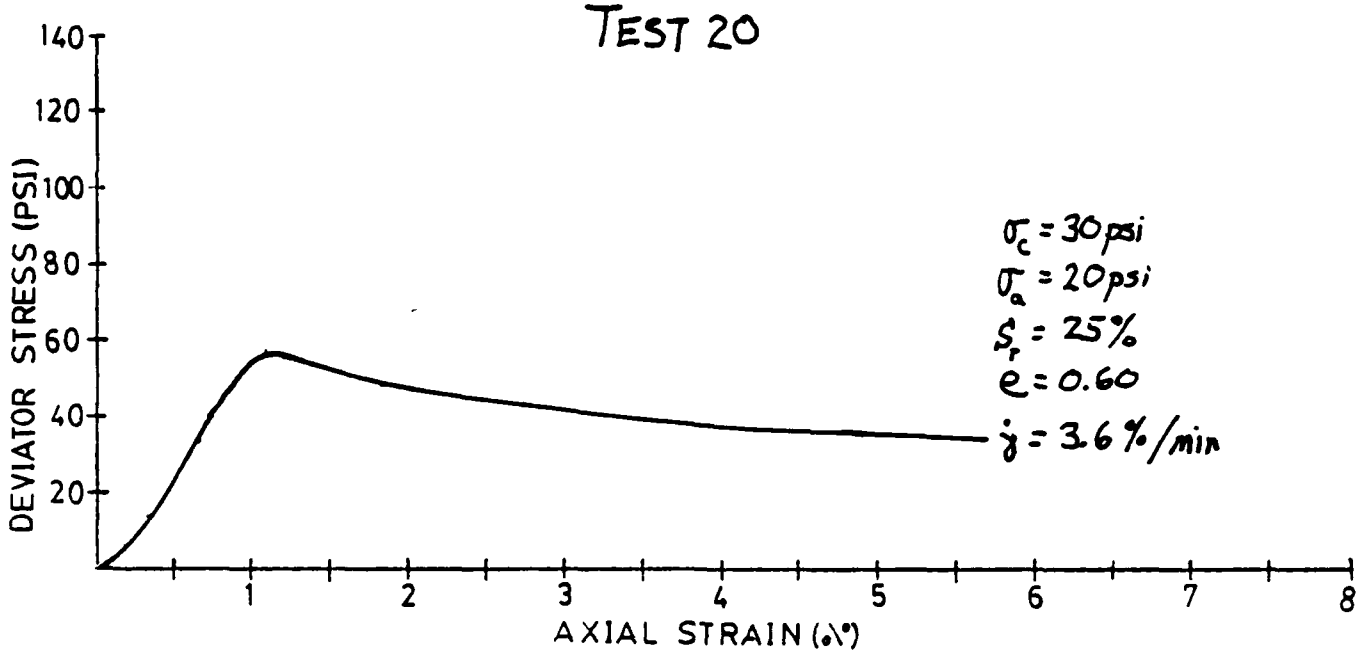
DEVIATOR STRESS (PSI)
140
120
100
80
60
40
20
1
2
3
4
5
6
7
8
AXIAL STRAIN (%)
σ_c = 30psi
σ_a = 20psi
ε_r = 25%
e = 0.60
$\dot{\gamma}$ = 3.6 %/min

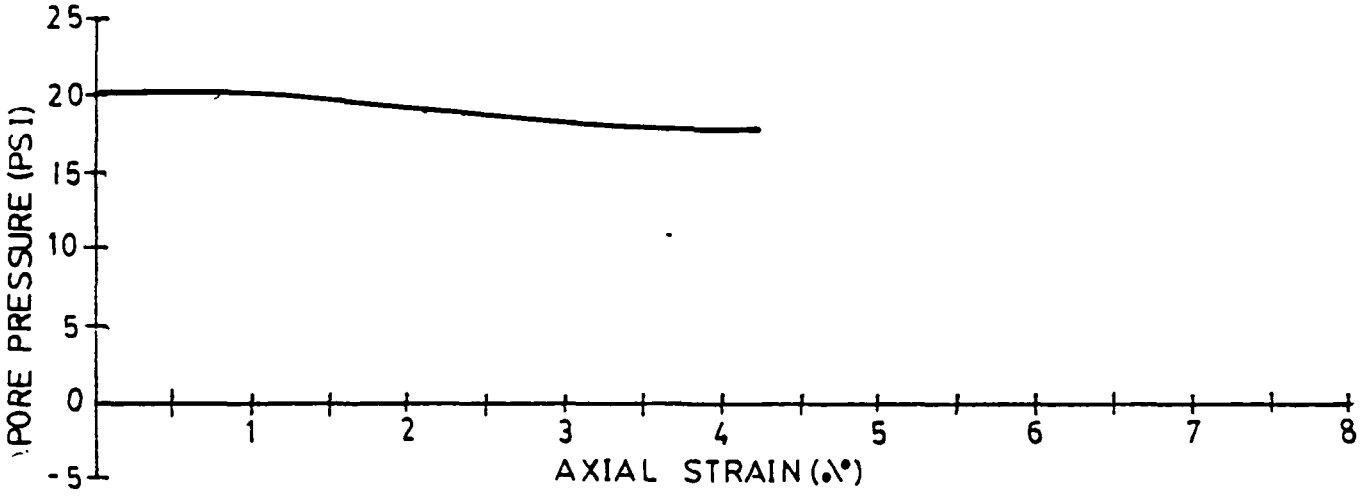
PORE PRESSURE (PSI)
25
20
15
10
5
0
-5
1
2
3
4
5
6
7
8
AXIAL STRAIN (%)

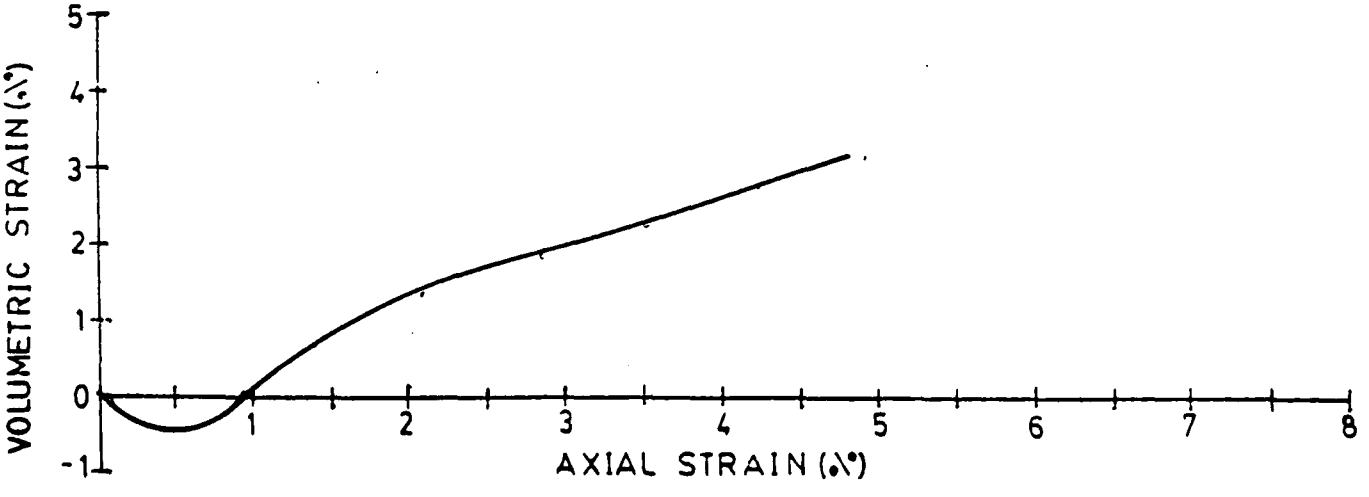
VOLUMETRIC STRAIN (%)
5
4
3
2
1
0
-1
1
2
3
4
5
6
7
8
AXIAL STRAIN (%)

TEST 21

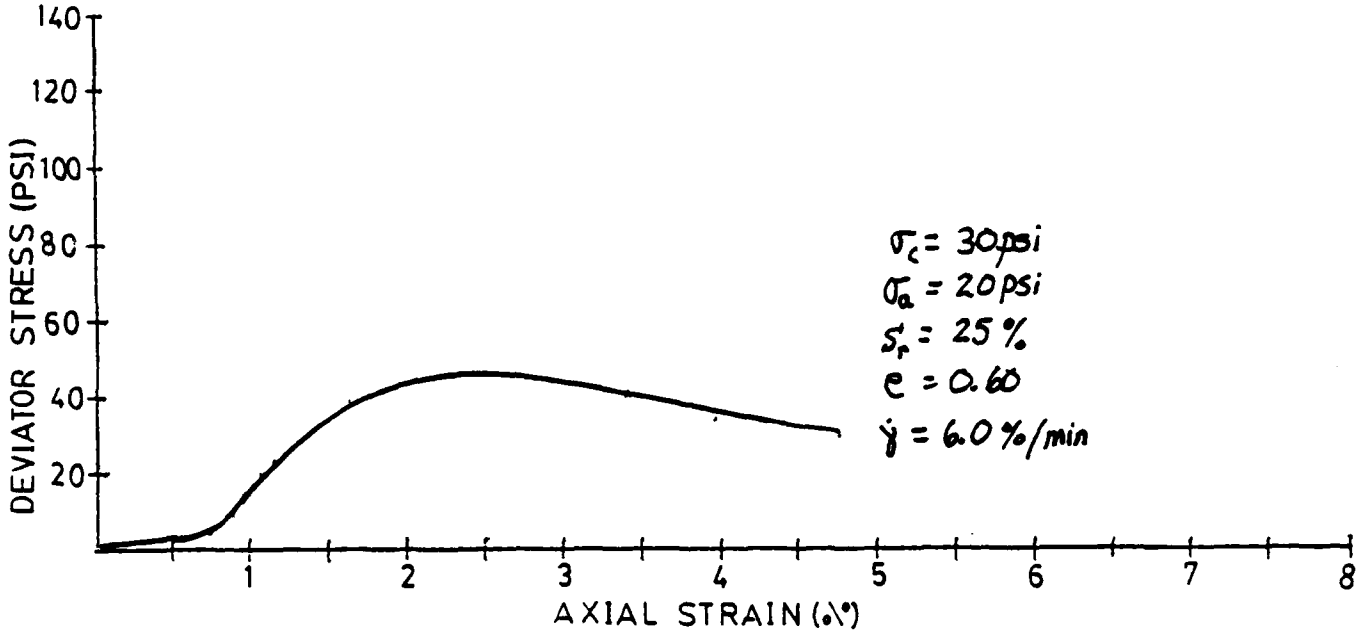
DEVIATOR STRESS (PSI)
140
120
100
80
60
40
20
1
2
3
4
5
6
7
8
AXIAL STRAIN (%)
σ_c = 30psi
σ_a = 20psi
S_r = 25 %
e = 0.60
$\dot{\gamma}$ = 6.0 %/min

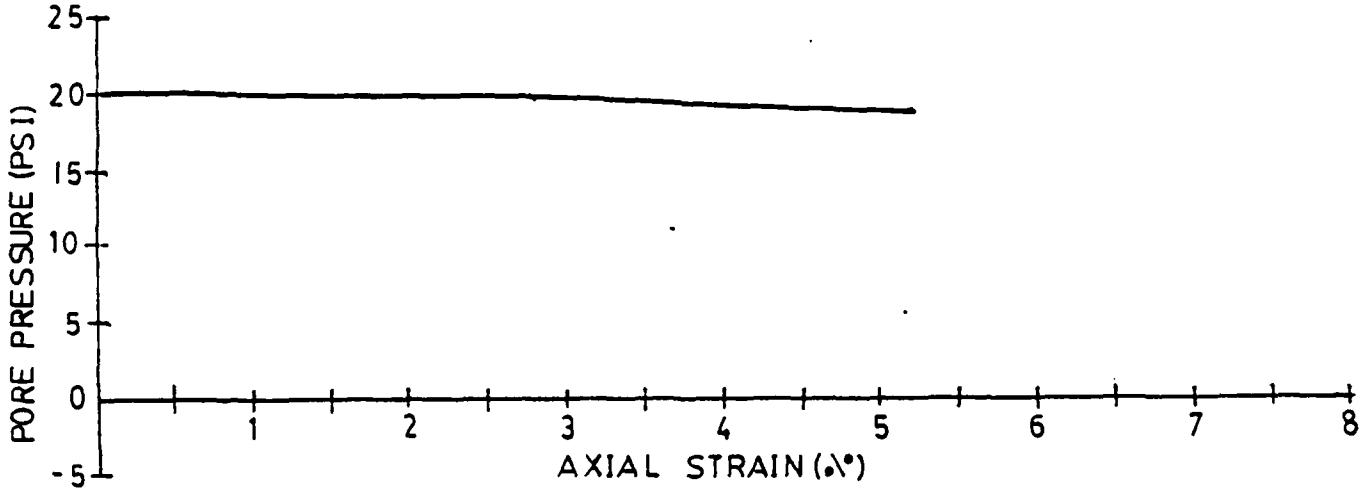
PORE PRESSURE (PSI)
25
20
15
10
5
0
-5
1
2
3
4
5
6
7
8
AXIAL STRAIN (%)

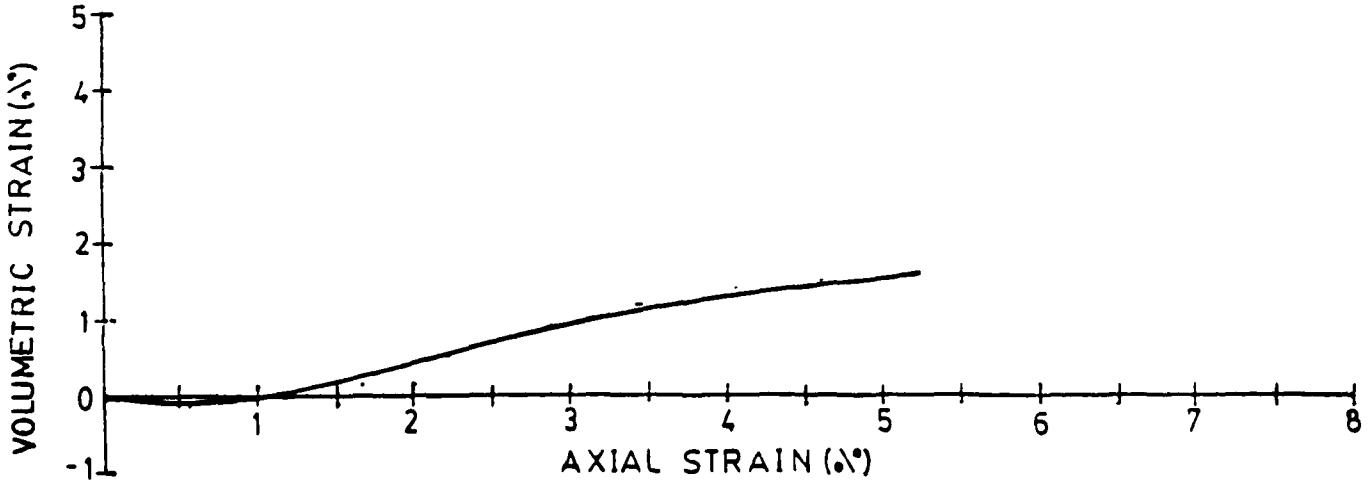
VOLUMETRIC STRAIN (%)
5
4
3
2
1
0
-1
1
2
3
4
5
6
7
8
AXIAL STRAIN (%)

TEST 22

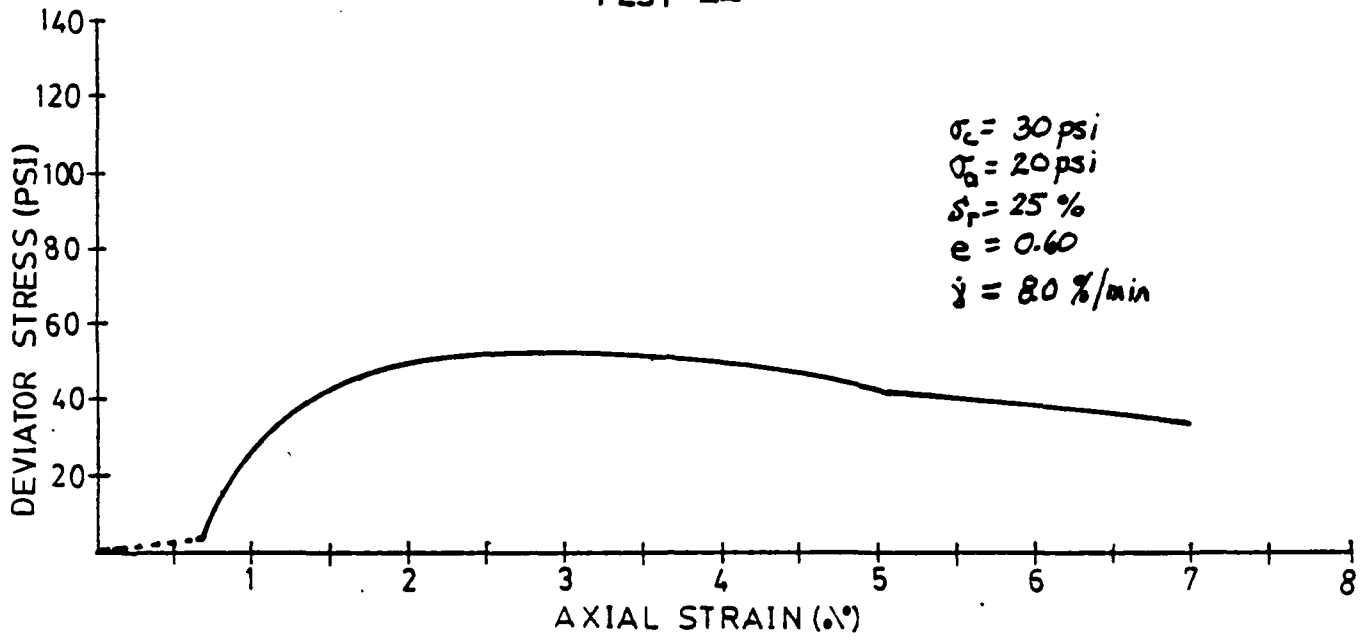
DEVIATOR STRESS (PSI)
140
120
100
80
60
40
20
1
2
3
4
5
6
7
8
AXIAL STRAIN (%)
σ_c = 30 psi
σ_a = 20 psi
δ_r = 25 %
e = 0.60
$\dot{\gamma}$ = 80 %/min

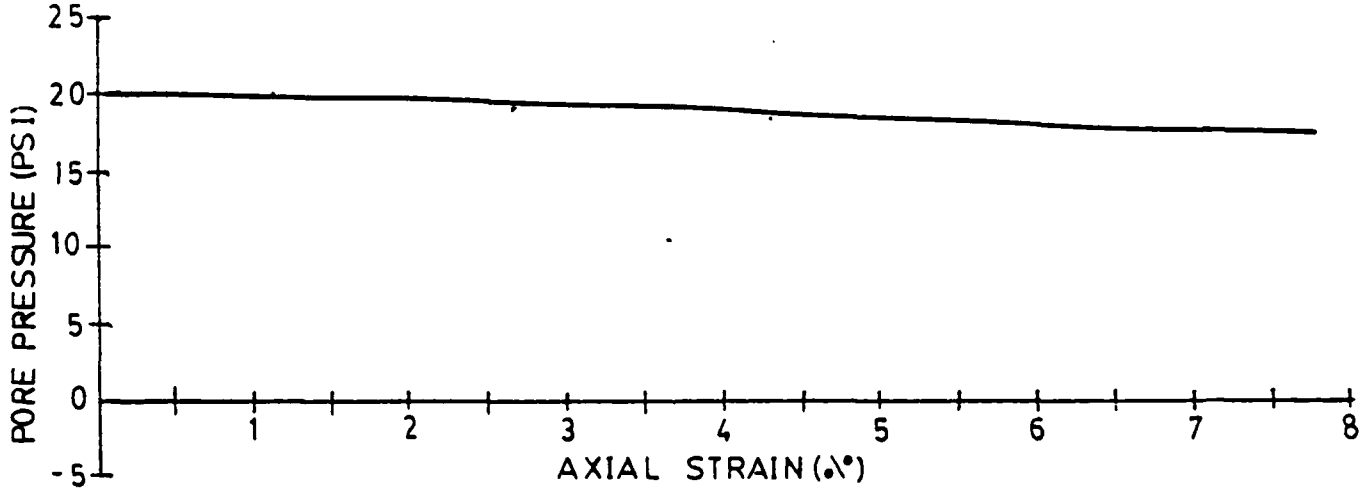
PORE PRESSURE (PSI)
25
20
15
10
5
0
-5
1
2
3
4
5
6
7
8
AXIAL STRAIN (%)

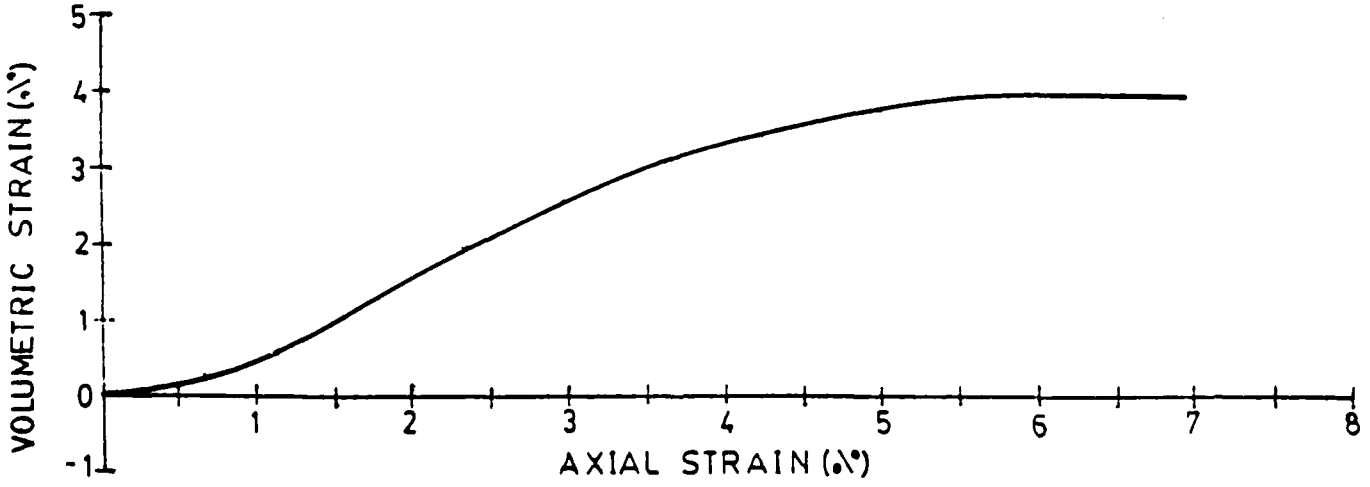
VOLUMETRIC STRAIN (%)
5
4
3
2
1
0
-1
1
2
3
4
5
6
7
8
AXIAL STRAIN (%)

TEST 23

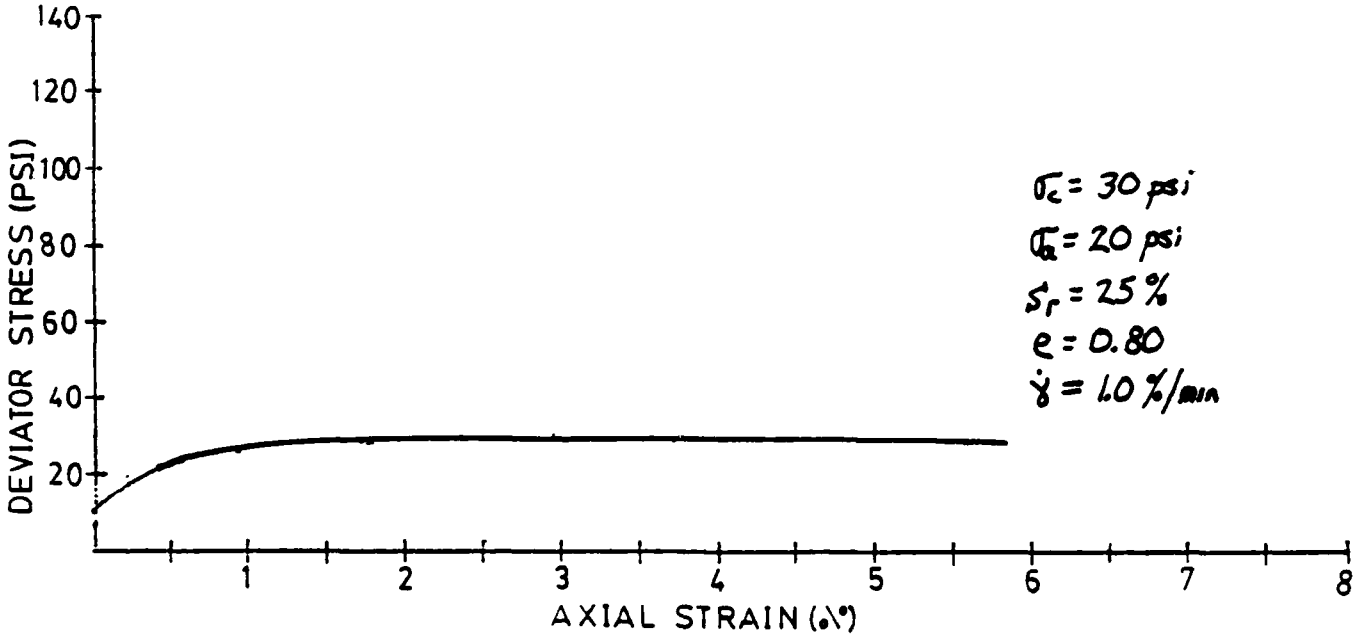
DEVIATOR STRESS (PSI)
140
120
100
80
60
40
20
1
2
3
4
5
6
7
8
AXIAL STRAIN (%)
σ_c = 30 psi
σ_a = 20 psi
S_r = 25 %
e = 0.80
$\dot{\varepsilon}$ = 1.0 %/min

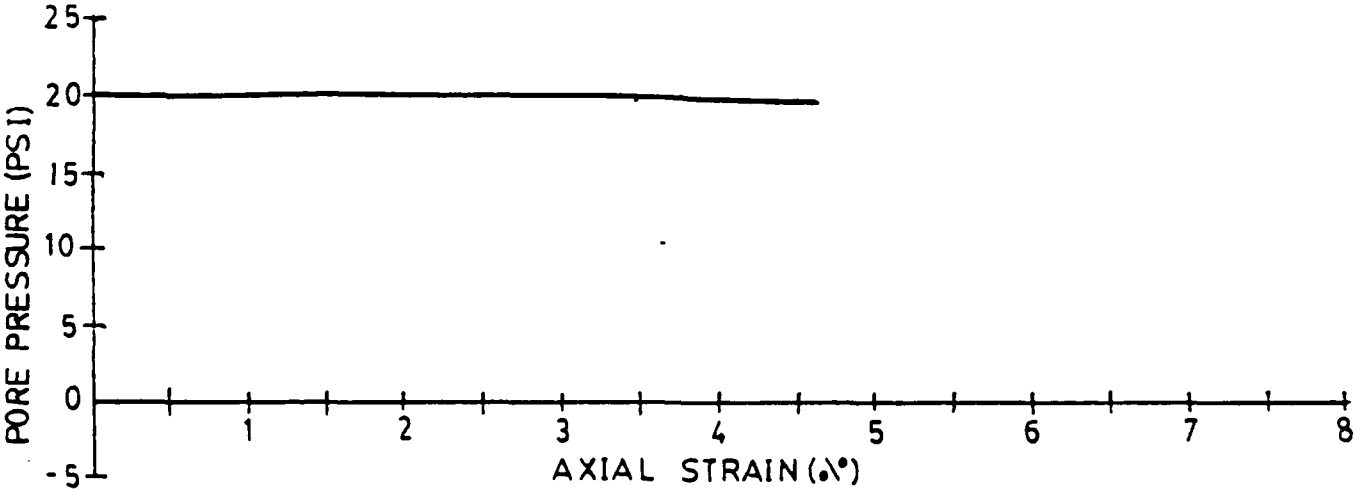
PORE PRESSURE (PSI)
25
20
15
10
5
0
-5
1
2
3
4
5
6
7
8
AXIAL STRAIN (%)

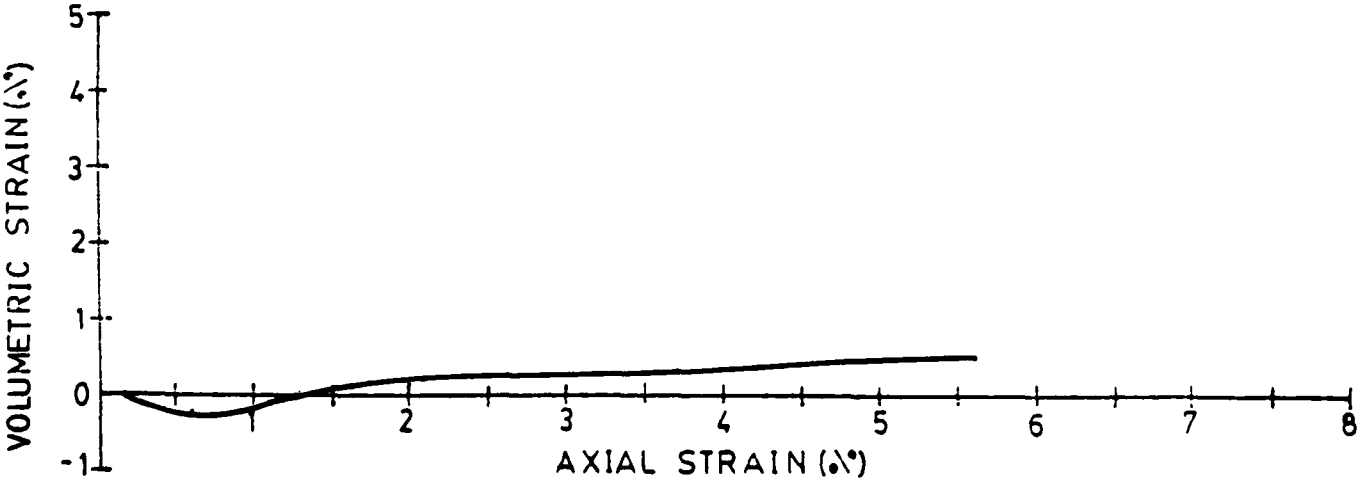
VOLUMETRIC STRAIN (%)
5
4
3
2
1
0
-1
2
3
4
5
6
7
8
AXIAL STRAIN (%)

TEST 24

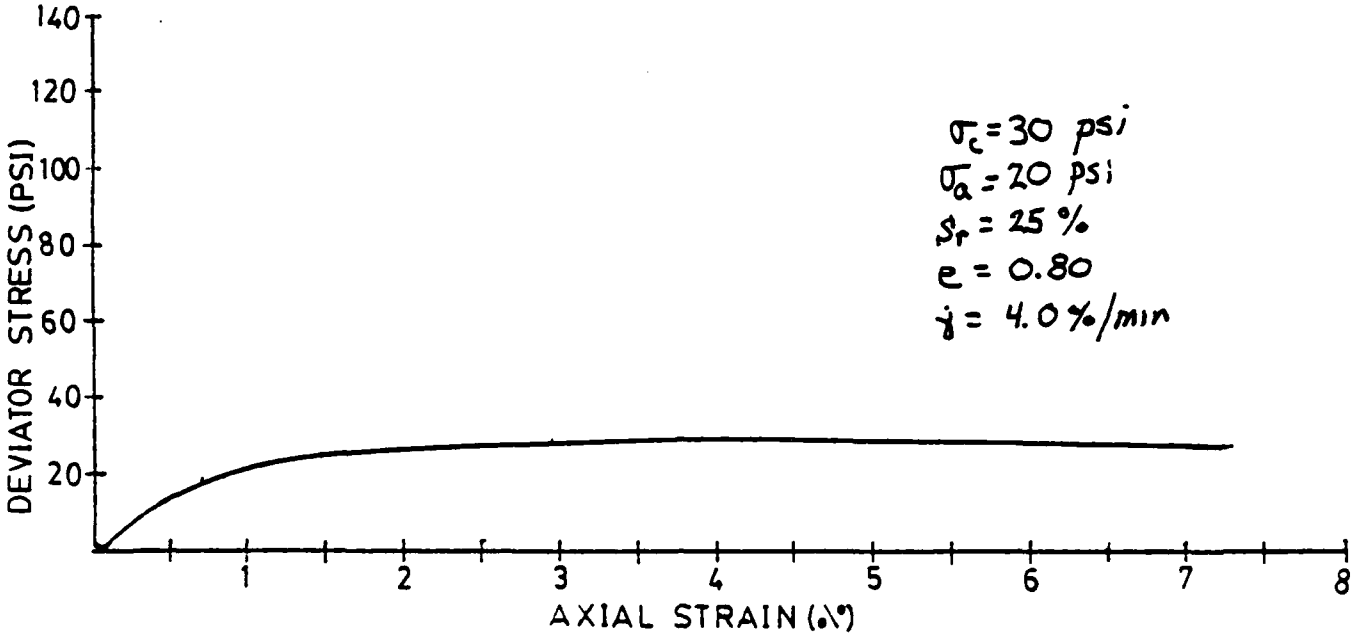
DEVIATOR STRESS (PSI)
140
120
100
80
60
40
20
1
2
3
4
5
6
7
8
AXIAL STRAIN (%)
σ_c = 30 psi
σ_a = 20 psi
S_r = 25 %
e = 0.80
$\dot{\varepsilon}$ = 4.0 %/min

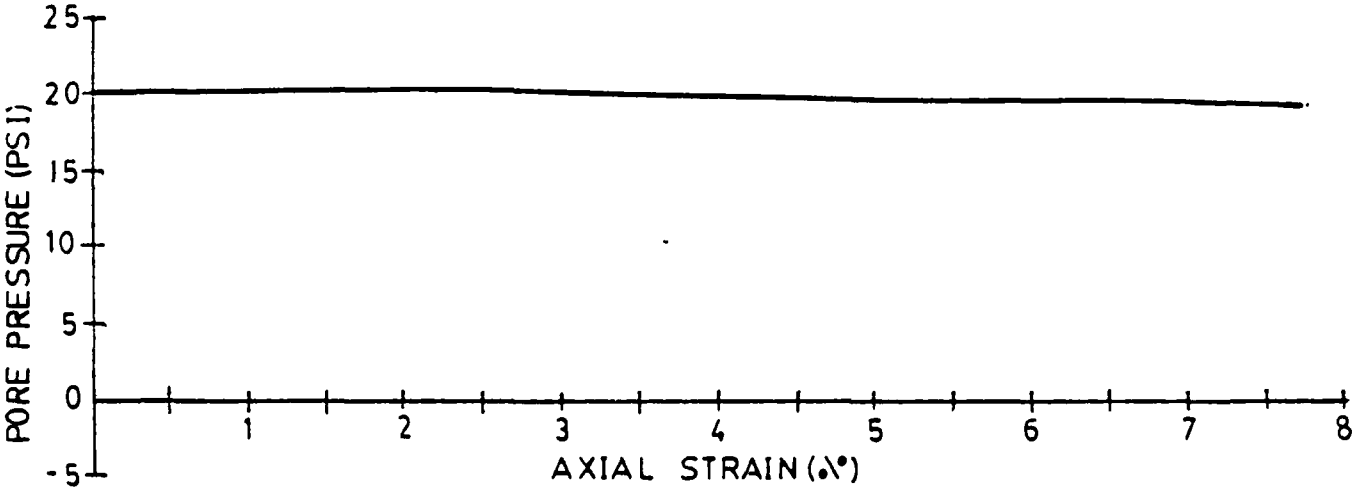
PORE PRESSURE (PSI)
25
20
15
10
5
0
-5
1
2
3
4
5
6
7
8
AXIAL STRAIN (%)

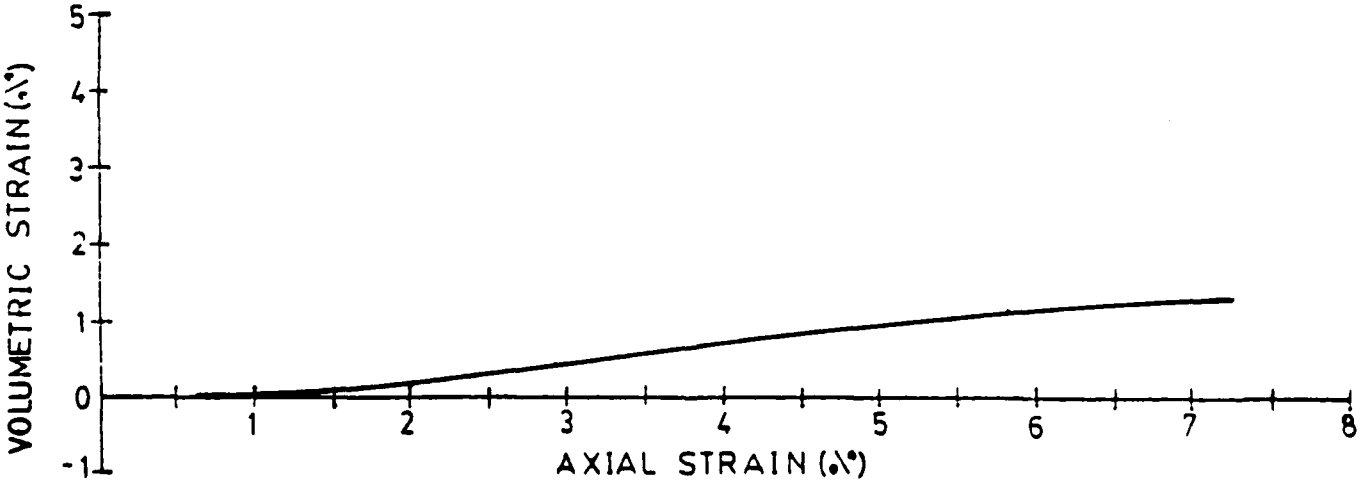
VOLUMETRIC STRAIN (%)
5
4
3
2
1
0
-1
1
2
3
4
5
6
7
8
AXIAL STRAIN (%)

TEST 25

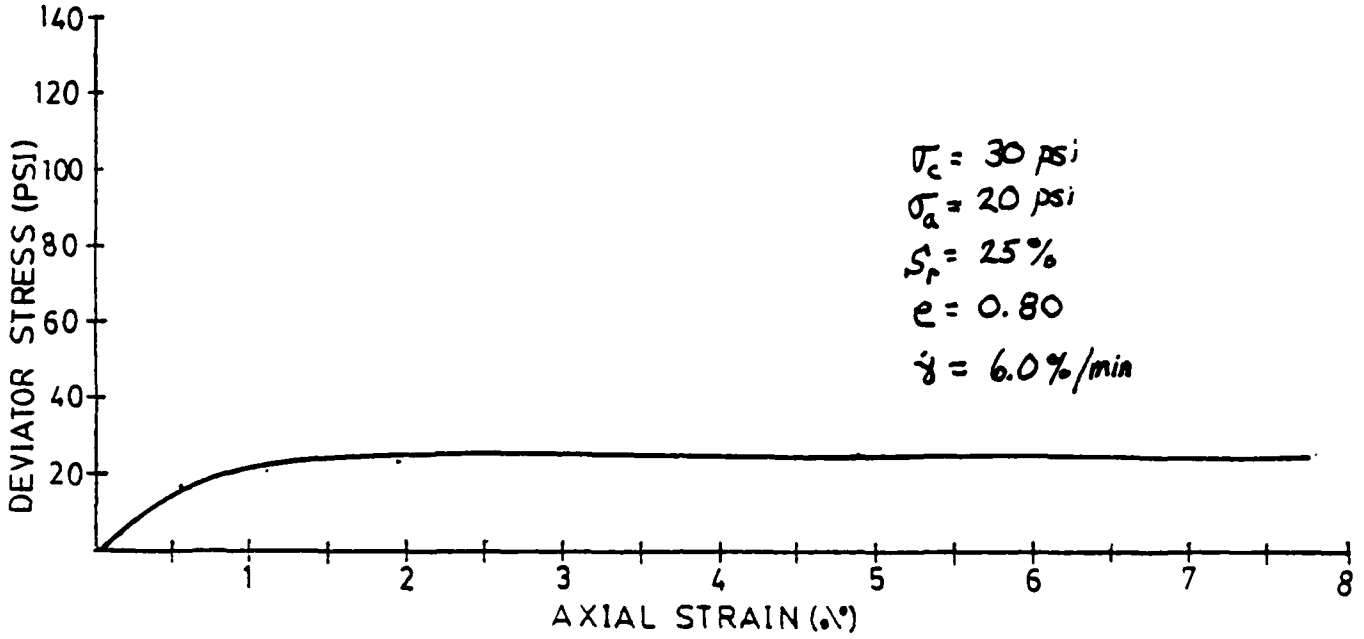

σ_c = 30 psi
σ_d = 20 psi
S_r = 25%
e = 0.80
$\dot{\gamma}$ = 6.0%/min

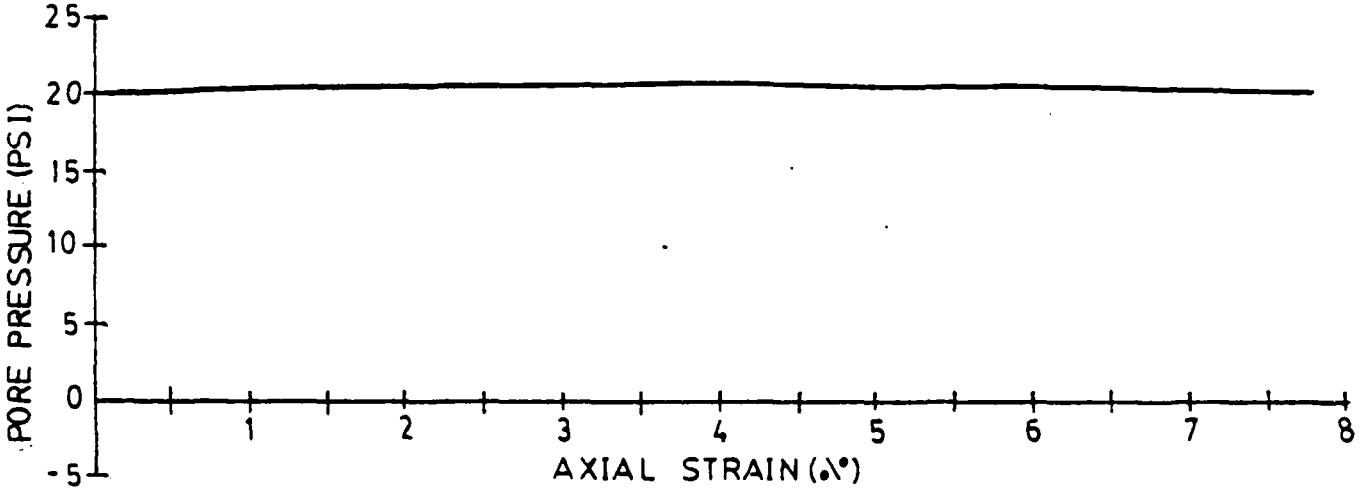

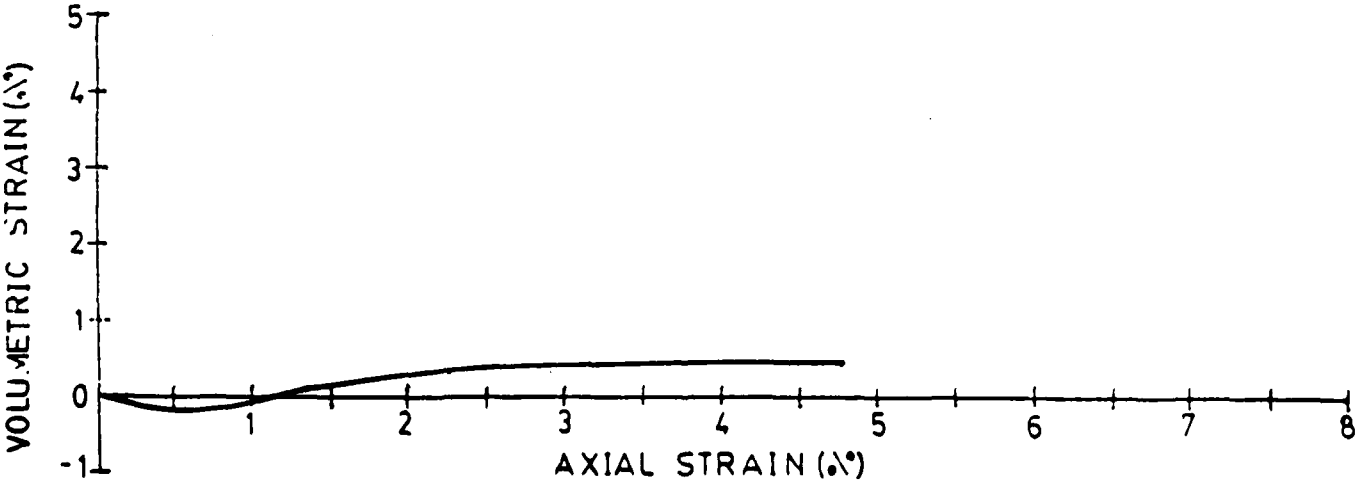

TEST 26

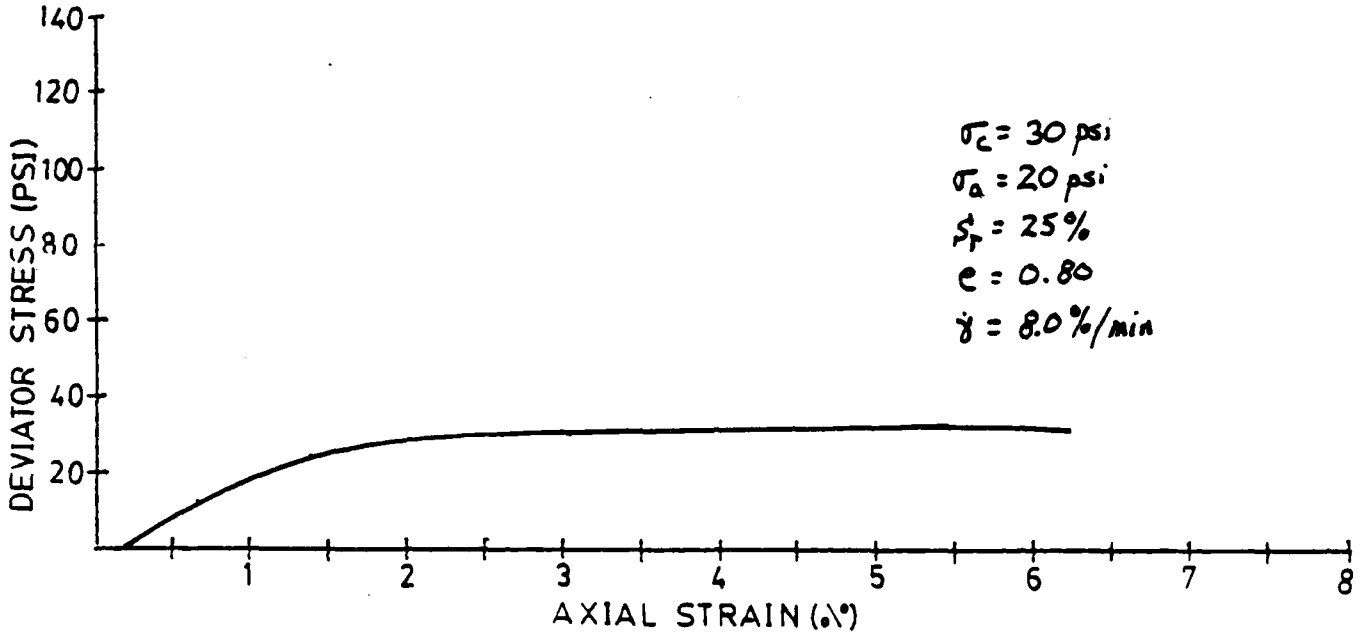
DEVIATOR STRESS (PSI)
140
120
100
80
60
40
20
1
2
3
4
5
6
7
8
AXIAL STRAIN (%)
σ_c = 30 psi
σ_a = 20 psi
S_r = 25%
e = 0.80
$\dot{\varepsilon}$ = 8.0%/min

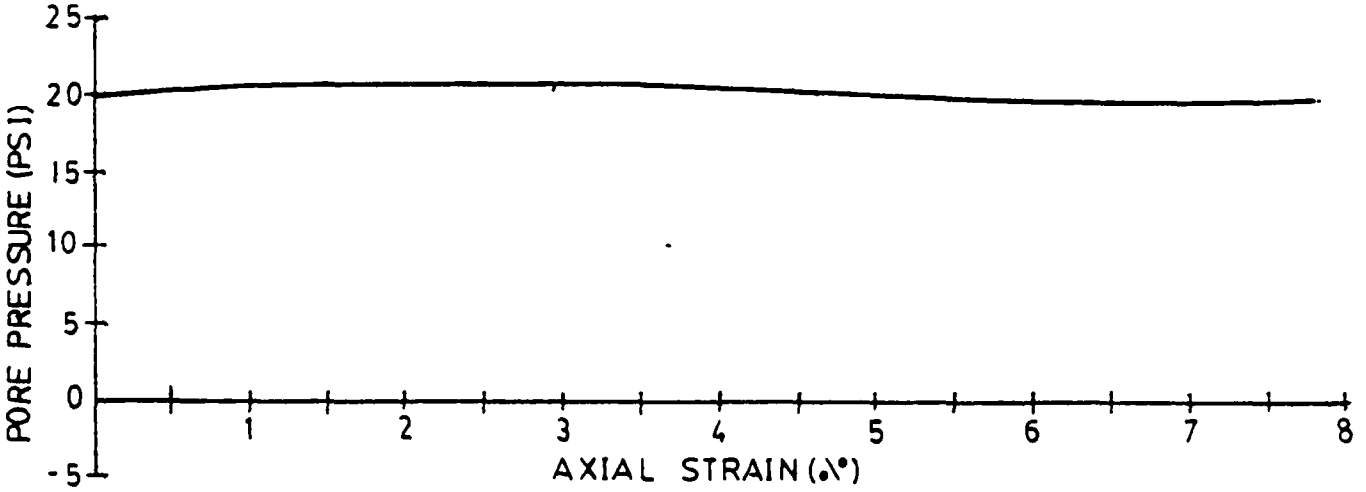
PORE PRESSURE (PSI)
25
20
15
10
5
0
-5
1
2
3
4
5
6
7
8
AXIAL STRAIN (%)

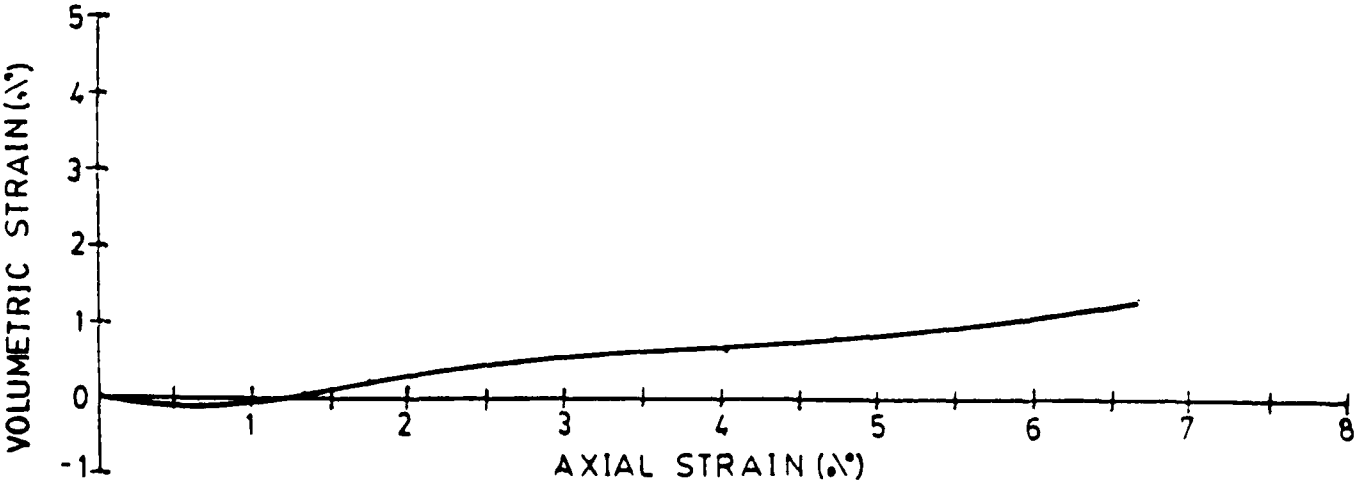
VOLUMETRIC STRAIN (%)
5
4
3
2
1
0
-1
1
2
3
4
5
6
7
8
AXIAL STRAIN (%)

END

DATE

FILMED

5-88

DTIC